

EVALUATION OF THE ENHANCED INTEGRATED CLIMATIC MODEL FOR SPECIFICATION OF SUBGRADE SOILS IN OKLAHOMA

FINAL REPORT ~ FHWA-OK-14-05
ODOT SP&R ITEM NUMBER 2160

Submitted to:

John R. Bowman, P.E.
Planning & Research Division Engineer
Oklahoma Department of Transportation

Submitted by:

Rifat Bulut, Ph.D.
Er Yue, Ph.D. Candidate
Lizhou Chen, Ph.D. Candidate
Oklahoma State University
and
K.K. "Muralee" Muraleetharan Ph.D., P.E.
Musharraf Zaman Ph.D., P.E.
Hoda Soltani, Ph.D. Candidate
Zahid Hossain, Ph.D.
The University of Oklahoma



January 2014

TECHNICAL REPORT DOCUMENTATION PAGE

1. REPORT NO. FHWA-OK- 14-05	2. GOVERNMENT ACCESSION NO.	3. RECIPIENT'S CATALOG NO.	
4. TITLE AND SUBTITLE Evaluation of the Enhanced Integrated Climatic Model for Specification of Subgrade Soils in Oklahoma		5. REPORT DATE Jan 2014	
		6. PERFORMING ORGANIZATION CODE	
7. AUTHOR(S) Rifat Bulut, K.K. "Muralee" Muraleetharan, Musharraf Zaman, Er Yue, Lizhou Chen, Hoda Soltani, and Zahid Hossain		8. PERFORMING ORGANIZATION REPORT Click here to enter text.	
9. PERFORMING ORGANIZATION NAME AND ADDRESS Oklahoma State University School of Civil and Environmental Engineering 207 Engineering South, Stillwater, OK 74078		10. WORK UNIT NO.	
		11. CONTRACT OR GRANT NO. ODOT SP&R Item Number 2160	
12. SPONSORING AGENCY NAME AND ADDRESS Oklahoma Department of Transportation Planning and Research Division 200 N.E. 21st Street, Room 3A7 Oklahoma City, OK 73105		13. TYPE OF REPORT AND PERIOD COVERED Final Report Oct 2011 - Dec 2013	
		14. SPONSORING AGENCY CODE	
15. SUPPLEMENTARY NOTES Oklahoma Transportation Center a University Transportation Center			
16. ABSTRACT The main objective of this study was to collect and evaluate climatic and soil data pertaining to Oklahoma for the climatic model (EICM) in the mechanistic-empirical design guide for pavements. The EICM climatic input files were updated and extended over a large area covering Oklahoma climatic conditions. Large cluster of raw climate and soil moisture data were obtained from the Oklahoma Mesonet for evaluation and use in creating the necessary input parameters for the climatic model. Historical climatic data were also employed for classifying climatic regions in Oklahoma using cluster analysis. Thornthwaite Moisture Index (TMI) contour maps were created using the climatic data and ArcGIS software. A comprehensive validation study was also undertaken in comparing the moisture migration processes in the EICM and commercially available software using the climatic and soil data in Oklahoma.			
17. KEY WORDS Climate, soil, EICM, TMI, moisture, suction		18. DISTRIBUTION STATEMENT No restrictions. This publication is available from the Planning & Research Div., Oklahoma DOT.	
19. SECURITY CLASSIF. (OF THIS REPORT) Unclassified	20. SECURITY CLASSIF. (OF THIS PAGE) Unclassified	21. NO. OF PAGES 118	22. PRICE N/A

The contents of this report reflect the views of the author(s) who is responsible for the facts and the accuracy of the data presented herein. The contents do not necessarily reflect the views of the Oklahoma Department of Transportation or the Federal Highway Administration. This report does not constitute a standard, specification, or regulation. While trade names may be used in this report, it is not intended as an endorsement of any machine, contractor, process, or product.

SI* (MODERN METRIC) CONVERSION FACTORS

APPROXIMATE CONVERSIONS TO SI UNITS				
SYMBOL	WHEN YOU KNOW	MULTIPLY BY	TO FIND	SYMBOL
LENGTH				
in	inches	25.4	millimeters	mm
ft	feet	0.305	meters	m
yd	yards	0.914	meters	m
mi	miles	1.61	kilometers	km
AREA				
in²	square inches	645.2	square millimeters	mm ²
ft²	square feet	0.093	square meters	m ²
yd²	square yard	0.836	square meters	m ²
ac	acres	0.405	hectares	ha
mi²	square miles	2.59	square kilometers	km ²
VOLUME				
fl oz	fluid ounces	29.57	milliliters	mL
gal	gallons	3.785	liters	L
ft³	cubic feet	0.028	cubic meters	m ³
yd³	cubic yards	0.765	cubic meters	m ³
NOTE: volumes greater than 1000 L shall be shown in m ³				
MASS				
oz	ounces	28.35	grams	g
lb	pounds	0.454	kilograms	kg
T	short tons (2000 lb)	0.907	megagrams (or "metric ton")	Mg (or "t")
TEMPERATURE (exact degrees)				
°F	Fahrenheit	5 (F-32)/9 or (F-32)/1.8	Celsius	°C
ILLUMINATION				
fc	foot-candles	10.76	lux	lx
fl	foot-Lamberts	3.426	candela/m ²	cd/m ²
FORCE and PRESSURE or STRESS				
lbf	poundforce	4.45	newtons	N
lbf/in²	poundforce per square inch	6.89	kilopascals	kPa

APPROXIMATE CONVERSIONS FROM SI UNITS				
SYMBOL	WHEN YOU KNOW	MULTIPLY BY	TO FIND	SYMBOL
LENGTH				
mm	millimeters	0.039	inches	in
m	meters	3.28	feet	ft
m	meters	1.09	yards	yd
km	kilometers	0.621	miles	mi
AREA				
mm ²	square millimeters	0.0016	square inches	in ²
m ²	square meters	10.764	square feet	ft ²
m ²	square meters	1.195	square yards	yd ²
ha	hectares	2.47	acres	ac
km ²	square kilometers	0.386	square miles	mi ²
VOLUME				
mL	milliliters	0.034	fluid ounces	fl oz
L	liters	0.264	gallons	gal
m ³	cubic meters	35.314	cubic feet	ft ³
m ³	cubic meters	1.307	cubic yards	yd ³
MASS				
g	grams	0.035	ounces	oz
kg	kilograms	2.202	pounds	lb
Mg (or "t")	megagrams (or "metric ton")	1.103	short tons (2000 lb)	T
TEMPERATURE (exact degrees)				
°C	Celsius	1.8C+32	Fahrenheit	°F
ILLUMINATION				
lx	lux	0.0929	foot-candles	fc
cd/m ²	candela/m ²	0.2919	foot-Lamberts	fl
FORCE and PRESSURE or STRESS				
N	newtons	0.225	poundforce	lbf
kPa	kilopascals	0.145	poundforce per square inch	lbf/in ²

*SI is the symbol for the International System of Units. Appropriate rounding should be made to comply with Section 4 of ASTM E380.

TABLE OF CONTENTS

1 INTRODUCTION.....	1
2 CLIMATIC INPUT FILES FOR EICM.....	3
2.1 Oklahoma Mesonet.....	3
2.1.1 Oklahoma Mesonet Station Layout	4
2.2 Climate and Soil Moisture/Suction Data	5
2.2.1 Percent Sunshine from Solar Radiation	9
2.3 EICM Input Files	10
2.3.1 Fortran Subroutine for Creating EICM Files	11
2.4 Validation of EICM Input Files.....	12
3 THORNTHWAITTE MOISTURE INDEX	17
3.1 Water Storage and Potential Evapotranspiration.....	18
3.2 Thornthwaite (1948) Equation	18
3.3 Thornthwaite and Mather (1955) Equation	21
3.4 Witczak et al. (2006) Equation	22
4 GROUNDWATER TABLE AND SOIL SUCTION PROFILES	25
4.1 Groundwater Table Depth	25
4.2 Soil Matric Suction Profile	27
5 CLIMATIC AND SOIL REGIONS.....	30
5.1 Climatic Regions.....	30
5.1.1 Climatic Parameters.....	31
5.1.2 SPSS and ARCGIS Software Models	32
5.1.3 Optimum Number of Climatic Regions	34
5.2 Soil Regions.....	37
5.2.1 Soil Parameters.....	38
5.2.1.1 Soil Parameters from USDA and Oklahoma Mesonet.....	38
5.2.1.2 SPSS and ARCGIS Software Models	39
5.2.2 New Soil Parameters	41

5.2.2.1 SPSS AND K-MEANS CLUSTER MODELS	42
6 VALIDATION OF A MOISTURE MIGRATION MODEL.....	45
6.1 Modeling of the Atmosphere-Soil Boundary	45
6.2 Validation Sites and Measured Data.....	46
6.3 SVFLUX Model	51
6.4 Results and Discussion	57
7 CONCLUSIONS.....	65
REFERENCES.....	67
APPENDICES.....	70
Appendix A	70
Appendix B Matric Suction versus Time Plots at Various Depths at STIL Mesonet Weather Station.....	76
Appendix C Maps Of Climatic Regions.....	86
Appendix D Maps Of Soil Regions Using Soil Parameters From USDA Web Soil Survey and The Oklahoma Mesonet	90
Appendix E Maps of Soil Regions Using New Soil Property Database.....	99

LIST OF FIGURES

Figure 2.1. Distribution of Mesonet Weather Stations Across Oklahoma (www.mesonet.org).....	3
Figure 2.2. A Schematic Drawing of an Oklahoma Mesonet Station.....	6
Figure 2.3. Campbell Scientific 229-L Sensor	7
Figure 2.4. Selected 77 Oklahoma Mesonet Weather Stations.....	11
Figure 2.5. Pavement Profile Used in the EICM Input File Verification.....	14
Figure 2.6. Typical Initial EICM Input Screen.	15
Figure 2.7. Typical EICM 3.4 Climate Data Input File.....	15
Figure 2.8. Typical Temperature-time Curves Predicted by EICM.	16
Figure 2.9. Typical Water Content-Time Curves Predicted by EICM.....	16
Figure 3.1. TMI Contour Map Based on Thornthwaite (1948) Equation.....	21
Figure 3.2. TMI Contour Map Based on Thornthwaite and Mather (1955) Equation.	22
Figure 3.3. TMI Contour Map Based on Witczak et al. (2006) Equation.....	23
Figure 4.1. The Oklahoma Water Resources Board Water Level Observation Wells. ..	26
Figure 4.2. The Color Contour Map of GWT Depths in Feet.	26
Figure 4.3. The Line Contour Map of GWT Depths in Feet.	27
Figure 4.4. Oklahoma Mesonet Sites with Installed Heat Dissipation Sensors (www.mesonet.org).....	28
Figure 4.5. Matric Suction Variation with Time at Different Depths in Stillwater during 2008.	29
Figure 5.1. U.S. Climatic Divisions	31
Figure 5.2. Oklahoma Climatic Divisions (http://climate.ok.gov).....	31
Figure 5.3. Eight Climatic Regions (Hierarchical Clustering).....	34
Figure 5.4. Eight Climatic Regions (K-means Clustering).	34
Figure 5.5. Optimum Number of Cluster of Climatic Regions (Hierarchical Cluster)	35
Figure 5.6. Optimum Number of Cluster of Climatic Regions (K-means Cluster).....	36
Figure 5.7. Six Soil Regions at 5 cm.	40
Figure 5.8. Ten Soil Regions at 5 cm.	41

Figure 5.9. Six Soil Regions (Weighted average).....	43
Figure 5.10. Six Soil Regions at 3 cm (K-means clustering).	44
Figure 6.1. Locations of the Validation Sites.	47
Figure 6.2. Rainfall at the Validation Sites in 2001.....	48
Figure 6.3. Air temperature at the validation sites in 2001.	49
Figure 6.4. Wind Speed at the Validation Sites in 2001.	49
Figure 6.5. Net Radiation Per Square Meter at Validation Sites in 2001.....	50
Figure 6.6. Relative Humidity at Validation Sites in 2001.....	50
Figure 6.7. Model Used in SVFLUX.	52
Figure 6.8. Measured and Predicted Pore Water Pressures at the BOWL Station – 8640 Hours.	59
Figure 6.9. Measured and Predicted Pore Water Pressures at BOWL Station – 3600 Hours.	60
Figure 6.10. Measured and Predicted Pore Water Pressures at the WAUR Station.	61
Figure 6.11. Measured and Predicted and Pore Water Pressures at the WIST Station.	62
Figure 6.12. Measured and Predicted Pore Water Pressures at the STIL Station.	63
Figure 6.13. Measured and Predicted Pore Water Pressures at the WAUR Station with Initial Conditions at 4320 Hours.	64
Figure B1. Matric Suction versus Time Plots For 1996.	76
Figure B2. Matric Suction versus Time Plots For 1997.	76
Figure B3. Matric Suction versus Time Plots For 1998.	77
Figure B4. Matric Suction versus Time Plots For 1999.	77
Figure B5. Matric Suction versus Time Plots For 2000.	78
Figure B6. Matric Suction versus Time Plots For 2001.	78
Figure B7. Matric Suction versus Time Plots For 2002.	79
Figure B8. Matric Suction versus Time Plots For 2003.	79
Figure B9. Matric Suction versus Time Plots For 2004.	80
Figure B10. Matric Suction versus Time Plots For 2005.	80
Figure B11. Matric Suction versus Time Plots For 2006.	81
Figure B12. Matric Suction versus Time Plots For 2007.	81
Figure B13. Matric Suction versus Time Plots For 2008.	82

Figure B14. Matric Suction versus Time Plots For 2009.	82
Figure B15. Matric Suction versus Time Plots For 2010.	83
Figure C1. Six Climatic Regions (Hierarchical Clustering)	86
Figure C2. Six Climatic Regions (K-Means Clustering)	86
Figure C3. Seven Climatic Regions (Hierarchical Clustering)	87
Figure C4. Seven Climatic Regions (K-Means Clustering).....	87
Figure C5. Nine Climatic Regions (Hierarchical Clustering).....	88
Figure C6. Nine Climatic Regions (K-Means Clustering).....	88
Figure C7. Ten Climatic Regions (Hierarchical Clustering).....	89
Figure C8. Ten Climatic Regions (K-Means Clustering).....	89
Figure D1. Seven Soil Regions at 5 cm.....	90
Figure D2. Eight Soil Regions at 5 cm.....	90
Figure D3. Nine Soil Regions at 5 cm.	91
Figure D4. Six Soil Regions at 25 cm.....	91
Figure D5. Seven Soil Regions at 25 cm.....	92
Figure D6. Eight Soil Regions at 25 cm.....	92
Figure D7. Nine Soil Regions at 25 cm.	93
Figure D8. Ten Soil Regions at 25 cm.....	93
Figure D9. Six Soil Regions at 60 cm.....	94
Figure D10. Seven Soil Regions at 60 cm.....	94
Figure D11. Eight Soil Regions at 60 cm.....	95
Figure D12. Nine Soil Regions at 60 cm.	95
Figure D13. Ten Soil Regions at 60 cm.....	96
Figure D14. Six Soil Regions at 75 cm.....	96
Figure D15. Seven Soil Regions at 75 cm.....	97
Figure D16. Eight Soil Regions at 75 cm.....	97
Figure D17. Nine Soil Regions at 75 cm.	98
Figure D18. Ten Soil Regions at 75 cm.....	98
Figure E1. Six Soil Regions at 20 cm.....	99
Figure E2. Seven Soil Regions at 3 cm.....	99
Figure E3. Seven Soil Regions at 20 cm.....	100

Figure E4. Eight Soil Regions at 3 cm.....	100
Figure E5. Eight Soil Regions at 20 cm.....	101
Figure E6. Nine Soil Regions at 3 cm.....	101
Figure E7. Nine Soil Regions at 20 cm.....	102
Figure E8. Ten Soil Regions at 3 cm.....	102
Figure E9. Ten Soil Regions at 20 cm.....	103
Figure E10. Seven Soil Regions (Weighted Average).....	103
Figure E11. Eight Soil Regions (Weighted Average).....	104
Figure E12. Nine Soil Regions (Weighted Average).	104
Figure E13. Ten Soil Regions (Weighted Average).....	105

LIST OF TABLES

Table 2.1. Climate and Soil Moisture Sensors Installed at Mesonet stations.	8
Table 2.2. A Truncated .hcd EICM Climatic Input File.....	12
Table 5.1. Soil Parameters for Soil Regions.....	39
Table 5.2. New Soil Dataset for Mesonet Stations	42
Table 6.1. Soil Properties at BOWL Station (from Scott et al. 2013).	53
Table 6.2. Soil Properties at WAUR Station (from Scott et al. 2013).....	54
Table 6.3. Soil Properties at WIST Station (from Scott et al. 2013).....	55
Table 6.4. Soil Properties at STIL Station (from Scott et al. 2013).	56
Table A1. Climatic Input Files.....	70
Table A2. Retired Station Information	75
Table B1. Time Period over which Matric Suction Measurements were Collected.....	84

ACKNOWLEDGEMENTS

This research was financially supported by the Oklahoma Department of Transportation (ODOT) under Grant No. SPR 2160 and the Oklahoma Transportation Center (OkTC) under Grant No. OTCREOS11.1-10. The authors would like to express their thanks to the Oklahoma Mesonet, Oklahoma Water Resources Board, and Dr. Tyson Ochsner for providing data for this study.

1 INTRODUCTION

Environmental conditions have a significant effect on the pavement performance. Of all the environmental factors, temperature and moisture have direct effect on the pavement layer and subgrade properties. As a result, improving the understanding of environmental interactions with pavement systems can predict the changes in pavement material properties over time. This study evaluates the appropriateness of the Enhanced Integrated Climatic Model (EICM) for the Oklahoma climatic conditions by creating historic climate files. It also leads to the estimation of site specific variation in environmental factors that are used in predicting seasonal variation and long-term properties of unbound materials.

The EICM is an integral component of the Mechanistic Empirical Pavement Design Guide (MEPDG) that involves analysis of water and heat flow through pavement layers in response to climatic, soil, and boundary conditions above and below the ground surface in the pavement structure. The performance of a pavement depends on many factors such as the structural integrity, the material properties, traffic loading, construction method, and climatic conditions (Puppala et al. 2009). The EICM plays a significant role in defining the material properties in the design guide.

The current study provides estimation of site specific variation in environmental factors that can be used in predicting seasonal and long-term variations in moduli of unbound materials. Using these site specific estimates, the EICM climatic input files were updated and extended over a large area covering Oklahoma climatic conditions. Validation of the EICM model is also critical for Oklahoma because of the state's unique topographical, geological, and geographical settings. Oklahoma has several microclimates and a large spatial variation in subgrade soils (Illston et al. 2004; McPherson 2007; Swenson et al. 2008). The EICM was originally developed by integrating several earlier models in order to predict the site-specific flow of water and heat through layered pavement materials (Zapata et al. 2007). However, due to the multiple phenomena considered by this model and the complexity of the boundary conditions, the results from the EICM model are not well understood. Accordingly, the

goal of this study was to review the different physical processes in the EICM to better understand the results obtained from this model. This study specifically focused on a detailed evaluation of the EICM for Oklahoma in order to reduce the sources of uncertainty in the MEPDG design. Validation of the EICM model is critical for Oklahoma because of the state's unique topographical, geological, and geographical settings.

This study mainly focused on improving our understanding of environmental interactions with pavement systems in Oklahoma to better predict the changes in pavement material properties over time. The main objective of this project was to develop realistic climatic input files and parameters for the EICM model in the pavement design. The climatic and soil parameters were also used to classify climatic and soil regions in Oklahoma. Furthermore, Thornthwaite Moisture Index (TMI) contour maps of Oklahoma were created using three different models.

The specific objectives of this study were:

1. To collect and check the quality of climatic and soil data pertaining to Oklahoma pavements;
2. To prepare input data files for the EICM program;
3. To prepare Thornthwaite Moisture Index (TMI) maps for Oklahoma;
4. To prepare ground water table depth maps and to prepare suction-time history plots for different depths for the soils at Mesonet sites;
5. To classify climatic and soil regions for Oklahoma; and
6. To validate EICM input files and moisture migration model.

2 CLIMATIC INPUT FILES FOR EICM

2.1 Oklahoma Mesonet

The climate data required for creating the EICM program input files and TMI contour maps were acquired from a large cluster of Mesonet weather stations dispersed across Oklahoma. The Oklahoma Mesonet program started in 1991 as a statewide mesoscale environmental monitoring network with at least one station in each of Oklahoma's 77 counties (Illston et al. 2008). The Oklahoma Mesonet is a network of 120 automated weather monitoring stations designed to measure the weather and soil moisture conditions. A number of counties have more than one weather station. Figure 2.1 shows the distribution of the stations in Oklahoma. There are six types of stations that focus on different functions, including OSU/OU Research, Academic/Foundation, Federal/City/State, Airport, Privately owned, and ARS Micronets. At each station, climate and soil moisture parameters including air and soil temperature, wind speed, precipitation, relative humidity, solar radiation, atmospheric pressure, and soil moisture are measured by a set of instruments every 5 to 15 minutes, 24 hours per day, and every day of the year. These observations are available free of charge to the researchers and public in Oklahoma.

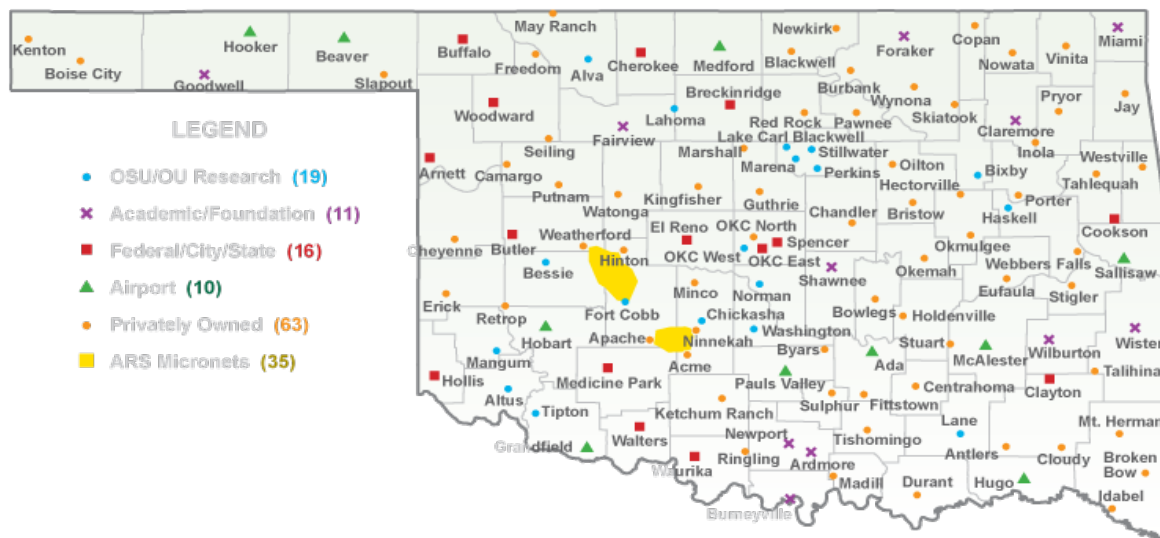


Figure 2.1. Distribution of Mesonet Weather Stations Across Oklahoma
(www.mesonet.org).

2.1.1 Oklahoma Mesonet Station Layout

Each Mesonet station send data every 5 to 15 minutes to an operation and collection center located at the Oklahoma Climatological Survey (OCS) for data quality assurance, data generation, storage, and dissemination. The mission of the OCS is to operate a world-class environmental monitoring network and to deliver high quality data to public and researchers (Illston et al. 2008). One of the main objectives in establishing the Mesonet network was to ensure that a station site be as representative of as large an area as possible. Therefore, site locations for Mesonet stations fulfill a number of general requirements for meteorological and environmental purposes (mesonet.org): (1) rural sites should be selected to avoid human influences present in urban and suburban areas, (2) the physical characteristics of a site, including soil properties, should be representative of as large an area as possible, (3) a site should be as far away as possible from irrigated areas, lakes and forests to minimize their influence, (4) the land surface should be as flat as possible, (5) there should be a minimum of obstructions that impede wind flow at the site, and (6) sites should have a uniform low-cover vegetation. Bare soil should not be visible except over the bare soil temperature measurements.

A Mesonet station occupies an area of about 100 m² and contains a datalogger, solar panel, radio transceiver, lightning rod, and climate and environmental sensors located on or surrounding a 10 m high tower, as shown in Figure 2.2. The sensors measure more than 20 environmental and soil variables, as listed in Table 2.1. As shown in Table 2.1, the primary sensors are installed in all Mesonet sites and the secondary sensors are in about 100 sites. The stations are equipped with the Campbell Scientific dataloggers CR10X-TD and CR23X-TD for enhanced data storage and download. The 10 m high tower records the 5-minute average wind speed. The 5-minute average air temperature is measured by a sensor at a height of 1.5 meters above the ground. The total amount of precipitation is measured just above the ground; it is measured in discrete tips of the bucket (approximately 0.01 inch per tip, or 0.254 millimeters). The average soil temperature during a 15-minute interval is measured at different depths below the ground; the surface under which the measurement is taken is not vegetated.

2.2 Climate and Soil Moisture/Suction Data

The primary focus of the Mesonet operations is to obtain research quality data in real time. The Oklahoma Mesonet follows a systematic, rigorous, and continuous monitoring protocol to verify the quality of all measurements (Illston et al. 2008). Among 120 Mesonet stations shown in Figure 2.1, one station in each 77 counties of Oklahoma was selected to represent the climate of that county and to collect the relevant climate and soil moisture parameters for this study.

The hourly climatic data for the 77 selected stations has been obtained from the Oklahoma Mesonet. Each climatic file consists of pressure, temperature, dew point, relative humidity, wind direction, wind speed, maximum wind speed, precipitation, and solar radiation. Since the EICM input files require only five parameters, only those five parameters from the Mesonet files are selected. Measured solar radiation from the Mesonet is selected to calculate the percent sunshine. The temperature is the average air temperature at a height of 1.5 meters above the ground. The wind speed is the average wind speed measured at a height of 10 meters above the ground. The total amount of precipitation is measured just above the ground, and it is measured in

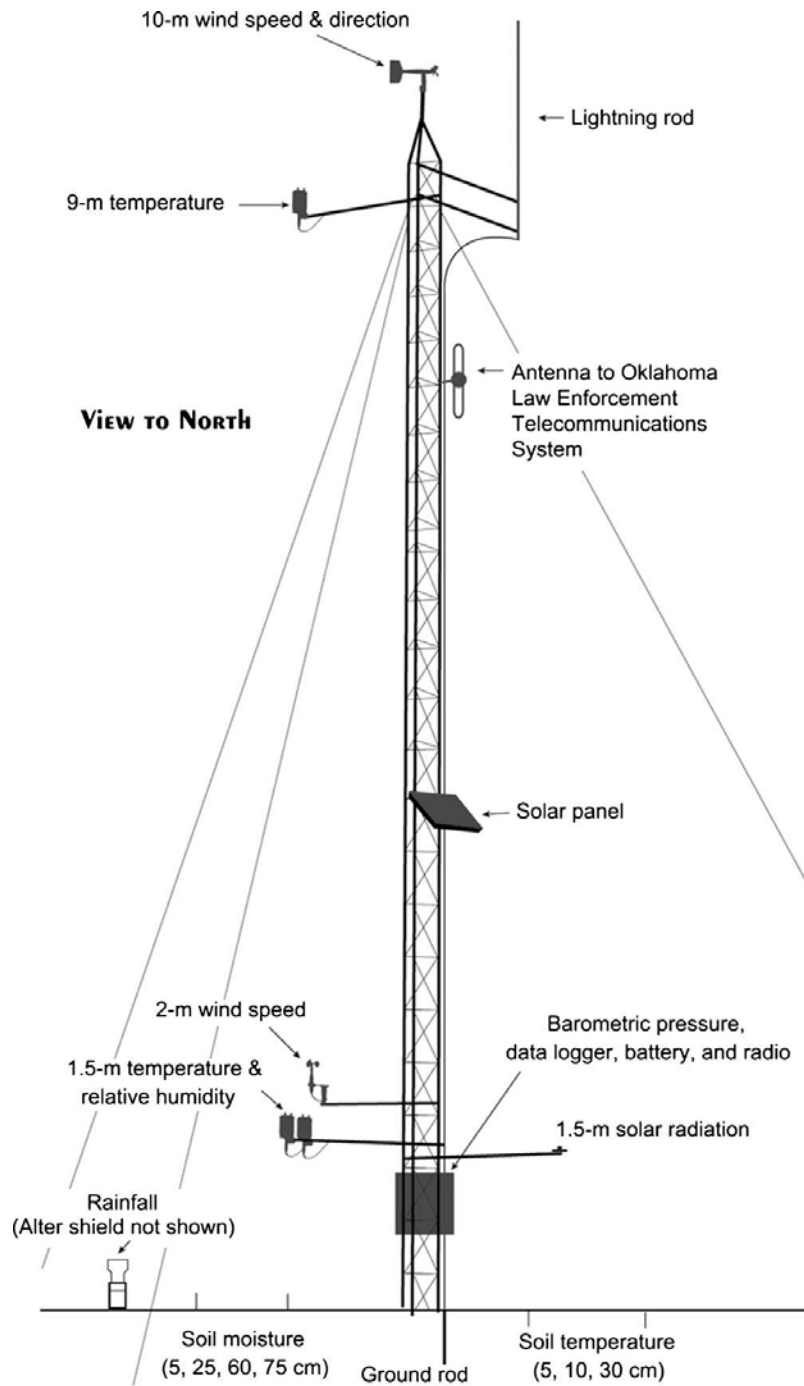


Figure 2.2. A Schematic Drawing of an Oklahoma Mesonet Station.

discrete tips of the bucket. Relative humidity changes when either the air moisture or the air temperature changes. The relative humidity is measured at a height of 1.5 meters above the ground. Because of the sensor's inaccuracy, all the measurements

above 100% are recorded as 100%. The solar radiation is measured by a sensor called Pyranometer. The pyranometer detect solar radiation which is reflected downward in the atmosphere (The Oklahoma Mesonet 2011).

Soil moisture is a fundamentally thermodynamic variable, and it is identical to the relative free energy of the soil moisture (Witczak et al. 2006). Recognizing the necessity of improving in-situ measurements of soil moisture, the Oklahoma Mesonet scientists designed the soil moisture measuring network to meet the needs from different disciplines. The soil moisture sensor installed at Oklahoma Mesonet sites is called the Campbell Scientific 229-L sensor (Figure 2.3) (Illston et al. 2008). This sensor records the temperature change after a heat pulse has been introduced. Soil water content and soil matric potential can be calculated using the measured temperature difference. This sensor was chosen because of its small size, easy incorporation into the whole network, and absence of harmful radiation (Illston et al. 2004).



Figure 2.3. Campbell Scientific 229-L Sensor

Before the installation, the sensors are calibrated in laboratory to remove the sensor-to-sensor variability. Next, the sensors are installed at multiple independent depths (5 cm, 25 cm, 60 cm, and 75 cm) and measure a temperature difference in the soil. The data are recorded every 30 minutes at each site, and the operation center, located at the Oklahoma Climatological Survey (OCS), remotely collects the data every 30 minutes as

well (McPherson et al. 2007, Illston et al. 2008) The soil matric suction can be derived from the calibrated change in temperature of the soil over time after a heat pulse is introduced.

Table 2.1. Climate and Soil Moisture Sensors Installed at Mesonet stations.

Climate/Soil Moisture Variable	Sensor Height	Primary Sensor	No. of Statio
Relative humidity	1.5 m	Vaisala HMP45C	116
Air temperature	1.5 m	Thermometrics UIM DC95	116
Rainfall	0.6 m	MetOne 380C	116
Pressure	0.75 m	Vaisala PTB202/PTB220	116
Wind speed and direction	10 m	R. M. Young 5103	116
Soil temperature under bare soil and	-10 cm	BetaTHERM 10K3D410	116
Air temperature	9.0 m	Thermometrics UIM DC95	100
Wind speed	2.0 m	R. M. Young 3101	116
Soil temperature under bare soil	-5 cm	BetaTHERM 10K3D410	111
Soil temperature under native sod	-5 cm	BetaTHERM 10K3D410	107
Soil temperature under native sod	-30 cm	BetaTHERM 10K3D410	106
Soil moisture/suction	-5 cm	Campbell Scientific 229-L	103
Soil moisture/suction	-25 cm	Campbell Scientific 229-L	101
Soil moisture/suction	-60 cm	Campbell Scientific 229-L	76
Soil moisture/suction	-75 cm	Campbell Scientific 229-L	37
Wind speed	9.0 m	R. M. Young 3101	2
Wind speed	3.5 m	R. M. Young 3101	2
Net radiation	1.5 m	Kipp & Zonen NR LITE	74
Soil heat flux	-5 cm	REBS HFT 3.1	2

2.2.1 Percent Sunshine from Solar Radiation

Based on the Guide for Mechanistic-Empirical Design of New and Rehabilitated Pavement Structures (NCHRP 2004), the percent sunshine (0% for cloudy and 100% for clear sky) is used to define the cloud cover in the sky. Therefore, it can be considered as the opposite of the percent cloud cover. There are different methods to calculate the percent sunshine. For example, Heitzman et al. (2011) assigned different percent sunshine values based on different categories of the sky coverage. On the other hand, a more universal approach has been outlined in the Allen et al. (2005) study as a part of an ASCE task force for the standardization of the evapotranspiration equation.

$$f_{cd} = 1.35R_s/R_{s0} - 0.35 \quad (2.1)$$

where, the ratio R_s/R_{s0} is the relative solar radiation (limited to $0.30 < R_s/R_{s0} < 1.00$), R_s is the measured or predicted solar radiation, R_{s0} is the predicted clear-sky radiation, and f_{cd} is the cloudiness function (limited to $0.05 < f_{cd} < 1.00$, which is dimensionless). The National Cooperative Highway Research Program (NCHRP Report 2004) also presents a similar equation for calculating the percent sunshine.

$$Q_s = a_s R^* [A + B(S_c/100)] \quad (2.2)$$

where, Q_s is the net short wave radiation, a_s is the surface short wave absorptivity, A and B are the constants that account for diffuse scattering and adsorption, respectively, S_c is the percent sunshine, and R^* is the extraterrestrial radiation. Both Equations 2.1 and 2.2 were evaluated in detail and the results were compared. The analysis has shown that there is a small difference in the final results of percent sunshine between these two methods.

This study adopts the NCHRP Equation 2.2 (as recommended by the MEPDG) for converting the measured solar radiation into an equivalent percent sunshine. Based on the recommendations provided in the NCHRP report, all the computed percent sunshine results above 100% are recorded as 100% and all the values below 0% are recorded as 0%. Based on the climate data obtained from Oklahoma Mesonet, the measured solar

radiation is zero during the night and reaches a maximum value around noon. After converting the measured solar radiation values into the equivalent percent sunshines, the computed results indicate that the values of percent sunshine are also zero during the night and reach the maximum around noon, and gradually decrease in the afternoon.

2.3 Eicm Input Files

Environmental factors play a key role in pavement design. Both external factors such as temperature, precipitation, wind speed, relative humidity, and percent sunshine, and internal factors such as drainability, permeability, and moisture stress state have significant effects on performance of pavements (NCHRP Report 2004). The Enhanced Integrated Climatic Model (EICM) is a major component of the new Mechanistic Empirical Pavement Design Guide (MEPDG) that simulates changes in the climatic conditions as well as pavement characteristics. The EICM program requires five climate-related parameters on an hourly basis: air temperature (F), wind speed (mi/h), percent sunshine (%), precipitation (in), and relative humidity (%). Since the current MEPDG climate files for Oklahoma only have 15 weather station data, the new historic climate files developed in this research study will enrich the database for Oklahoma.

Seventy seven weather stations (one in each county) have been selected in Oklahoma to represent the state's climate condition. Several counties have more than one weather station. In this case, the station located near the center of the county is selected. The distribution of the selected 77 stations is well dispersed, which would benefit the spatial interpolation of the climatic variables. Figure 2.4 shows the distribution of the selected stations with their station ID numbers. The hourly climate data required for the creation of the EICM input files have been acquired from the Oklahoma Mesonet weather stations.

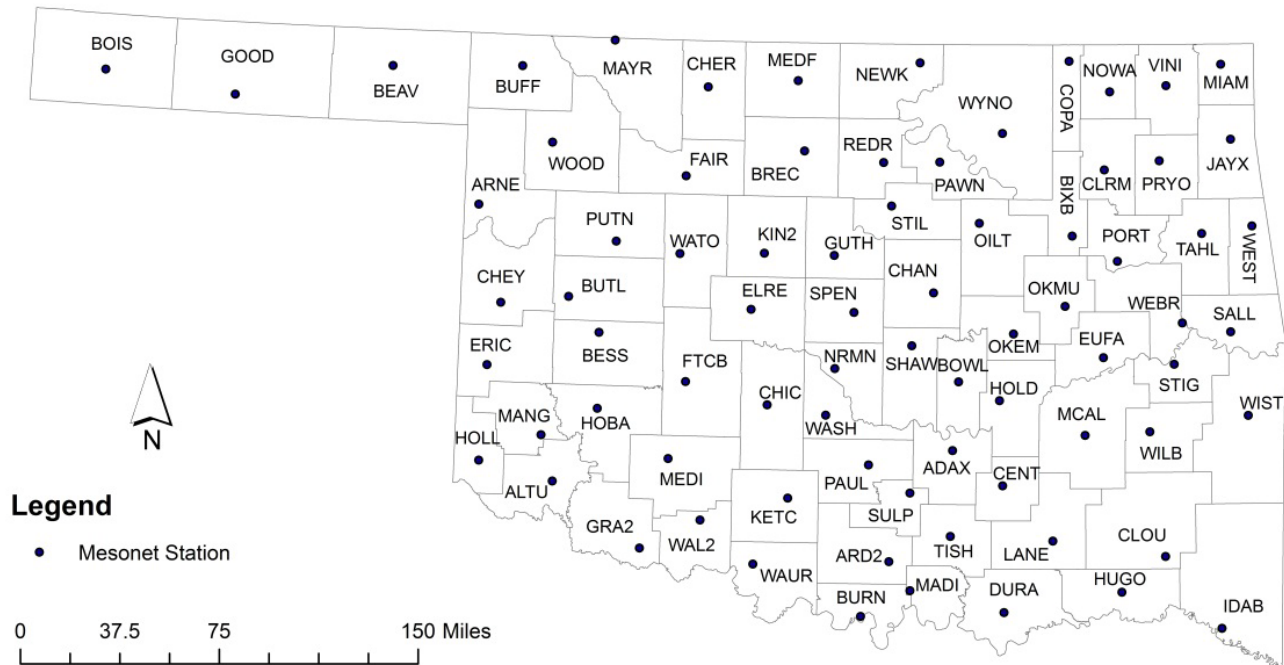


Figure 2.4. Selected 77 Oklahoma Mesonet Weather Stations.

2.3.1 Fortran Subroutine for Creating EICM Files

Large amount of climate data (18 years of hourly precipitation, temperature, relative humidity, wind speed, and solar radiation) were obtained from Oklahoma Mesonet for processing, evaluation, and creation of the relevant parameters for the EICM program. In order to handle the large cluster of climate data, FORTRAN subroutines were developed. One subroutine was developed for computing the percent sunshine from measured solar radiation and another subroutine was developed for the creation of the EICM program input files. Table 2.2 shows a truncated climatic input file. These files are very long and it is not convenient to list the whole file in the report. All the 77 climatic input files are provided in a digital media (CD-ROM) as part of this study. Information about each of the 77 climatic input files is given in Appendix A.

Table 2.2. A Truncated .hcd EICM Climatic Input File.

Year-Month- Day-Hour	Temperature (F)	Wind Speed (mi/h)	Percent Sunshine (%)	Precipitation (in)	Relative Humidity (%)
1994010100	48	12	0	0	56
1994010101	48	9	0	0	62
1994010102	48	11	0	0	65
1994010103	46	6	0	0	72
1994010104	42	3	0	0	80
1994010105	38	4	0	0	87
1994010106	37	7	0	0	89
1994010107	38	8	0	0	84
1994010108	42	8	100	0	73
1994010109	48	10	100	0	56
1994010110	53	12	100	0	46
1994010111	56	14	100	0	43
1994010112	58	12	100	0	40
1994010113	60	11	93	0	36
1994010114	61	12	82	0	35
1994010115	61	11	64	0	36
1994010116	58	11	31	0	40
1994010117	52	7	0	0	46
...

2.4 Validation of EICM Input Files

Verification of the created EICM input files was carried out by running the stand-alone version of the EICM program for a typical flexible pavement section. The latest version of the stand-alone EICM software (Version 3.4) was obtained through personal communication with Mr. Chris Wagner of the Federal Highway Administration. The

EICM software requires at least two layers of paving materials in the pavement profile and the top layer must either be asphalt or Portland cement concrete. The Oklahoma Mesonet sites, however, have a surface soil layer and therefore the EICM software could not be used to predict moisture profiles at the Mesonet sites. Mr. Gregg Larson from Applied Research Associates, Inc. (ARA) also confirmed this limitation of the EICM software. Mr. Larson further indicated,

1. ARA is in the process of developing a software tool for agriculture applications that can be used for sites with soil surface layers. This software will, however, not be part of the MEPDG software.
2. The critical issue related to using EICM 3.4 for soil surface sites is the wetting of the surface layer for rainfall events. There is a work around of the aforementioned issue but it is unpublished work. The work around involves using drainage models other than those used in MEPDG. The programmers at ARA can bypass the climate input data by entering soil suction and temperature of the surface layer as input and use EICM 3.4 for soil surface sites.

For the verification of the EICM input files, a typical pavement section with two layers as shown in Figure 2.5 was considered. At least one year of analysis was conducted for each of the 77 input files. For BOWL, ADAX, and ALTU input files, the analysis was conducted for five years. A typical EICM initial input screen is shown in Figure 2.6. The EICM 3.4 requires depth to water table at a site as an input. This information is not part of the EICM input files created in this project for use in DARWin-ME and therefore depth to water table was added to the input files before EICM 3.4 analyses were conducted. A typical EICM 3.4 climate input data file is shown in Figure 2.7. All the analyses ran to completion without any errors. Selected output files were examined to ensure predicted values are reasonable. Typical temperature-time curves predicted by EICM 3.4 are shown in Figure 2.8 and water content-time curves are given in Figure 2.9.

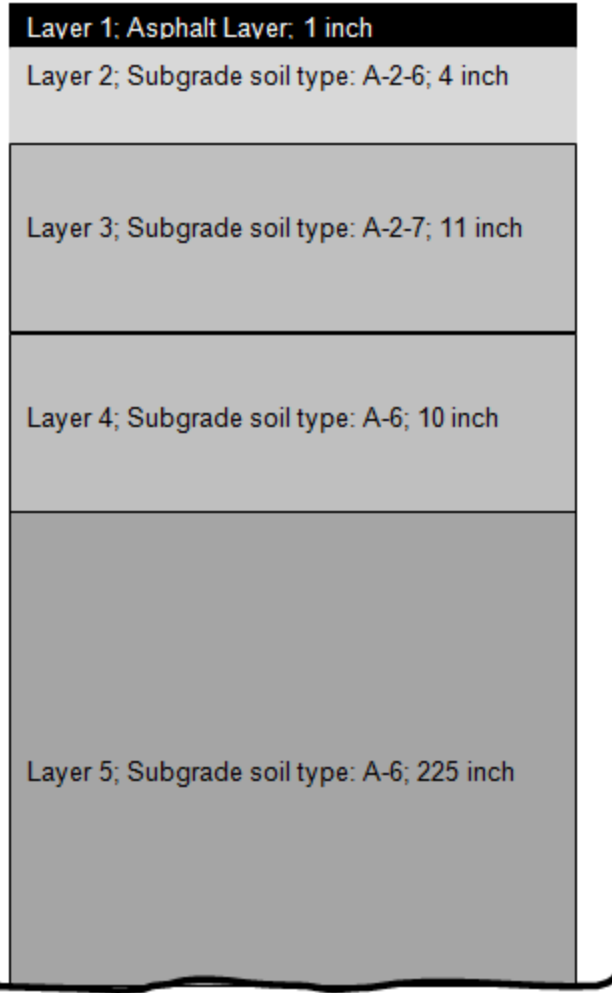


Figure 2.5. Pavement Profile Used in the EICM Input File Verification.

Integrated Model Initialization

Model Description: ARNE - as is rainfall

Year to be modeled: 2001

First month in analysis period: January

First day of month in analysis period: 1

Length of analysis period (days): 365

Time increment for output (hours): 1

Time increment for calculation (hours): 0.1

Enter latitude (degrees.minutes): 35.1716

Longitude (degree.minutes): -96.6312

Elevation(ft)(optional): 600

Example(30° 15' = 30.15)

Buttons: Previous, Next, OK, Cancel

Figure 2.6. Typical Initial EICM Input Screen.

Climatic Data Input

Use Hourly Climatic Data

Convert Daily/Hourly Interpolate Missing Climatic Database Import Export

Date/Time	Temperature (°F)	Windspeed (mph)	Sunshine (%)	Precipitation (in)	Humidity (%)	Watertable (ft)
01/01/2001 00:00	12	5	0	0	92	75
01/01/2001 01:00	13	2	0	0	92	75
01/01/2001 02:00	14	4	0	0	92	75
01/01/2001 03:00	13	4	0	0	93	75
01/01/2001 04:00	14	4	0	0	93	75
01/01/2001 05:00	16	5	0	0	93	75
01/01/2001 06:00	18	5	0	0	94	75
01/01/2001 07:00	20	4	0	0	95	75
01/01/2001 08:00	22	5	100	0	96	75
01/01/2001 09:00	24	7	48	0	96	75
01/01/2001 10:00	24	8	44	0	95	75
01/01/2001 11:00	24	8	39	0	94	75
01/01/2001 12:00	25	7	28	0	93	75
01/01/2001 13:00	26	6	32	0	91	75
01/01/2001 14:00	26	6	20	0	90	75
01/01/2001 15:00	26	6	0	0	91	75
01/01/2001 16:00	25	6	0	0	92	75
01/01/2001 17:00	25	7	0	0	93	75
01/01/2001 18:00	24	7	0	0	94	75
01/01/2001 19:00	23	7	0	0	95	75
01/01/2001 20:00	22	5	0	0	95	75
01/01/2001 21:00	21	5	0	0	95	75
01/01/2001 22:00	21	5	0	0	95	75
01/01/2001 23:00	21	4	0	0	96	75
01/02/2001 00:00	21	3	0	0	96	75

Buttons: Previous, Next, OK, Cancel

Figure 2.7. Typical EICM 3.4 Climate Data Input File.

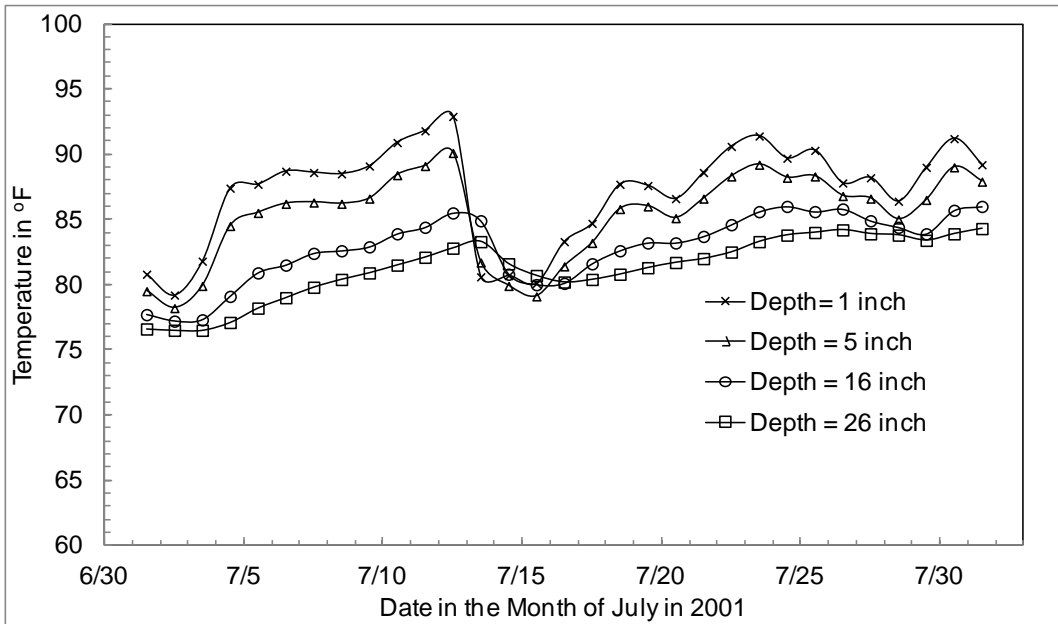


Figure 2.8. Typical Temperature-time Curves Predicted by EICM.

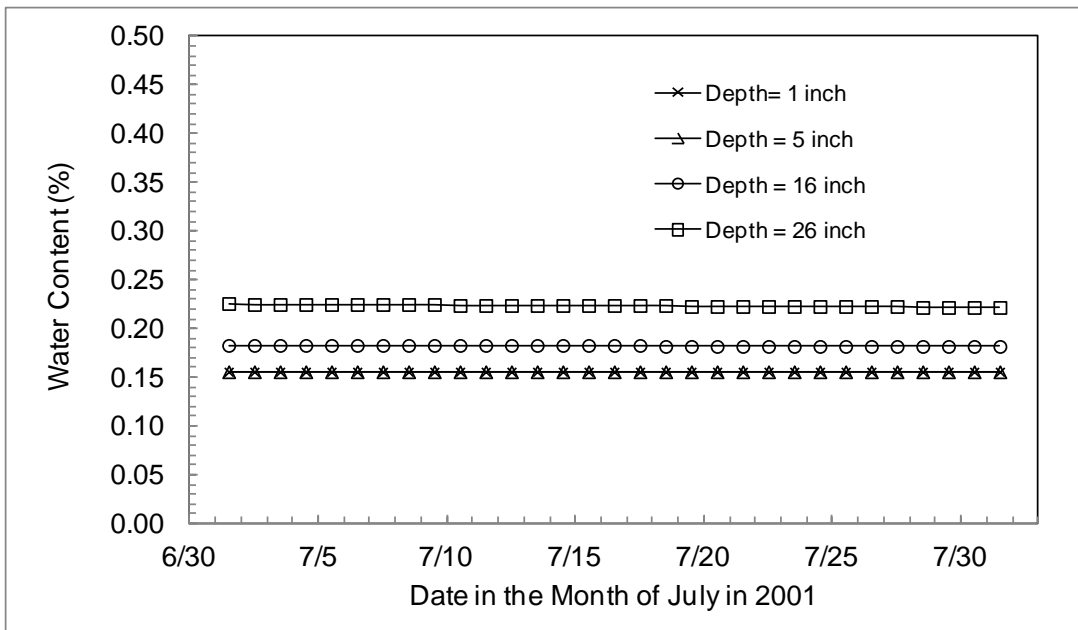


Figure 2.9. Typical Water Content-Time Curves Predicted by EICM.

3 THORNTHWAITE MOISTURE INDEX

This chapter evaluates historical climate data acquired from Oklahoma Mesonet weather stations for computing the Thornthwaite Moisture Index (TMI) parameter and for creating maps for Oklahoma. TMI is a climatic parameter widely used in geotechnical and pavement engineering to evaluate the changes in moisture conditions in near surface soils in the unsaturated zone. It has become an important parameter for predicting the equilibrium soil suction beneath the moisture active zone, as well as the depth to constant suction.

The TMI, originally developed by Thornthwaite in 1948, is determined by annual water surplus, water deficiency, and water need. The water surplus and deficiency are determined using the maximum water storage of the soil by performing a water balance computation. The process also requires an estimate of the initial water storage. The whole process is computationally intensive and requires soil and moisture storage information that may not be readily available in many places. In 1955, the original TMI equation was revised by Thornthwaite and Mather (1955). The modified TMI is only related to the precipitation and potential evapotranspiration at monthly intervals in evaluating the annual soil moisture balance. Recently, the TMI has been modified further by Witczak et al. (2006) as part of the Enhanced Integrated Climatic Model (EICM) in the Mechanistic Empirical Pavement Design Guide (MEPDG), and correlations have been established between the TMI and equilibrium suction at depth in the pavement profile.

The current study evaluates the three different TMI computation methods (Thornthwaite 1948; Thornthwaite and Mather 1955; and Witczak et al. 2006) and produces TMI-based contour maps for Oklahoma using the climate data from Mesonet weather stations across Oklahoma. The results are analyzed and compared within the three methods.

3.1 Water Storage and Potential Evapotranspiration

The water stored in the soil is a fundamental property and depends on the soil type and climatic conditions. The water storage is an important parameter in the water balance computations for determining the Thornthwaite Moisture Index (TMI) parameter (Thornthwaite 1948). The water storage can simply be defined as the water holding capacity of the soil profile in cm of water (McKeen and Johnson 1990). The unit of water storage is usually in centimeters of water per centimeter of soil for each soil layer.

Evaporation represents a transfer of mass and energy from the soil to the atmosphere. Evaporation also means the downward flow of energy from the sun can be balanced. Thornthwaite (1948) defined one further term, the “potential evapotranspiration”, as the water loss from the vegetation cover that never suffers from a lack of water. Potential evapotranspiration is different from actual evapotranspiration. Actual evapotranspiration depends on (1) climatic factors; (2) soil types; (3) soil moisture contents; (4) vegetation types; and (5) land uses; while potential evapotranspiration depends almost completely on the energy from the sun (Mather 1974). Potential evapotranspiration is an important component of the TMI parameter.

3.2 Thornthwaite (1948) Equation

Thornthwaite (1948) adopted a relatively simple model for the calculation of the adjusted potential evapotranspiration as compared to some of the sophisticated (yet complex in terms of the parameters involved) models available in the literature. Due to its simplicity, the TMI equations given by Thornthwaite and Mather (1955) and Witczak et al. (2006) also employ the same model for the calculation of the potential evapotranspiration. For the computation of the potential evapotranspiration, the heat index for each month is determined using the mean monthly temperature as follows:

$$h_i = (0.2t_i)^{1.514} \quad (3.1)$$

where, h_i is the monthly heat index and t_i is the mean monthly temperature. The annual heat index is simply calculated by summing the monthly heat index values as:

$$H_y = \sum_{i=1}^{12} h_i \quad (3.2)$$

where, H_y is the yearly heat index. The unadjusted potential evapotranspiration is then determined for each month as follows:

$$e_i = 1.6 (10^{t_i}/H_y)^a \quad (3.3)$$

where, e_i is the unadjusted potential evapotranspiration for a month with 30 days and a is a coefficient given by:

$$a = 6.75 \cdot 10^{-7} H_y^3 - 7.17 \cdot 10^{-5} H_y^2 + 0.19721 H_y + 0.49239 \quad (3.4)$$

The unadjusted potential evapotranspiration is then corrected for the location (latitude) and the number of days in the month as:

$$PE_i = e_i (d_i n_i / 30) \quad (3.5)$$

where, PE_i is the adjusted potential evapotranspiration for the month i , d_i is the day length correction factor (provided in McKeen and Johnson 1990), and n_i is the number of days in the month i . The yearly total potential evapotranspiration is then obtained by summing Equation 3.5 over 12 months of the year.

Thornthwaite (1948) defined a moisture index (known as the Thornthwaite Moisture Index or TMI) as a relative measure indicating the wetness or dryness of a particular region. The TMI has been a popular and attractive parameter in the geotechnical and pavement engineering communities due to the fact that the data required for its determination are usually readily available from local weather stations and it is based on a simple climatic model as compared to some of the rigorous models in the literature. Thornthwaite (1948) equation is given as:

$$\text{TMI} = (100R - 60D)/\text{PE} \quad (3.6)$$

where, D is the moisture deficit, R is the runoff, and PE is the net potential evapotranspiration. TMI computations are based on a period of one year with monthly values of precipitation, adjusted potential evapotranspiration, storage, runoff, and deficit by conducting a moisture balance approach. The standards for TMI climate classification are:

$20 \leq \text{TMI} \leq 100$	Humid
$0 \leq \text{TMI} \leq 20$	Moist Sub-Humid
$-20 \leq \text{TMI} \leq 0$	Dry Sub-Humid
$-40 \leq \text{TMI} \leq -20$	Semi-Arid
$\text{TMI} \leq -40$	Arid

Oklahoma has a variety of climates ranging from humid to semi-arid. The 0 TMI value line go across central Oklahoma, as a result, the climate in central Oklahoma ranges from moist sub-humid to dry sub-humid.

The calculation process requires the total monthly precipitation, average monthly temperature, initial and maximum water storage values, the day length correction factor, and the number of days for each month. The precipitation and temperature values can be obtained from the local weather stations. The maximum water storage is a function of the soil type and the initial water storage depends on the climate and site conditions. The day length correction factor is a constant for a given month and location (latitude). Figure 3.1 shows the TMI contour map developed using the original Thornthwaite (1948) method.

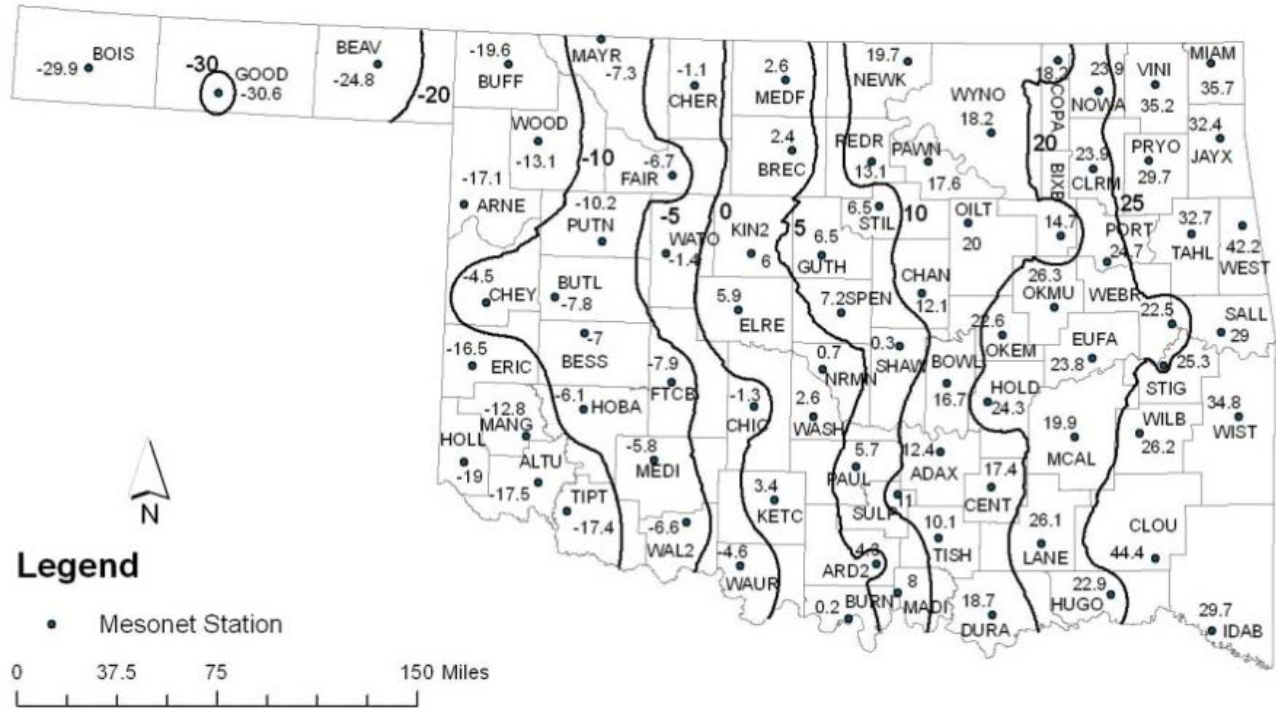


Figure 3.1. TMI Contour Map Based on Thornthwaite (1948) Equation.

3.3 Thornthwaite and Mather (1955) Equation

As mentioned previously, the original TMI method given by Thornthwaite (1948) is computationally intensive and requires soil and moisture storage information that may not be readily available at many locations in Oklahoma or in the U.S. Thornthwaite and Mather (1955) simplified the original approach by eliminating the water balance computations. The modified method requires only precipitation and potential evapotranspiration at monthly intervals in evaluating the annual moisture index. The simplified equation is given as:

$$\text{TMI} = 100 (P/PE - 1) \tag{3.7}$$

where, P is the annual precipitation and PE is the potential evapotranspiration as explained above. Figure 3.2 depicts the TMI contour map developed using the modified Thornthwaite and Mather (1955) method.

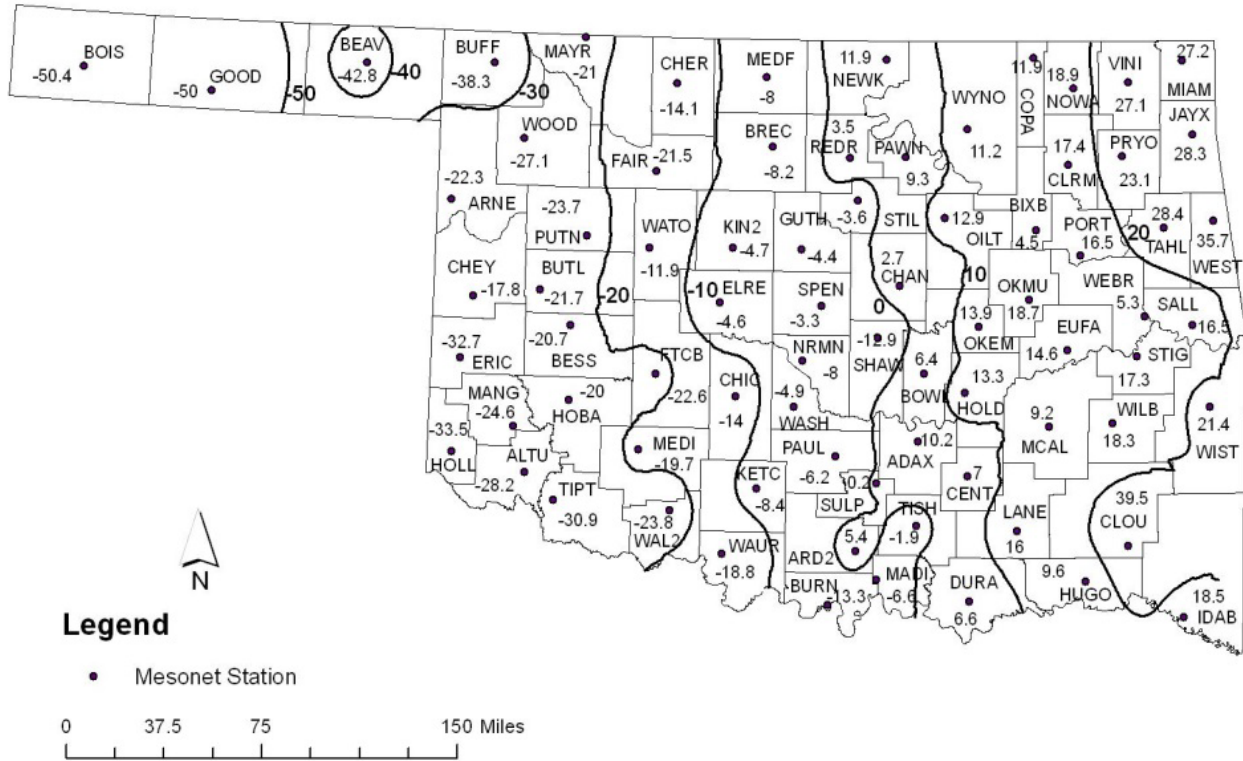


Figure 3.2. TMI Contour Map Based on Thornthwaite and Mather (1955) Equation.

3.4 Witczak et al. (2006) Equation

As part of the NCHRP 1-40D research project for the development of the MEPDG, Witczak et al. (2006) modified Equation 3.7 in the form given below:

$$TMI = 75 (P/PE - 1) + 10 \tag{3.8}$$

Figure 3.3 shows the TMI contour map developed using the Witczak et al. (2006) method. TMI contour maps were produced based on the three models (Equations 3.6, 3.7, and 3.8) given above using the climatic data obtained from 77 Oklahoma Mesonet weather stations representing 77 counties in the state. Contour maps consist of lines connecting points of equal values of TMI for a certain region. To create the contour maps of TMI, the method of Inverse Distance Weighting (IDW) was used in ArcGIS software. IDW is a type of interpolation scheme with a known scattered set of points.

4 GROUNDWATER TABLE AND SOIL SUCTION PROFILES

The Ground Water Table (GWT) depth is an important input parameter for the EICM program. The GWT controls the moisture boundary condition at the bottom boundary in a pavement. The depth of GWT has a significant effect on the performance of pavements. A change in GWT depth influences the moisture content of the unbound and subgrade soils, and thus their shear strength and modulus. The GWT controls the equilibrium suction and the depth to the constant suction when it is shallow.

The Oklahoma Mesonet monitors the soil moisture conditions with depth at more than 100 weather stations across Oklahoma to understand the impacts of various soil moisture conditions on climate and soil moisture storage. Among the selected 77 weather stations (one station in one county), 71 stations had thermal conductivity moisture sensors at different depths below the ground surface. The recordings from these sensors were used to compute matric suction values at Mesonet sites.

4.1 Groundwater Table Depth

The Oklahoma Water Resources Board (OWRB) conducts a statewide ground water level measurement program utilizing approximately 825 observation wells (of which about 530 are active wells and about 300 are historical wells). Figure 4.1 shows the mass measurement wells in Oklahoma. The OWRB measures the static (equilibrium) water levels in these wells during the first quarter of each year. The OWRB obtains the water level measurements using graduated steel tapes that are marked in hundredths, tenths, and one foot increments (www.owrb.ok.gov). The tapes are lowered into the well bore through access ports constructed in the base of the well pump. The OWRB collects and compiles the ground water table (GWT) depths, and makes the data accessible on its website.

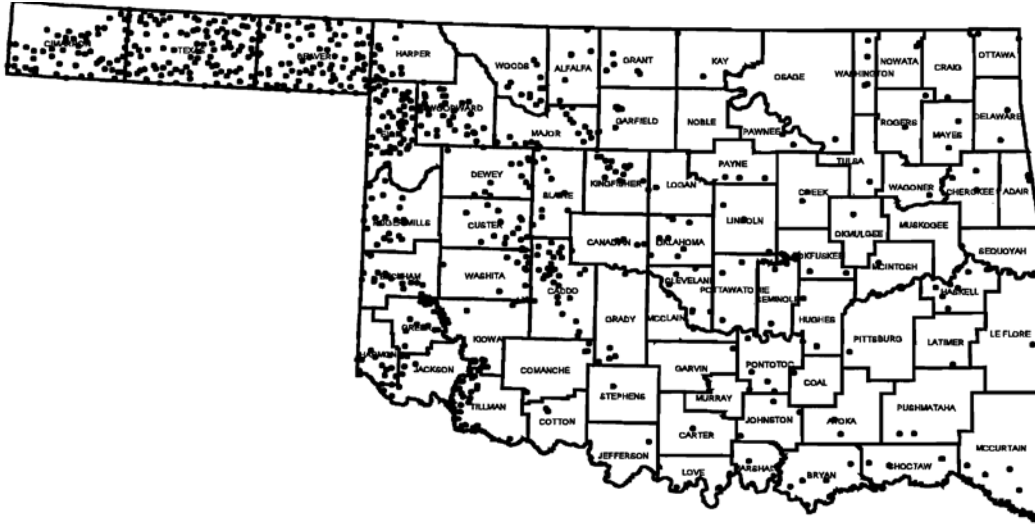


Figure 4.1. The Oklahoma Water Resources Board Water Level Observation Wells.

Approximately, 5,600 water level measurement records were obtained from OWRB. The data was processed and an average of the last 10 years water level measurements for each well was obtained. These average values were used in ArcGIS software for creating maps of the GWT depths in Oklahoma. Figures 4.2 and 4.3 depict the color and line contour maps of the GWT depths in Oklahoma, respectively. In the map, blue color indicates shallow groundwater depth and red color indicates deep depth.

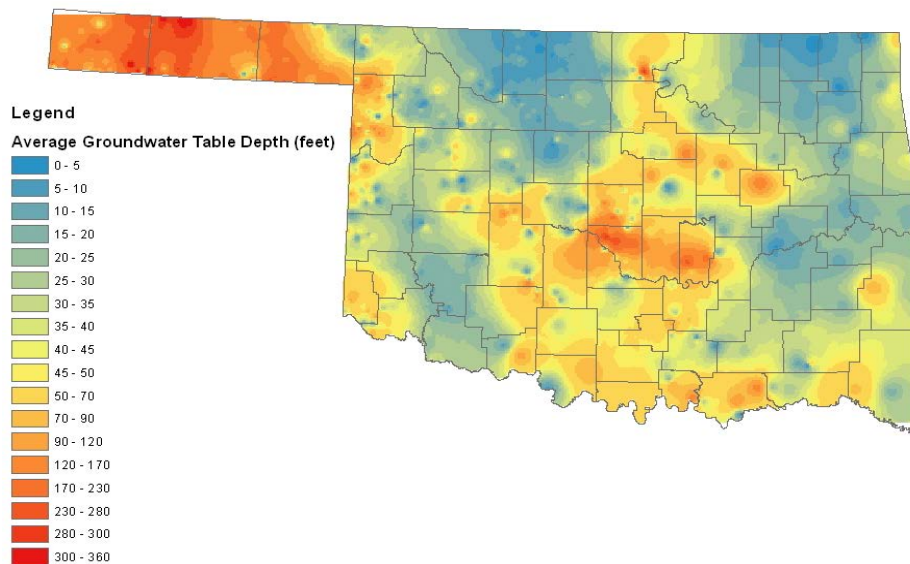


Figure 4.2. The Color Contour Map of GWT Depths in Feet.

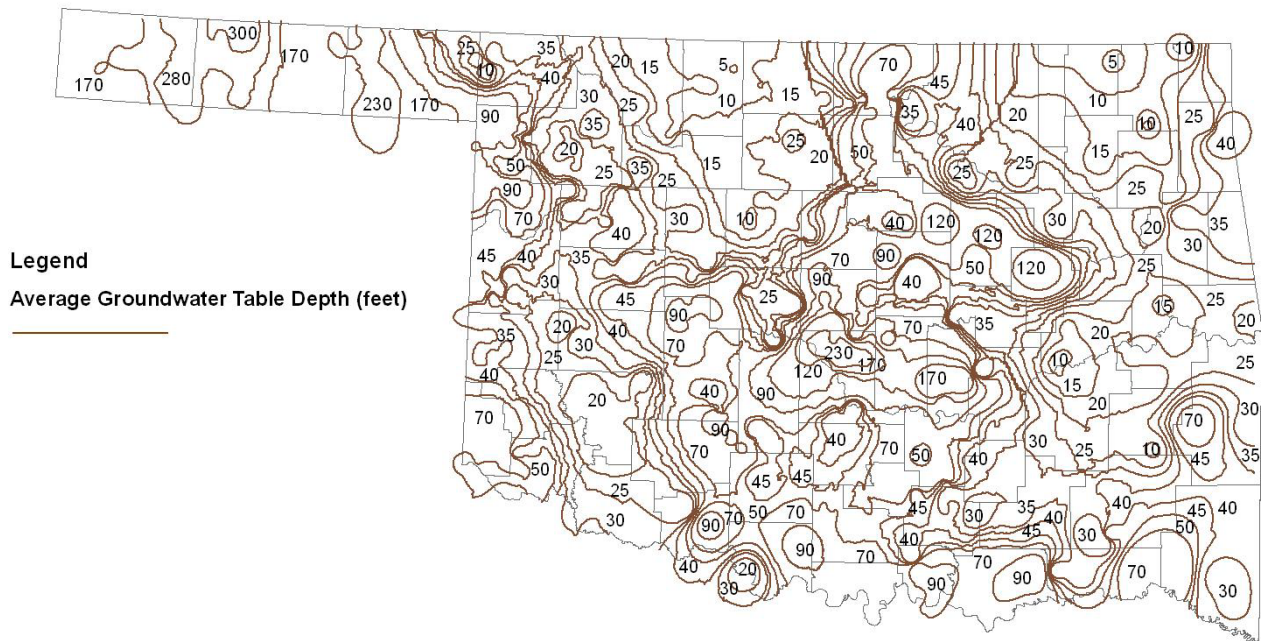


Figure 4.3. The Line Contour Map of GWT Depths in Feet.

4.2 Soil Matric Suction Profile

The Oklahoma Mesonet installed CSI 229-L heat dissipation sensors at a depth of 5 cm at 103 sites, at a depth of 25 cm at 101 sites, at a depth of 60 cm at 76 sites, and at a depth of 75 cm at 53 sites. The weather stations with installed sensors are shown in Figure 4.4. In the figure, red stations are installed with soil moisture measurements. The sensors are used to infer matric suction of the soil indirectly using the heat dissipation capacity of the soil by measuring a temperature difference between two reference points. The temperature difference is related to matric suction of the soil using the following calibration equation (Illston et al. 2008):

$$h_m = -0.717e^{1.788\Delta T_{ref}} \quad (4.1)$$

where, h_m is the soil matric suction in kPa and ΔT_{ref} is the reference temperature difference in °C. The Oklahoma Mesonet collects the reference temperature differences at 5 cm, 25 cm, 60 cm, and 75 cm depths at every 15 minutes.

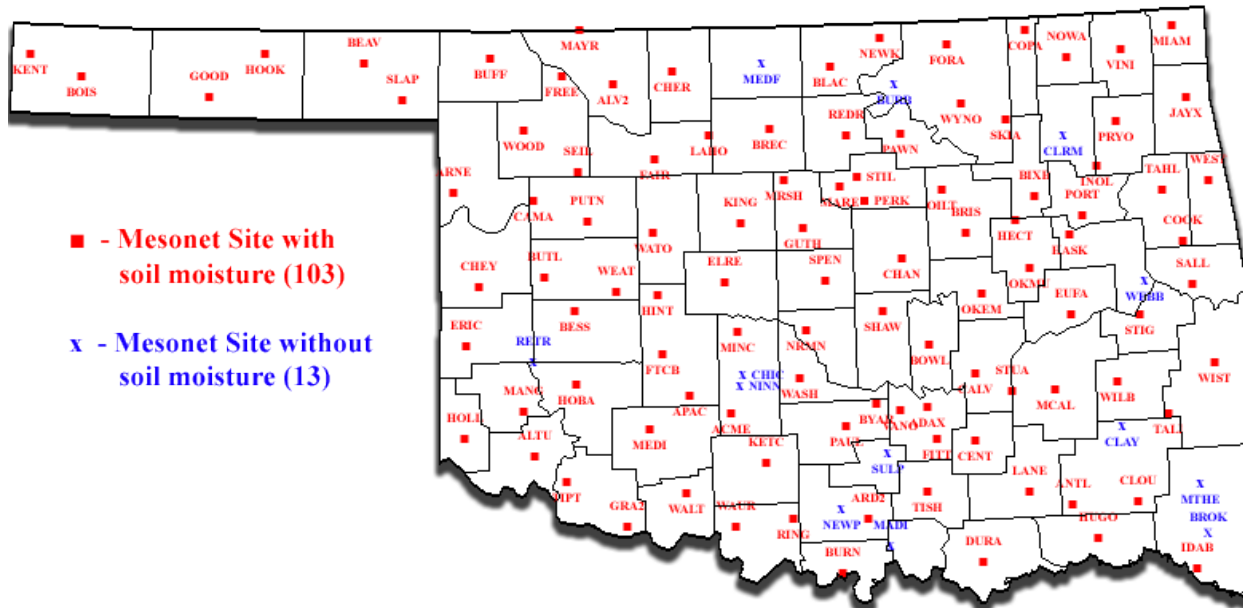


Figure 4.4. Oklahoma Mesonet Sites with Installed Heat Dissipation Sensors (www.mesonet.org).

The reference temperature difference values were obtained from Mesonet for 71 counties in Oklahoma. Equation 4.1 was used to calculate matric suction values with time at various depths in the soil profile. Figure 4.5 shows a typical suction versus time plot for 2008 in Stillwater, Oklahoma. Appendix B contains the suction-time history plots for Stillwater, Oklahoma from 1996 to 2010. The suction-time history plots of all the 71 stations are provided in the digital media (CD-ROM) as part of this study.

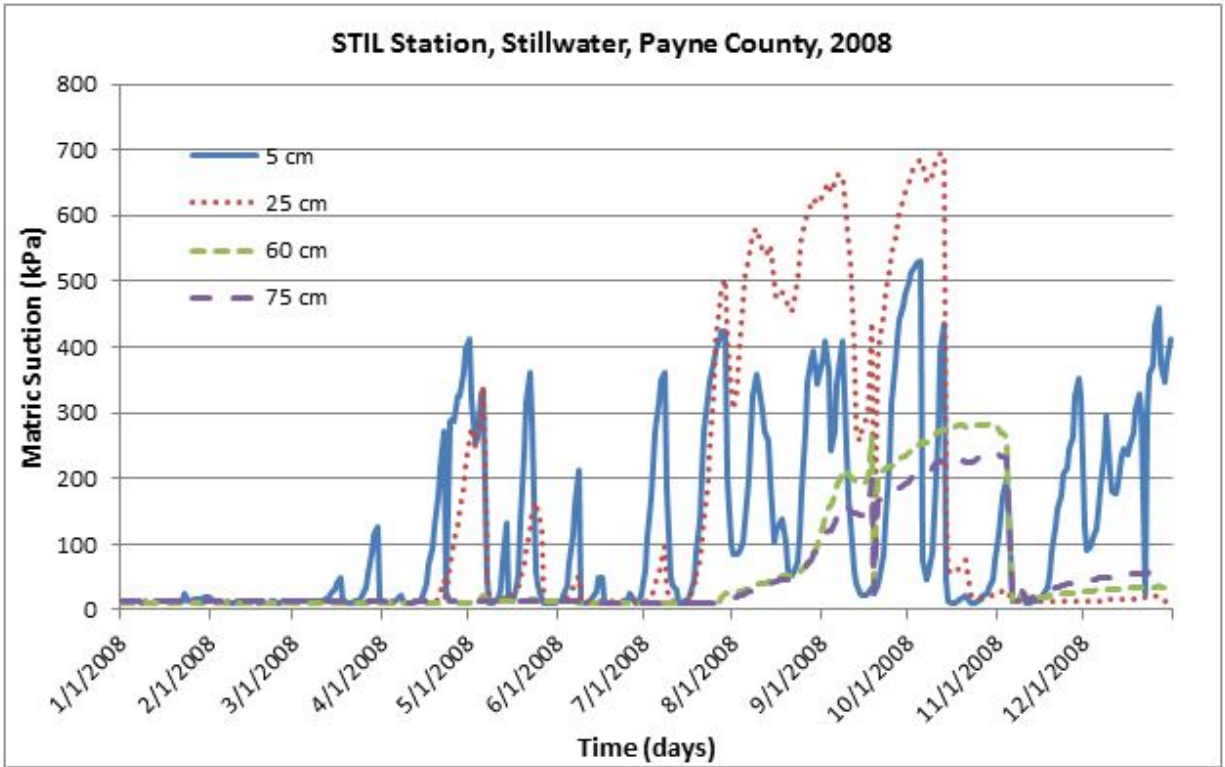


Figure 4.5. Matric Suction Variation with Time at Different Depths in Stillwater during 2008.

5 CLIMATIC AND SOIL REGIONS

5.1 Climatic Regions

The 48 contiguous U.S. states have been subdivided into 344 climate divisions based on long-term climate data maintained by National Climatic Data Center (NCDC) (Guttman and Quayle 1985). These divisions are classified mainly for agricultural purpose (Illston et al. 2004). Figure 5.1 shows 344 climate divisions across contiguous U.S states. Each of the 48 states has been classified up to 10 divisions. There are nine climate divisions in Oklahoma (Figure 5.2). These nine divisions correspond to the nine crop divisions designated by the US Department of Agriculture. Each climate division also has homogeneous weather and climate patterns. The climate of Oklahoma varies significantly across the state (Illston et al. 2004).

The U.S. divisional climate data are used to large-scale and long-period climate features for a variety of climatic applications. The divisions often coincide with county boundaries. A divisional dataset is based on year-monthly averages of temperature and precipitation since 1895. These divisions show climatic coherence in space and time. However, this computation of divisional averages also has some weaknesses (Guttman and Quayle 1985). First, divisional boundary may not show the best climatological homogeneity. In some regions, these boundaries are not related to climate. Second, the weather stations within a division are not constant. For example, in a same region, different years may have the data from different weather stations. Third, the data used to classify divisions is long-term averages since early 1900s. Since climate has changes during the recent 100 years, the climatic data is needed to be updated.

By avoiding those listed weaknesses, this research uses the data from 1994 to 2011 for climatic region classification. All the Oklahoma Mesonet stations are built since 1994. As a result, the weather stations within a division are constant. However, the boundaries are still based on the county boundary, since only one weather station is selected in each of the 77 counties in Oklahoma.



Figure 5.1. U.S. Climatic Divisions

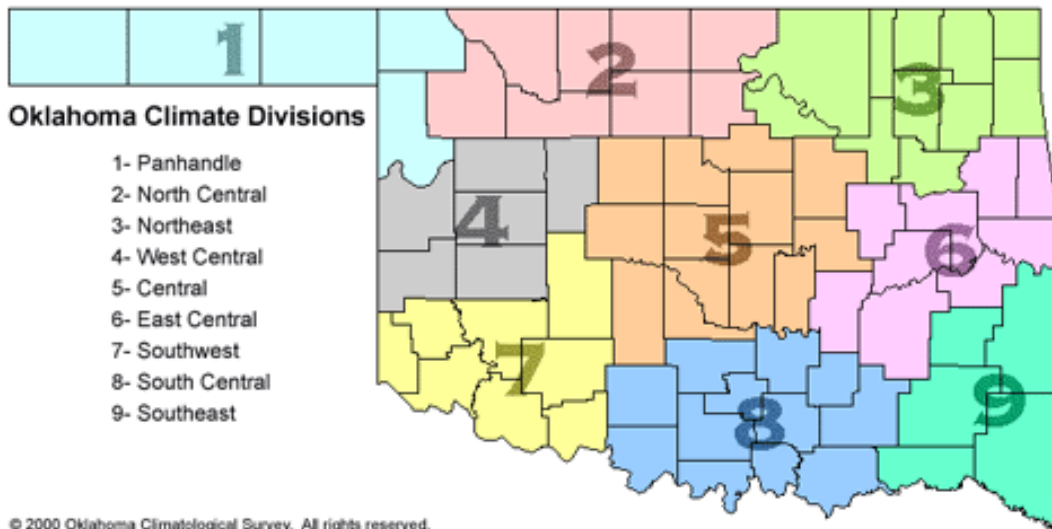


Figure 5.2. Oklahoma Climatic Divisions (<http://climate.ok.gov>)

5.1.1 Climatic Parameters

The climatic parameters used to classify climatic regions in this research are: air temperature, wind speed, percent sunshine, precipitation, and relative humidity. All of

these parameters are 18-year averages. Since TMI is a function of temperature and precipitation, and the distribution of TMI across Oklahoma is also similar to the distributions of temperature and precipitation, the classification of climatic regions does not include TMI. Each of the 77 stations has five parameters ready for the classification. The station represents the county where the station located.

5.1.2 SPSS and ARCGIS Software Models

The basic idea of classification is called cluster analysis. Cluster analysis takes a large number of variables and reduces them to a smaller number of groups based on the similarity of the data values within the same group. Cluster analysis calculates a similarity or a distance measured between each observation and groups the two observations that have the greatest similarity or the shortest distance into a cluster. It repeats this step all over again and combines the next two observations with the cluster of two already existed observations. This procedure continues until all observations are grouped into one larger cluster containing all similar observations (Mallery and George 2012). Clustering algorithms include hierarchical clustering, K-means clustering, distribution-based clustering, density-based clustering, etc. This research applies two clustering methods - hierarchical clustering and K-means clustering using two different software programs – SPSS and Matlab.

SPSS Statistics (Software Package used for Statistical Analysis) is one of the software used to classify climatic regions. The Hierarchical Cluster (also known as Connectivity based clustering) analysis is based on the core idea of observations being more related to nearby observations than to those farther away. Hierarchical cluster is the most widely used method in different fields. Hierarchical clustering connects "objects" to form "clusters" based on their distance. A cluster can be described largely by the maximum distance needed to connect parts of the cluster. At different distances, different clusters will form. In SPSS, the hierarchical cluster method is applied to classify the climatic regions in Oklahoma. Two counties with similar values of the five climatic variables can be classified into the same climatic region or, alternatively, into two distinct regions if the counties are dissimilar.

In the K-means cluster (also known as Centroid-based clustering), the clusters are represented by a central vector, which may not necessarily be a member of the dataset. K-means method requires the number of clusters, K, to be determined in advance. Furthermore, the algorithms prefer clusters of approximately similar size, as they will always assign an object to the nearest centroid. In this project, K-means cluster is done by Matlab. In addition to five climatic parameters used in hierarchical clustering, latitude and longitude are also included in K-means method. By considering latitude and longitude, counties with long distance are not likely to be classified in one region. When cluster analysis is completed, each county is designated by a cluster number, then this information is input into ArcGIS software for creating the maps.

ArcGIS is geographic software that is widely used in map creation and data management. Using geographic information system (GIS) database, the spatial analysis of data can be conducted to integrate other solutions and systems. GIS is playing an increasingly important role in Civil Engineering by supporting the infrastructure management. Choropleth maps, created by ArcGIS, are used to show different climatic regions. The choropleth map offers an easy way to display how a measurement varies across a geographic area or it shows the level of variability within a region. Different colors on the map represent different regions. In this project, counties in the same color mean they are in the same climatic region. Figure 5.3 and 5.4 show the maps of eight climatic regions using two different methods. Appendix C includes the maps for number of other regions evaluated in this study.

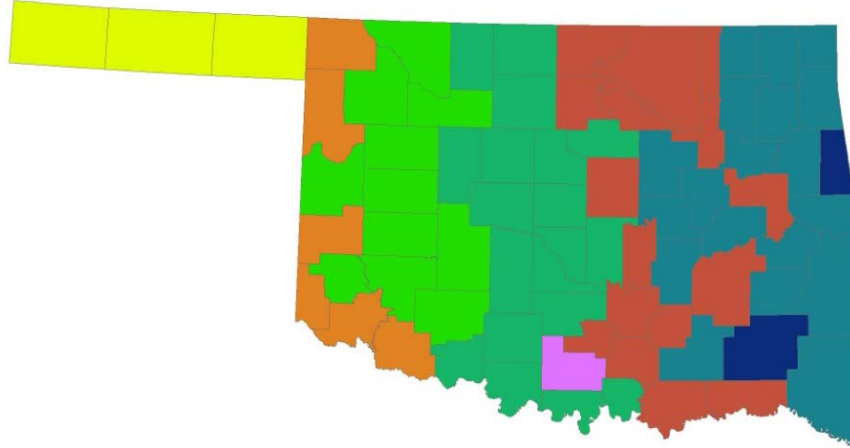


Figure 5.3. Eight Climatic Regions (Hierarchical Clustering).

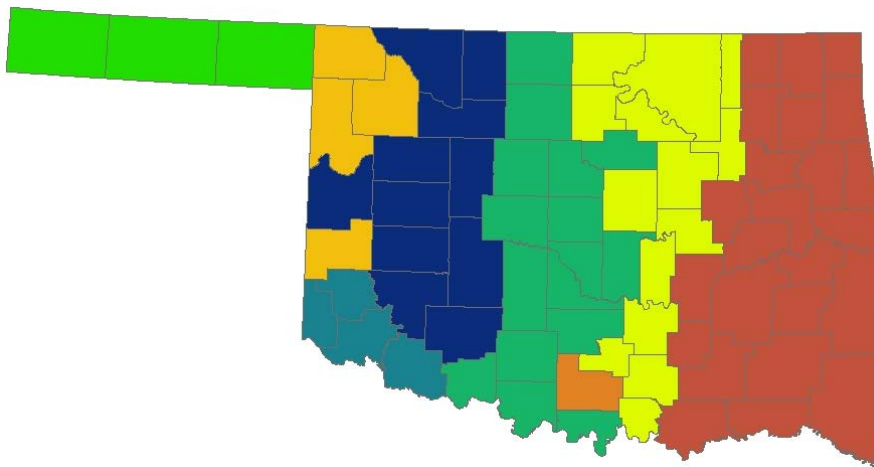


Figure 5.4. Eight Climatic Regions (K-means Clustering).

5.1.3 Optimum Number of Climatic Regions

To decide on the appropriate number of climatic regions for characterizing climatic conditions, we examined the change in the mean square error statistic. In statistics, the mean squared error (MSE) of an estimator is one of many ways to quantify the difference between values implied by an estimator and the true values of the quantity

being estimated. MSE measures the average of the squares of the "errors." The error is the amount by which the value implied by the estimator differs from the quantity to be estimated. The equation of calculating MSE is

$$MSE = \sum_{i=1}^5 \sum_{j=6}^{J_c} \sum_{k=1}^k (X_{ijk} - x_{ij})^2 / 5(77 - J_c) \quad (5.1)$$

This analysis is used for the results from hierarchical cluster. In Equation 5.1, 5 means 5 climatic parameters, and 77 means a total of 77 counties in Oklahoma. Let X_{ijk} be the i^{th} climatic variable for the k^{th} county classified in the j^{th} (j ranges from 6 to 10) cluster. Then, for the given number of clusters J_c , the mean square error indicates the variability of climatic conditions for J_c clusters.

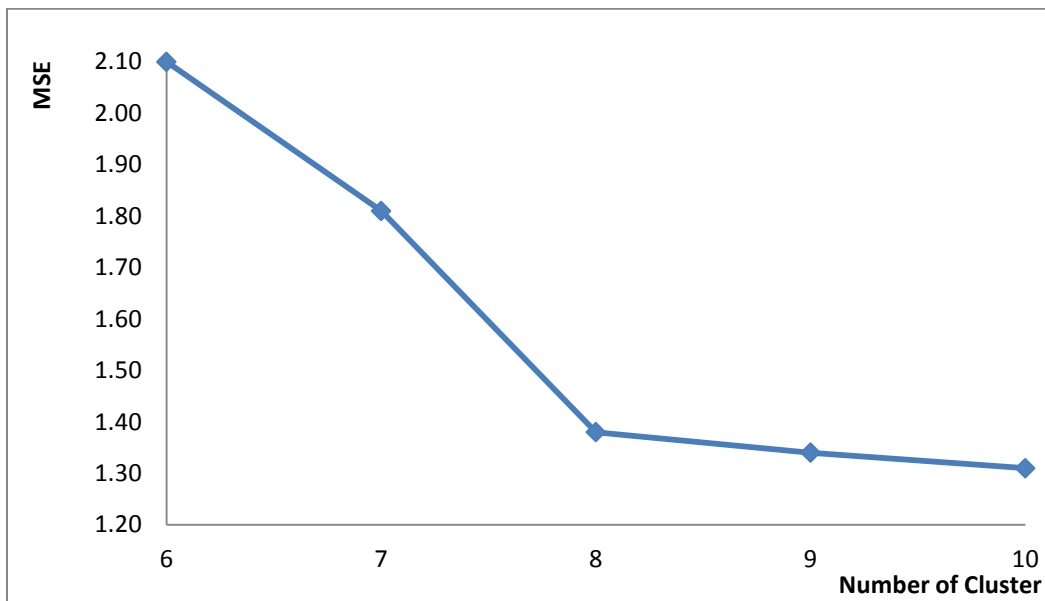


Figure 5.5. Optimum Number of Cluster of Climatic Regions (Hierarchical Cluster)

As shown in Figure 5.5, when 8 clusters are considered, increasing the number of clusters does not contribute significantly to the reduction of the MSE. Therefore, 8 clusters adequately capture the variation in climatic conditions across Oklahoma and represent a good compromise between reducing the MSE and keeping the number of clusters small for simplicity. However, both Figure 5.3 and Figure 5.4 indicate that there is one region that is defined by one county (Carter County located in south central

Oklahoma). The reason that Carter County becomes a region might be that the Mesonet station in that county is surrounded by active agricultural research fields, which change throughout the year. Irrigation and ground cover surrounding the station can affect air temperature and humidity (Personal Communication, Oklahoma Mesonet). If this county can be classified within neighboring regions, then for hierarchical method, 7 is the optimum number of climatic regions.

In K-means analysis, to measure the quality of a clustering, the sum of the squared error (SSE) is used. SSE is the total sum of the distance between a data point and its corresponding cluster for all data points. The SSE is normally defined as follows:

$$SSE = \sum_{i=1}^K \sum (c_i - x)^2 \tag{5.2}$$

where C_i is the i^{th} cluster, x is the point in C_i , and c_i is the mean of the i^{th} cluster. In our problem, one data point is a vector consisting seven parameters, and the number of clusters ranges from 3 to 20, and their corresponding total sum values is shown in the Figure 5.6.

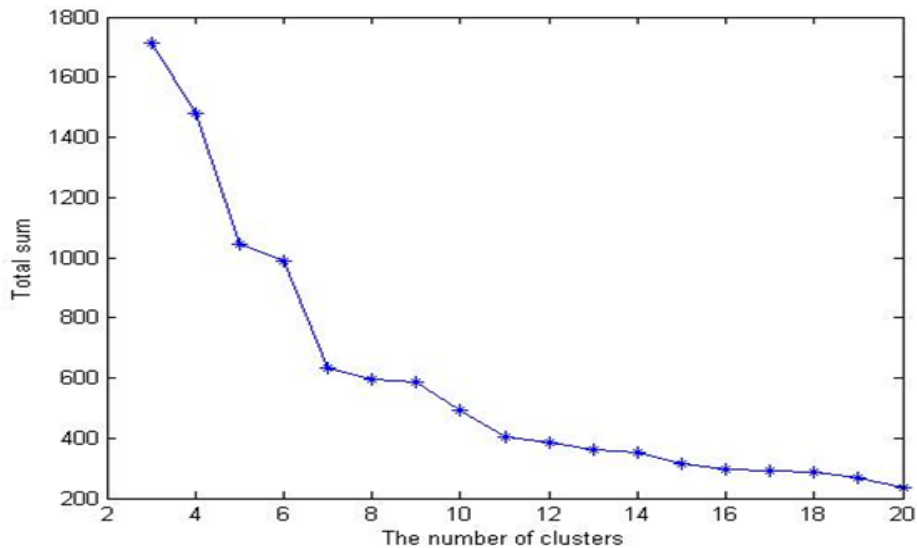


Figure 5.6. Optimum Number of Cluster of Climatic Regions (K-means Cluster)

Given different sets of clusters that are produced by different runs of K-means, researchers prefer the one with smallest SSE since this means the centroids of this clustering are a better representation of the points in this cluster. Figure 5.4 shows that when the number of clusters reaches 8, the SSE does not change a lot. Similar to the hierarchical method, there is still one region that contains only county (e.g., Carter County). If we put this single county to its neighboring regions, the optimum number of climatic regions for K-means method is 7.

From the maps of climatic regions in Figure 5.3, Figure 5.4 and the figures given in Appendix C for the other clusters evaluated in this study, we can see that the regions created by K-means method have better patterns than the ones created by hierarchical method. That might be due to the consideration of latitude and longitude in K-means method. These climatic regions have been created using five climatic parameters: precipitation, temperature, percent sunshine, wind speed, and relative humidity. These regions can be used for subsurface moisture conditions, similar to the interpretation of the TMI maps. The equilibrium suction and depth to the equilibrium suction could be considered very similar across each of these regions.

5.2 Soil Regions

In addition to the climatic regions that have been created using five climatic parameters and the cluster analyses, the research team attempted to apply a similar approach for creating soil regions across Oklahoma in terms of some typical engineering properties of the soils. To establish the soil regions, soil parameters from different sources were reviewed and evaluated. A soil database for 77 Oklahoma Mesonet stations has been established for creating the regions. All the soil parameters are measured at four depths: 5 cm, 25 cm, 60 cm, and 75 cm. Attempts were made to create soil regions at these four depths. Like climatic regions, the number of soil regions ranges from 6 to 10 at each depth based on the cluster analysis. The regions were created from two sources containing different soil properties. The following section describes the regions created using the soil parameters obtained from the USDA and Oklahoma Mesonet, and from a

new soil database obtained from the soils at the locations of the weather stations in the Oklahoma Mesonet network.

5.2.1 Soil Parameters

5.2.1.1 Soil Parameters from USDA and Oklahoma Mesonet

Soil parameters were obtained from two sources: the United States Department of Agriculture (USDA) Web Soil Survey (WSS) and the Oklahoma Mesonet. The WSS provides soil data and information produced by the National Cooperative Soil Survey. The soil dataset is operated by the USDA Natural Resources Conservation Service (NRCS) and provides access to the largest dataset of natural resources in the world. The NRCS has soil properties and maps available online for more than 95 percent of the U.S. counties and anticipates having 100 percent in the near future. The soil dataset is updated and maintained online as the single authoritative source of soil survey information. Soil parameters obtained from the WSS include: cation exchange capacity (meq/100grams), liquid limit (%), plasticity index (%), linear extensibility (%), clay (%), sand (%), and silt (%).

The other source of soil parameters is from van Genuchten et al. (1991) soil water characteristic curve (SWCC) model. The Oklahoma Mesonet has the data derived from this model. The Oklahoma Mesonet collected or estimated soil bulk density at each sensor location. The estimated soil water retention curves were derived using Arya and Paris (1981) methodology, from which four empirical coefficients α , n , WC_r , and WC_s are determined (Illston et al. 2008), where

α = empirical constant (kPa⁻¹),

n = empirical constant (unitless),

WC_r = residual volumetric water content (cm³/cm³),

WC_s = saturated volumetric water content (cm³/cm³).

For each soil sample, water content and water pressure values are inserted into van Genuchten et al. (1991) model for calculating the model coefficients. The WC_s is determined from bulk density. Other three coefficients α , n , WC_r are determined from the SWCC curve. Table 5.1 gives all the soil parameters used for soil region classification based on the soil information from USDA and Oklahoma Mesonet.

Table 5.1. Soil Parameters for Soil Regions.

Soil Parameters	Data Source	Depth
cation exchange capacity (meq/100grams), liquid limit (%), plasticity index (%), linear extensibility (%), clay (%), sand (%), and silt (%)	The USDA Web Soil Survey (WSS)	5 cm, 25 cm, 60 cm, and 75 cm
α : empirical constant (kPa ⁻¹) n: empirical constant (unitless) WC_r : residual water content (cm ³ /cm ³) WC_s : saturated water content (cm ³ /cm ³)	The Oklahoma Mesonet	5 cm, 25 cm, 60 cm, and 75 cm

5.2.1.2 SPSS and ARCGIS Software Models

Similar to the creation of the climatic regions in the previous section, an attempt was made for the soil region using the model in the SPSS software package and ArcGIS for the maps. The hierarchical cluster model in the SPSS was employed for the analysis. Following the hierarchical analysis, the ArcGIS was used in creating the maps. The soil dataset of 77 Oklahoma counties was used in the analysis. The procedure was repeated for each of the four depths mentioned in Table 5.1. Figure 5.7 shows the map

of six soil regions at 5 cm, and Figure 5.8 shows the map of ten soil regions at 5 cm. The maps for other depths at different levels of clusters (groups) are listed in Appendix D.

Unlike the climatic region maps, the soil regions do not have any unique clustering patterns. There are probably a number of reasons behind these trends. The most obvious reason is that the distribution of the soils across a region is not uniform. Furthermore, only the soil properties at the location of the Mesonet weather station were used in the analysis. In other words, it was assumed that the soil properties at one location represent the whole county where that weather station is located. Next section describes another attempt in creating the soil regions using a new soil database.

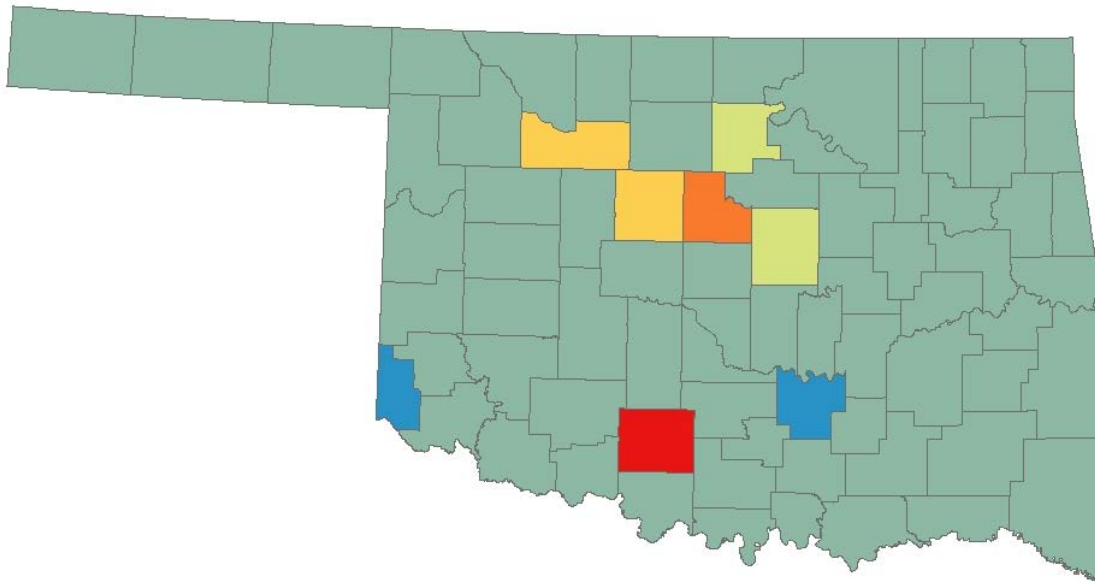


Figure 5.7. Six Soil Regions at 5 cm.

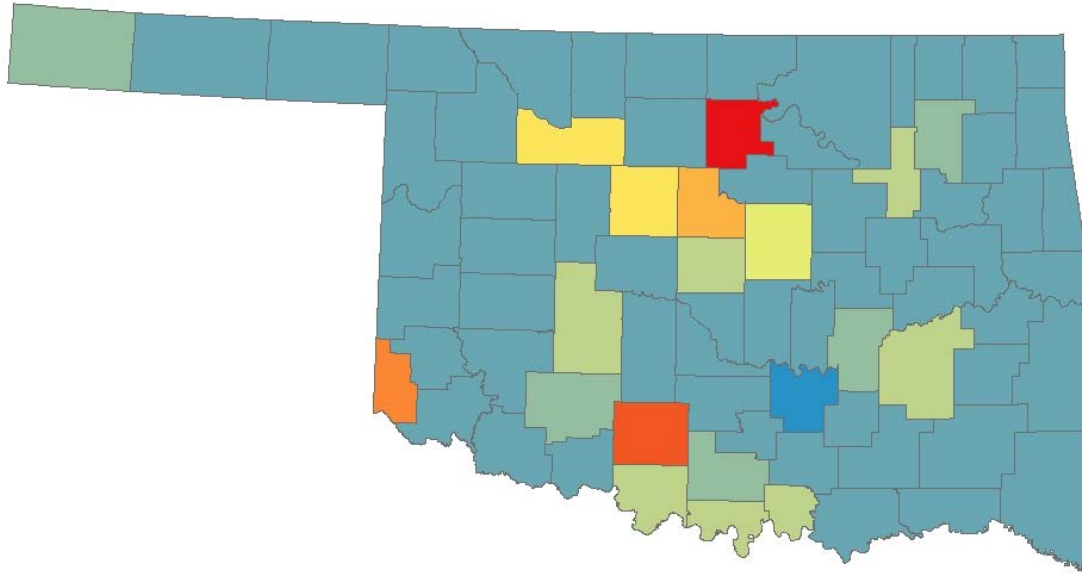


Figure 5.8. Ten Soil Regions at 5 cm.

5.2.2 New Soil Parameters

To increase the accuracy of the Oklahoma Mesonet soil and soil moisture data, and to improve the van Genuchten parameters for each site, a research team from Oklahoma State University and University of Oklahoma has conducted a comprehensive field sampling and laboratory tests to obtain new measurements of soil parameters (Scott et al. 2013). The new Mesonet soil database contains 12 soil properties using the samples from 545 sites and depth combinations from 117 Oklahoma Mesonet stations (Scott et al. 2013). Table 5.2 gives the description of this soil dataset.

This data set contains soil physical property data for the soils of the Oklahoma Mesonet stations. Sand, silt, and clay contents, bulk density, and volumetric water content at -33 and -1500 kPa matric suctions were measured using duplicate samples from five depth layers (3 cm, 20 cm, 40 cm, 55 cm, 70 cm) at 117 Oklahoma Mesonet stations. These soil properties were used as inputs for the Rosetta pedotransfer function which predicted parameters describing the water retention curve and hydraulic conductivity function for each site and depth. Rosetta is an artificial neural network model for

estimating van Genuchten parameters (Scott et al. 2013). Rosetta also provides estimates of saturated hydraulic conductivity (K_s).

In this study, a second attempt was made for using the new soil database in creating soil regions across Oklahoma using two models: The hierarchical cluster method in SPSS and the K-means cluster method using Matlab.

Table 5.2. New Soil Dataset for Mesonet Stations

Soil	Units	Description
Sand	%	percent sand
Silt	%	percent silt
Clay	%	percent clay
BulkD	g/cm^3	bulk density
Th33	cm^3/cm^3	volumetric water content at -33 kPa (measured)
Th1500	cm^3/cm^3	volumetric water content at -1500 kPa (measured)
Theta_r	cm^3/cm^3	residual water content
Theta_s	cm^3/cm^3	saturated water content
Alpha	1/kPa	fitting parameter for van Genuchten water retention curve
N	No units	fitting parameter for van Genuchten water retention curve
K_s	cm/day	saturated hydraulic conductivity
L	No units	exponent of van Genuchten-Mualem conductivity function

5.2.2.1 SPSS AND K-MEANS CLUSTER MODELS

Based on the new dataset, soil regions are reclassified using hierarchical cluster method in SPSS and K-means cluster method in Matlab, which have been discussed in the previous section for the classification of the climatic regions. For the cluster analysis in soil region classification, the weighted averages of the soil parameters were calculated, with the trials of 6 to 10 soil regions. For instance, Figure 5.9 shows the map for 6 regions using the weighted method.

Not all the 77 stations selected in this study have measurements at all five depths; however, all the 77 stations have measurements at 3 cm and 20 cm. In this case, soil regions are classified from 6 to 10 regions at 3 cm and 20 cm. Figure 5.10 shows six soil regions at 5 cm using the K-means method. All other maps using the hierarchical and K-means methods are listed in Appendix E. Since with the new soil data, the analysis did not result in any unique patterns of soil regions, no optimum number of clusters was analyzed at this step.

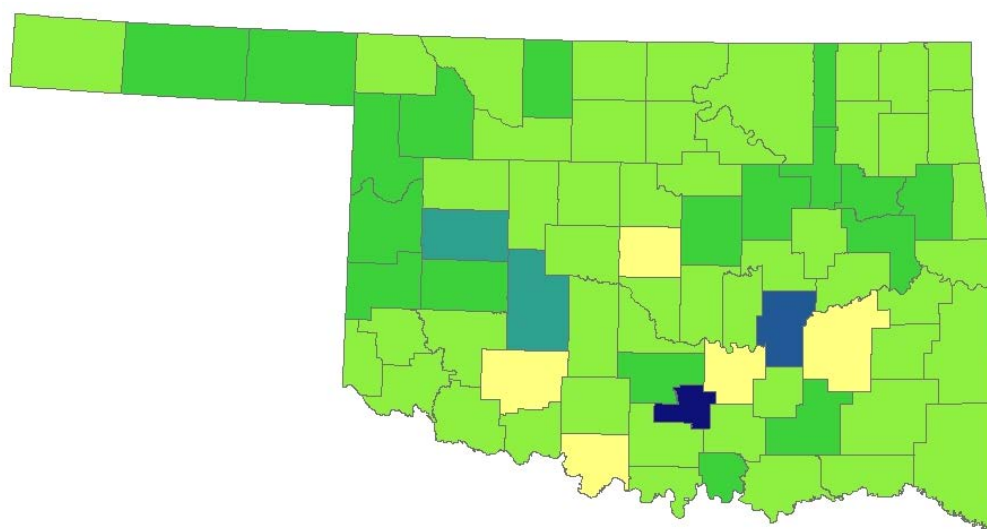


Figure 5.9. Six Soil Regions (Weighted average).

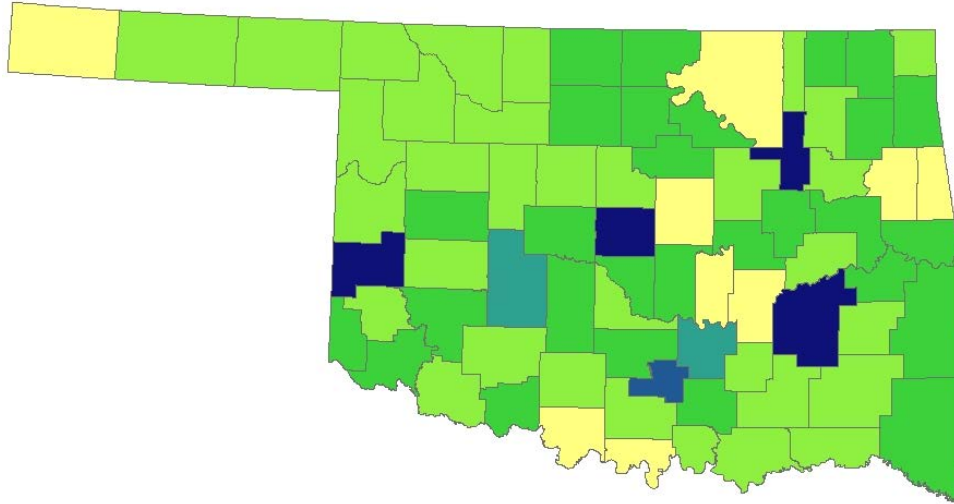


Figure 5.10. Six Soil Regions at 3 cm (K-means clustering).

6 VALIDATION OF A MOISTURE MIGRATION MODEL

As described in Chapter 2, the current version of the EICM software is not capable of predicting moisture migration at sites with a soil surface layer. Oklahoma Mesonet data described in Chapter 2, collected at sites with soil surface layer, is yet very valuable to validate moisture migration models. Once the EICM version with soil surface layer becomes available, it can be validated using the Mesonet data. In this chapter, moisture migration at selected Mesonet sites is predicted using a computer program similar to EICM (SVFLUX (Thode et al. 2011)). In addition to showing the capabilities of a moisture migration model, these predictions will give insights into the quality of soil suction (related to moisture content) measured at Mesonet sites. A moisture migration model solves four simultaneous differential equations associated with liquid water, water vapor, air, and heat flows (Fredlund and Rahardjo 1993).

6.1 Modeling of the Atmosphere-Soil Boundary

One of the key considerations in the moisture migration modeling is the proper modeling of the atmosphere-soil surface boundary. In one-dimensional moisture migration modeling, water that infiltrates through the soil surface is considered a flux boundary condition at the soil surface for solving the liquid water flow differential equation. The water flux at the soil surface depends on the rainfall, runoff, and actual evaporation. The water vapor pressure gradient between the soil surface and the air immediately above it determines evaporation. The evaporative flux at the soil surface is the flux boundary condition for solving the differential equation for water vapor flow. When the surface is fully saturated the evaporation is the maximum and referred to as the potential evaporation. The original Penman equation given below is used to calculate the potential evaporation in this study.

$$PE = [(rQ_n + \eta E_a)/(\gamma + \eta)] \gamma \quad (6.1)$$

Where, PE = potential evaporation (m/day)

E_a = flux associated with mixing, a function of wind speed, relative humidity in the air above the ground surface, and saturated vapor pressure

γ = slope of saturation vapor pressure vs. temperature curve (kPa/C),

Q_n = net radiation (m/day)

η = psychrometric constant = 0.06733 kPa/C (Thode et al. 2011).

As the soil surface becomes unsaturated the actual evaporation rate decreases. Actual evaporation can be calculated from fundamental thermodynamic considerations. In this study, Wilson-Penman method is used in formulating climatic boundary conditions (Thode et al. 2011). In this method, soil temperature at the ground surface can be different from the air temperature above it, and ground thermal flux is assumed to be zero beneath the soil surface.

6.2 Validation Sites and Measured Data

Four Mesonet sites (Figure 6.1) were selected for validation purposes. They are:

- BOWL Station: Bowlegs, Seminole County
- WAUR Station: Waurika, Jefferson County
- WIST Station: Wister, Le Flore County
- STIL Station: Stillwater, Payne County

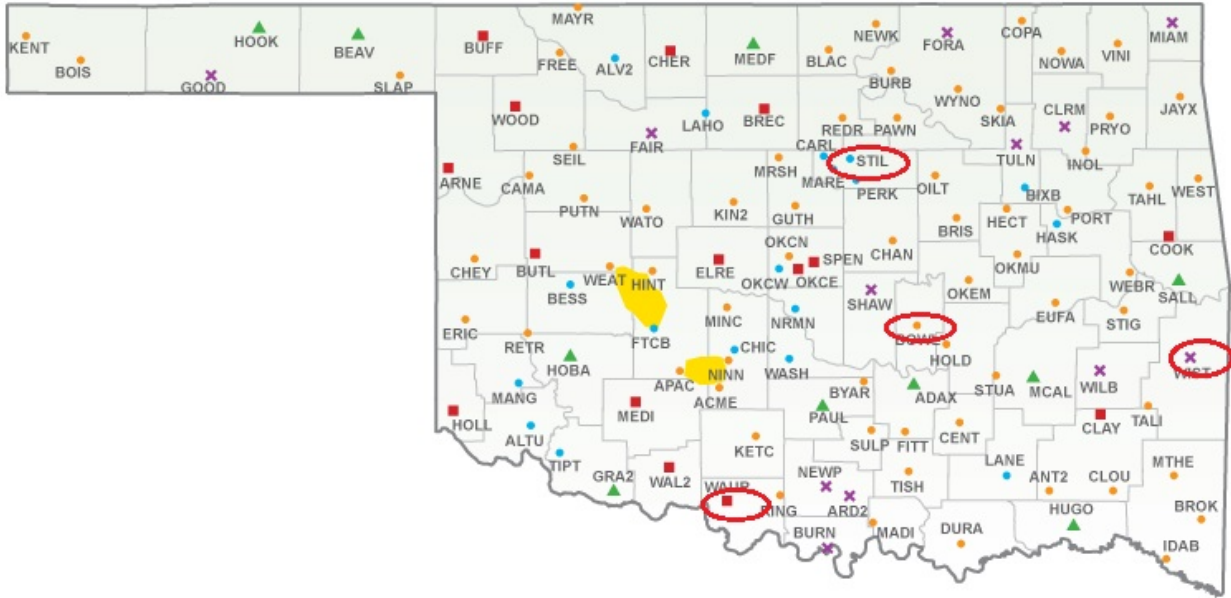


Figure 6.1. Locations of the Validation Sites.

Following data measured at the above given Mesonet sites were used as input to SVFLUX

- rainfall
- air temperature measured at 1.5 m above the ground
- wind speed and direction measured at 2 m above the ground
- incoming solar radiation
- relative humidity measured at 1.5 m above the ground

The hourly measurements of the above given quantities are shown in Figures 6.2-6.6 for a period of 8640 hours (360 days) in 2001. The zero on the time axis corresponds to 12 AM on January 1, 2001. The time span between vertical grid lines is 720 hours or 30 days. The net radiation values, a required input for SVFLUX, shown in Figure 6.5 were obtained using the percent sunshine values discussed in Chapter 2 and the

methodology described in ASCE Standardization of Reference Evapotranspiration Task Committee report (2005).

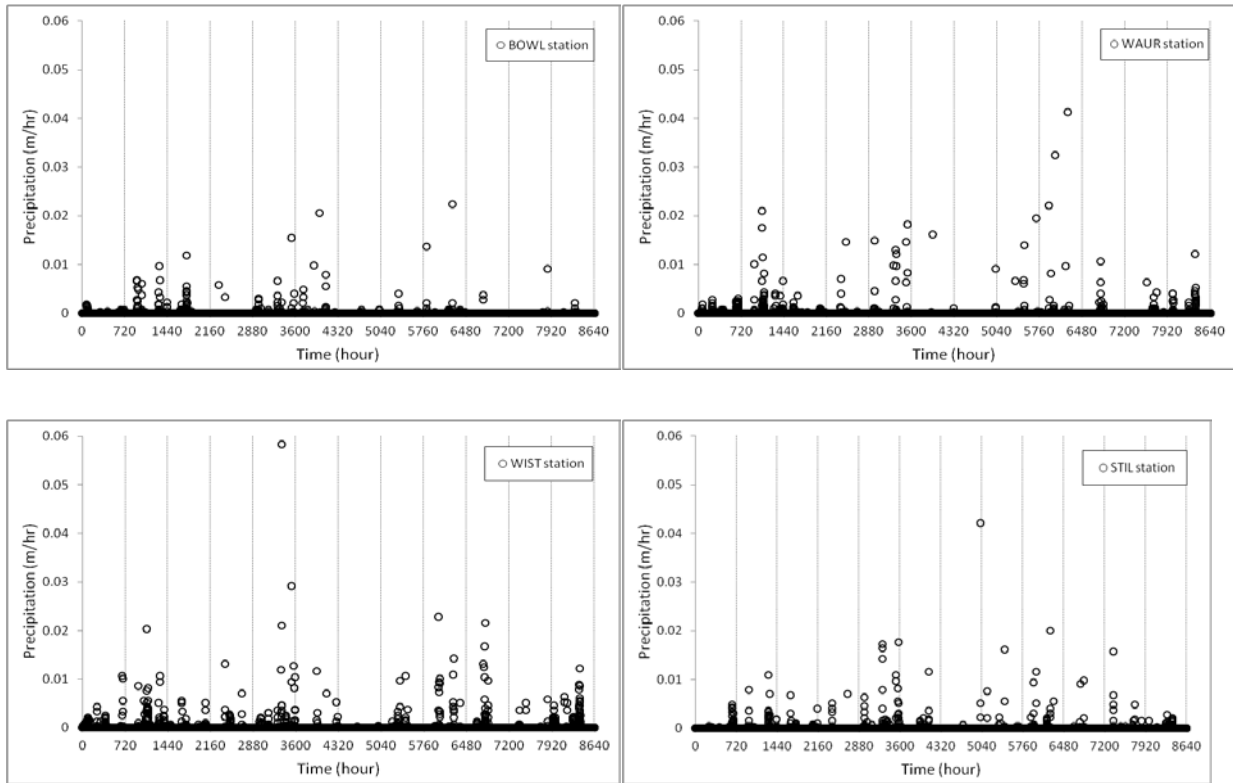


Figure 6.2. Rainfall at the Validation Sites in 2001.

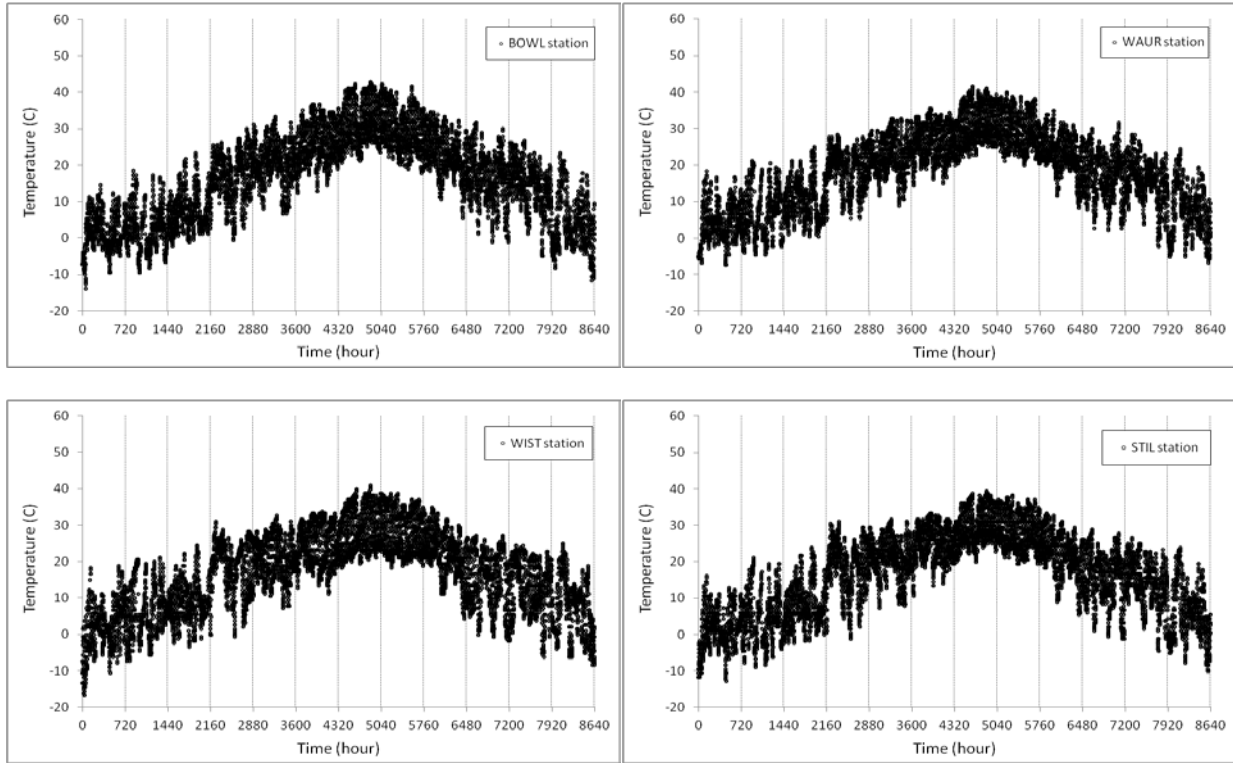


Figure 6.3. Air temperature at the validation sites in 2001.

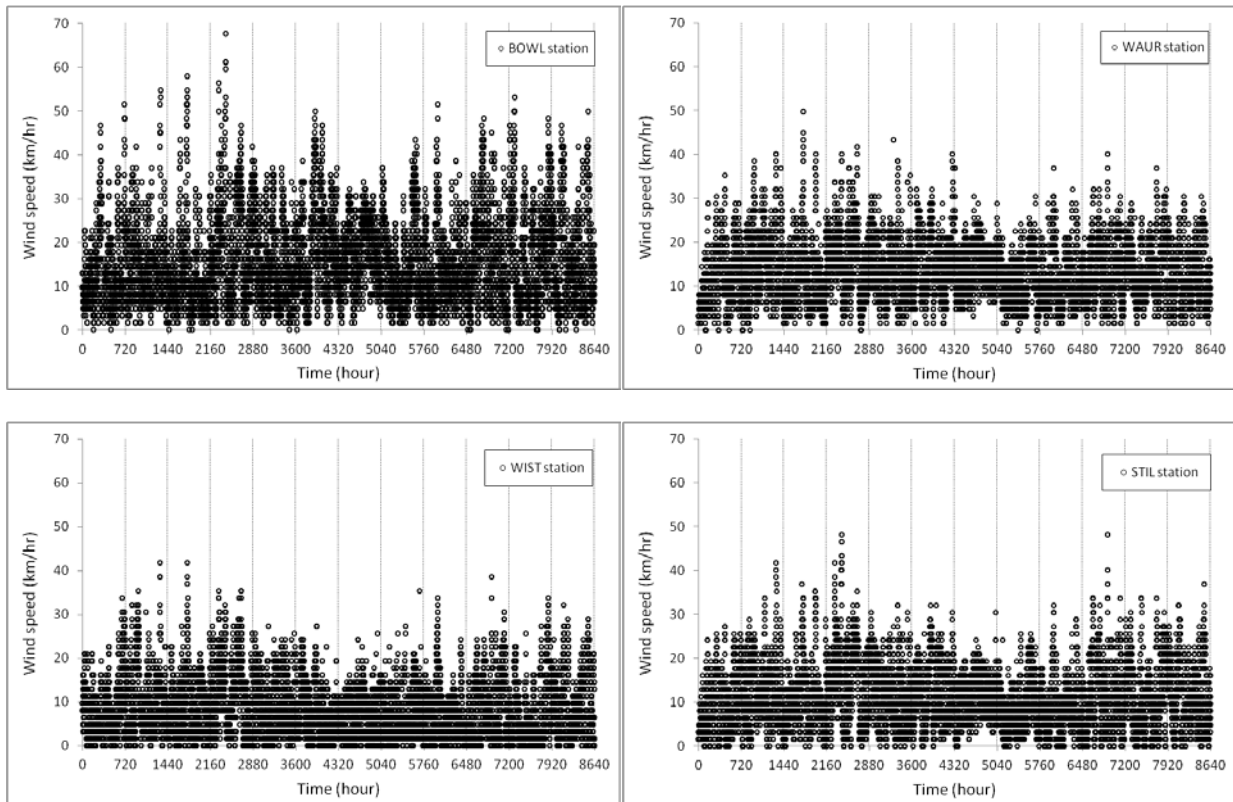


Figure 6.4. Wind Speed at the Validation Sites in 2001.

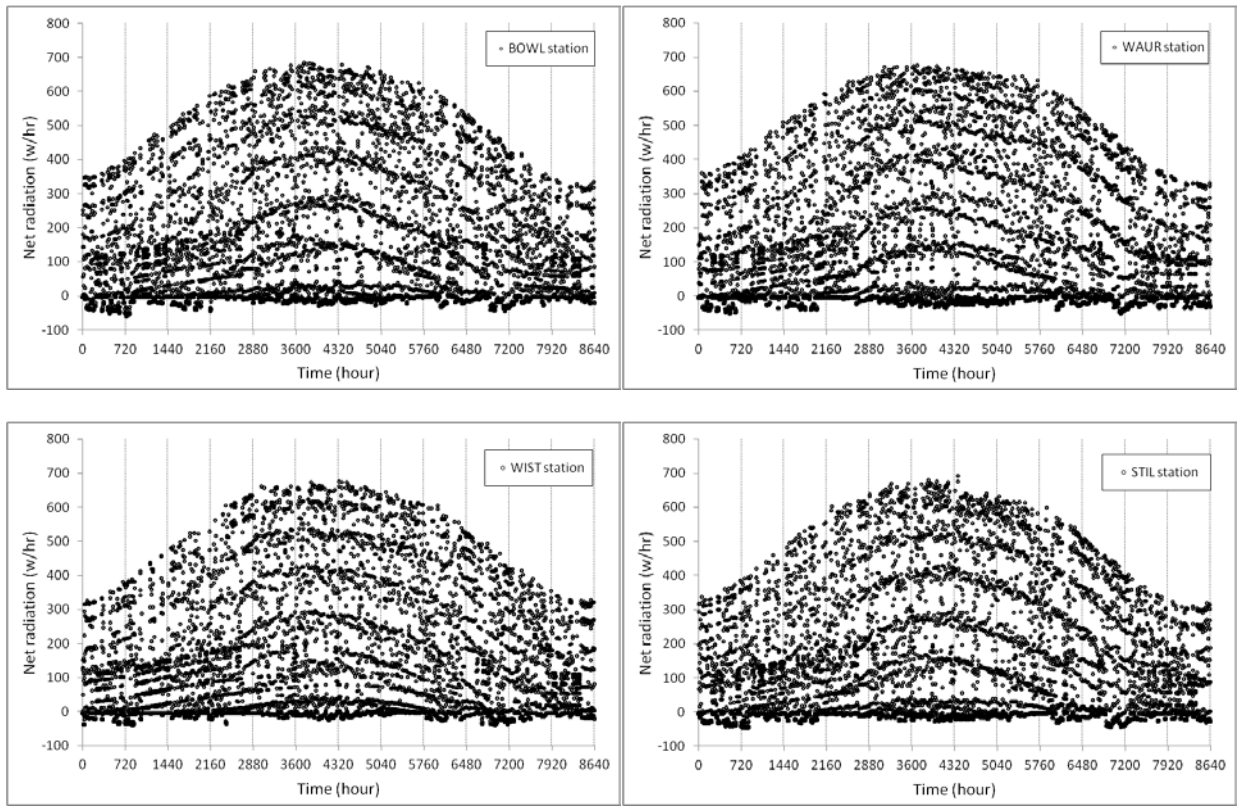


Figure 6.5. Net Radiation Per Square Meter at Validation Sites in 2001.

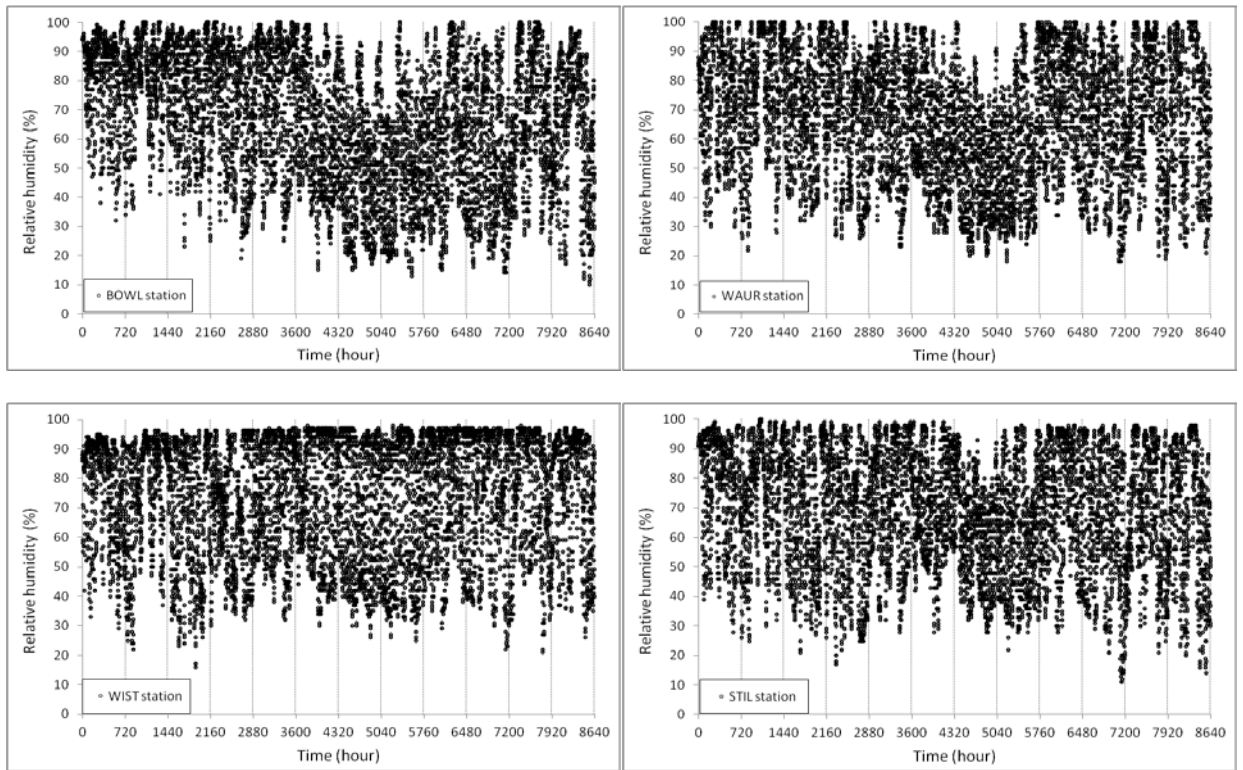


Figure 6.6. Relative Humidity at Validation Sites in 2001.

In addition to the climatic data described above, soil suction measurements were collected at four different depths (5, 25, 60, and 75 cm) below the ground surface at each site. The soil suction data can be related to soil moisture through calibration of the sensors. The sensors used to collect data at the Mesonet sites are heat-dissipation sensors with the pore water pressure sensitivity of -8.5 kPa to -852 kPa (Illston et al. 2008). The measured suction data are presented together with predicted data later.

6.3 SVFLUX Model

The SVFLUX model used is shown in Figure 6.7. The locations of the soil suction (moisture) sensors are also shown in in this figure. The input soil properties were obtained from a study conducted by Scott et al. (2013). Scott et al. (2013) measured various soils properties on soil samples collected at all Mesonet sites. Thicknesses of their soil samples were 10 cm, except for the sample near the ground surface, which was 7 cm-thick. The center of the Scott et al. (2013) soil samples are also indicated in Figure 6.7. The SVFLUX model was created using the locations of soil property measurements as a guideline. The fifth layer was extended to a sufficient depth to make sure that the bottom boundary condition did not influence the predicted suction values. The measured soil properties at various sites are summarized in Tables 6.1-6.4. As can be seen from these tables that the surficial soils at BOWL and WAUR sites are primarily sand and the soil at other two sites are primarily silt/clay.

At the soil surface, climate data described in Section 6.2 was applied and the ponding height was set to zero. Therefore the maximum pore water pressure at the surface is restricted to zero. At the bottom boundary a constant pressure head was applied. This pressure head was calculated assuming negative hydrostatic water pressure above the ground water table. Measured suction values at 12 AM on January 1, 2001 were specified as the initial conditions. Pore air pressures were assumed to be negligible throughout the analyses.

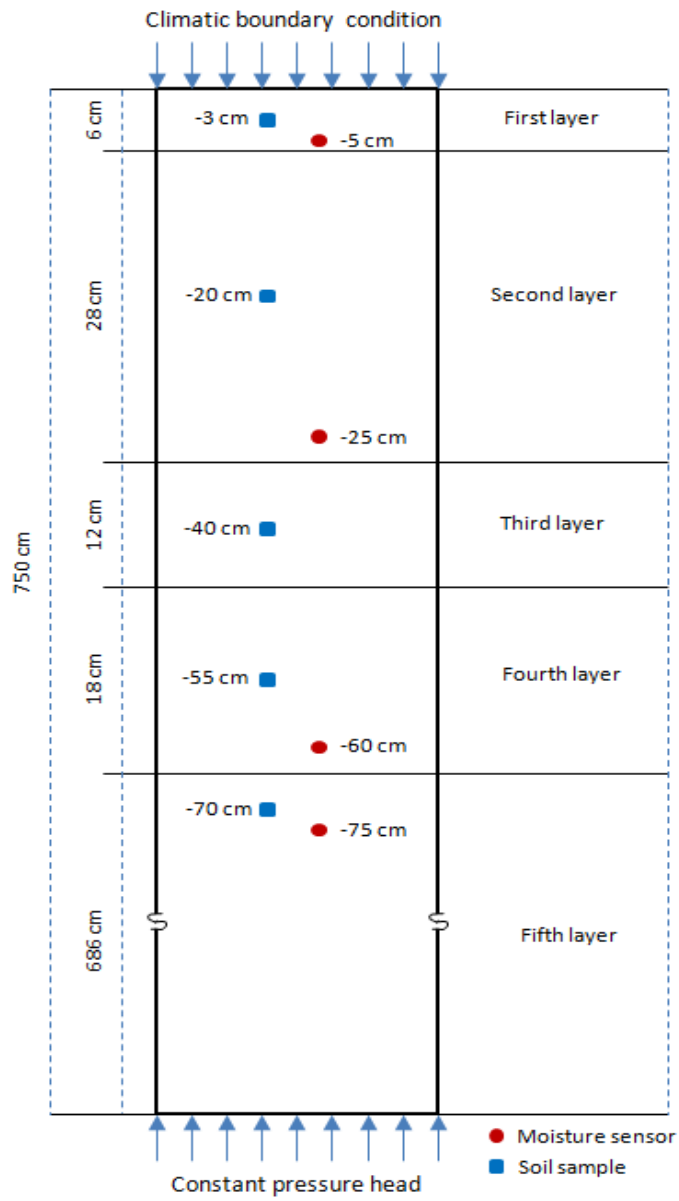


Figure 6.7. Model Used in SVFLUX.

Table 6.1. Soil Properties at BOWL Station (from Scott et al. 2013).

	Soil contents (%)	Saturated volumetric water content	Residual volumetric water content	Saturated hydraulic conductivity (m/hr)	Fitting parameters for Van Genuchten curve :α (1/kPa), n
First layer	Sand= 58 Silt= 28.8 Clay= 13.2	0.428	0.021	0.03712	α = 0.246 n=1.35
Second layer	Sand= 47.3 Silt= 26.4 Clay= 26.4	0.356	0.044	0.00371	α = 0.246 n=1.35
Third layer	Sand= 38.3 Silt= 28.3 Clay= 33.4	0.382	0.055	0.00258	α = 0.246 n=1.35
Fourth layer	Sand= 31.5 Silt= 31.4 Clay= 37.1	0.380	0.057	0.00137	α = 0.246 n=1.35
Fifth layer	Sand= 27 Silt= 35.3 Clay= 37.8	0.376	0.059	0.00167	α = 0.246 n=1.35

Table 6.2. Soil Properties at WAUR Station (from Scott et al. 2013).

	Soil contents (%)	Saturated volumetric water content	Residual volumetric water content	Saturated hydraulic conductivity (m/hr)	Fitting parameters for Van Genuchten curve :α (1/kPa), n
First layer	Sand= 66.1 Silt= 20.7 Clay= 13.2	0.388	0.027	0.0304	α = 0.321 n=1.36
Second layer	Sand= 53.2 Silt= 20.9 Clay= 25.9	0.373	0.046	0.0053	α = 0.132 n=1.33
Third layer	Sand= 54 Silt= 25.9 Clay= 20.2	0.346	0.040	0.0053	α = 0.195 n=1.32
Fourth layer	Sand= 62.2 Silt= 22.7 Clay= 15.1	0.351	0.034	0.0143	α = 0.318 n=1.35
Fifth layer	Sand= 68.6 Silt= 19.5 Clay= 11.9	0.313	0.027	0.0063	α = 0.226 n=1.34

Table 6.3. Soil Properties at WIST Station (from Scott et al. 2013).

	Soil contents (%)	Saturated volumetric water content	Residual volumetric water content	Saturated hydraulic conductivity (m/hr)	Fitting parameters for Van Genuchten curve :α (1/kPa), n
First layer	Sand= 17.6 Silt= 61.7 Clay= 20.7	0.398	0.053	0.0045	α = 0.028 n=1.69
Second layer	Sand= 10.0 Silt= 61.1 Clay= 28.9	0.405	0.052	0.0051	α = 0.118 n=1.38
Third layer	Sand= 5.9 Silt= 29.1 Clay= 65.0	0.486	0.087	0.0056	α = 0.180 n=1.19
Fourth layer	Sand= 9.2 Silt= 17.8 Clay= 73.0	0.514	0.082	0.0084	α = 0.111 n=1.22
Fifth layer	Sand= 4.8 Silt= 24.8 Clay= 70.5	0.486	0.079	0.0042	α = 0.107 n=1.20

Table 6.4. Soil Properties at STIL Station (from Scott et al. 2013).

	Soil contents (%)	Saturated volumetric water content	Residual volumetric water content	Saturated hydraulic conductivity (m/hr)	Fitting parameters for Van Genuchten curve :α (1/kPa), n
First layer	Sand= 16.8 Silt= 48.9 Clay= 34.3	0.474	0.091	0.00866	α = 0.253 n=1.27
Second layer	Sand= 24.9 Silt= 47.1 Clay= 28.0	0.386	0.055	0.00179	α = 0.073 n=1.36
Third layer	Sand= 27.6 Silt= 44.5 Clay= 27.9	0.396	0.050	0.00458	α = 0.107 n=1.38
Fourth layer	Sand= 29.4 Silt= 42.0 Clay= 28.6	0.381	0.052	0.00258	α = 0.095 n=1.36
Fifth layer	Sand= 25.2 Silt= 29.7 Clay= 45.1	0.397	0.058	0.00030	α = 0.068 n=1.21

6.4 Results and Discussion

The measured and predicted pore water pressure (pwp) – time histories at various depths for the BOWL Station are given in Figures 6.8 and 6.9. Note that soil suction is equal to $-pwp$ assuming pore air pressure is negligible. Predictions for the first 3600 hours are presented in Figure 6.9, while the predictions for the entire 8640 hours are given in Figure 6.8. Predictions are compared to the measured values for the WAUR, WIST, and STIL Stations in Figures 6.10, 6.11, and 6.12, respectively. Also given in these figures are the measured rainfall values.

In general, measured and predicted pore water pressures show more variation near the surface. From Figure 6.9 it can be seen that, while both measured and predicted pore water pressures respond to rainfall events near the surface (-5 cm), the predicted values respond more quickly, especially for small rainfall events. It is a well-known fact that the heat-dissipation sensors used at the Mesonet sites respond to moisture changes slowly. The major discrepancies between measured and predicted values at all sites occur between 3600 hours to 6000 hours. This is during the hot summer months. At this time, the reasons for this discrepancy are not very clear and are being investigated. Two possibilities are that the evaporation modeling in SVFLUX is not accurate or the sensor used is not very accurate under low moisture conditions.

Overall trends in pore water pressures and therefore moisture contents are predicted reasonably well by SVFLUX. It is recommended that the above mentioned discrepancy is resolved before proceeding with the validation of the EICM moisture migration model using Mesonet data.

In order to investigate the location of the lower boundary (Figure 6.7) and its effects on the predicted pore water pressures, the specified constant pressure head at the bottom of the model was changed from its original value of -18.4 m at the BOWL site to -40 m and 5 m and the SVFLUX was ran again. The predicted pore water pressures were same for all three analyses at all four depths (5, 25, 60, and 75 cm). These analyses confirmed that the bottom boundary is at sufficiently large depth and did not influence the behavior at the depths of interest. At the WAUR Station, the analysis was started at

4320 hours instead of 0 hour with the measured low pore water pressures (e.g. -478 kPa at 5 cm) as the initial conditions. The predictions, however, quickly reached previous predictions (see Figure 6.13) pointing to the fact that the initial conditions have influence on the predicted values over only a short time period. Similar behavior was also observed at the BOWL Station.

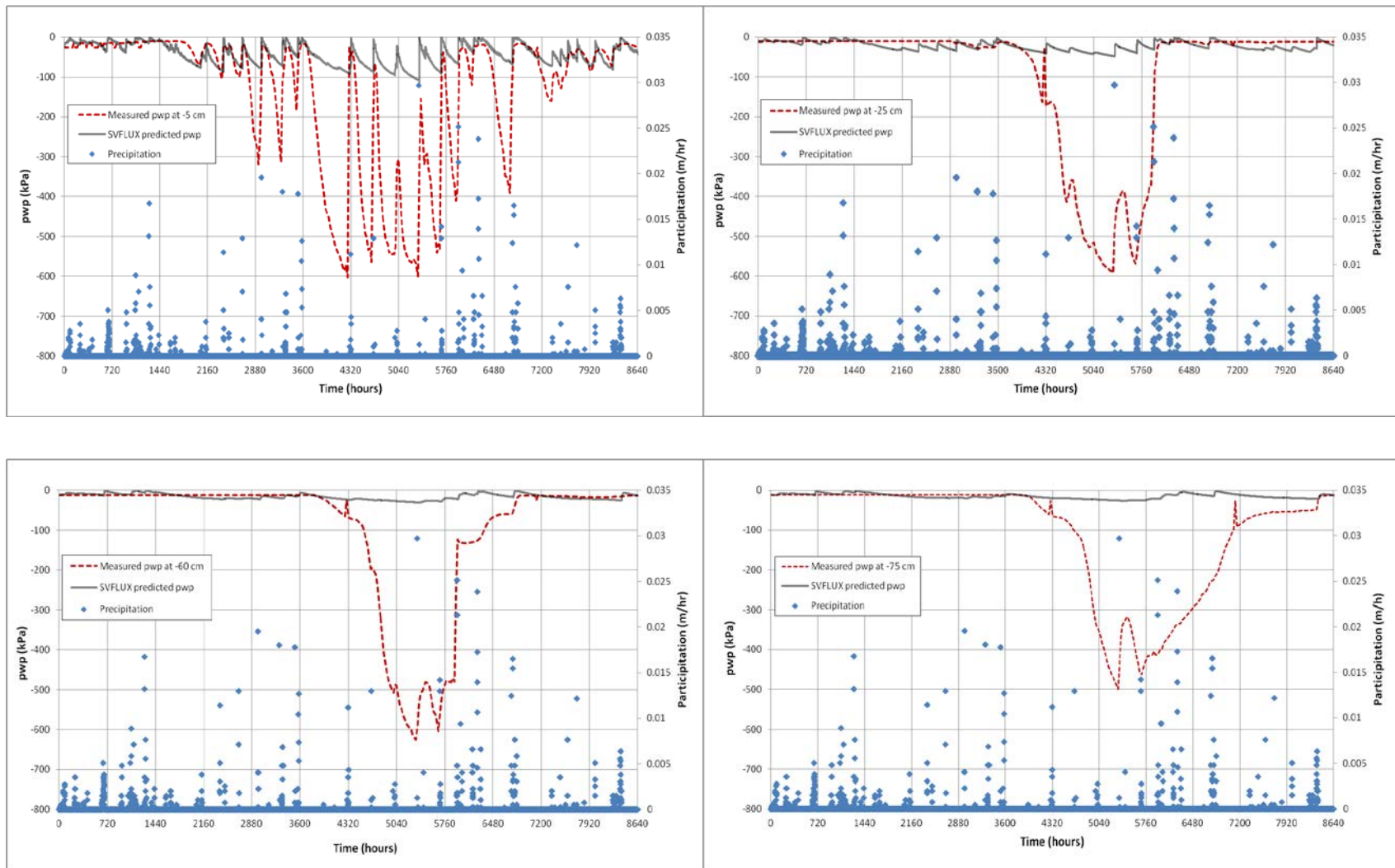


Figure 6.8. Measured and Predicted Pore Water Pressures at the BOWL Station – 8640 Hours.

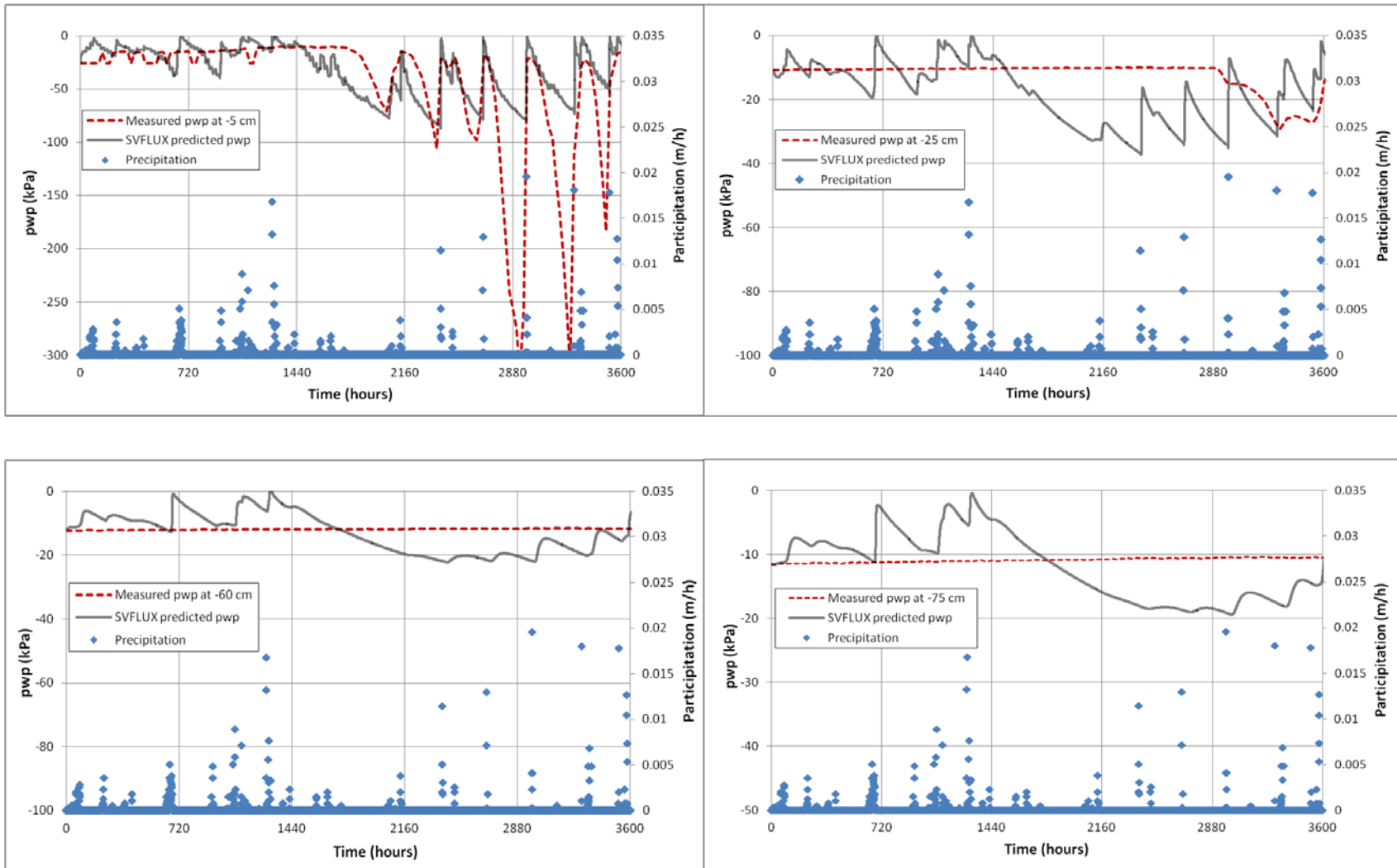


Figure 6.9. Measured and Predicted Pore Water Pressures at BOWL Station – 3600 Hours.

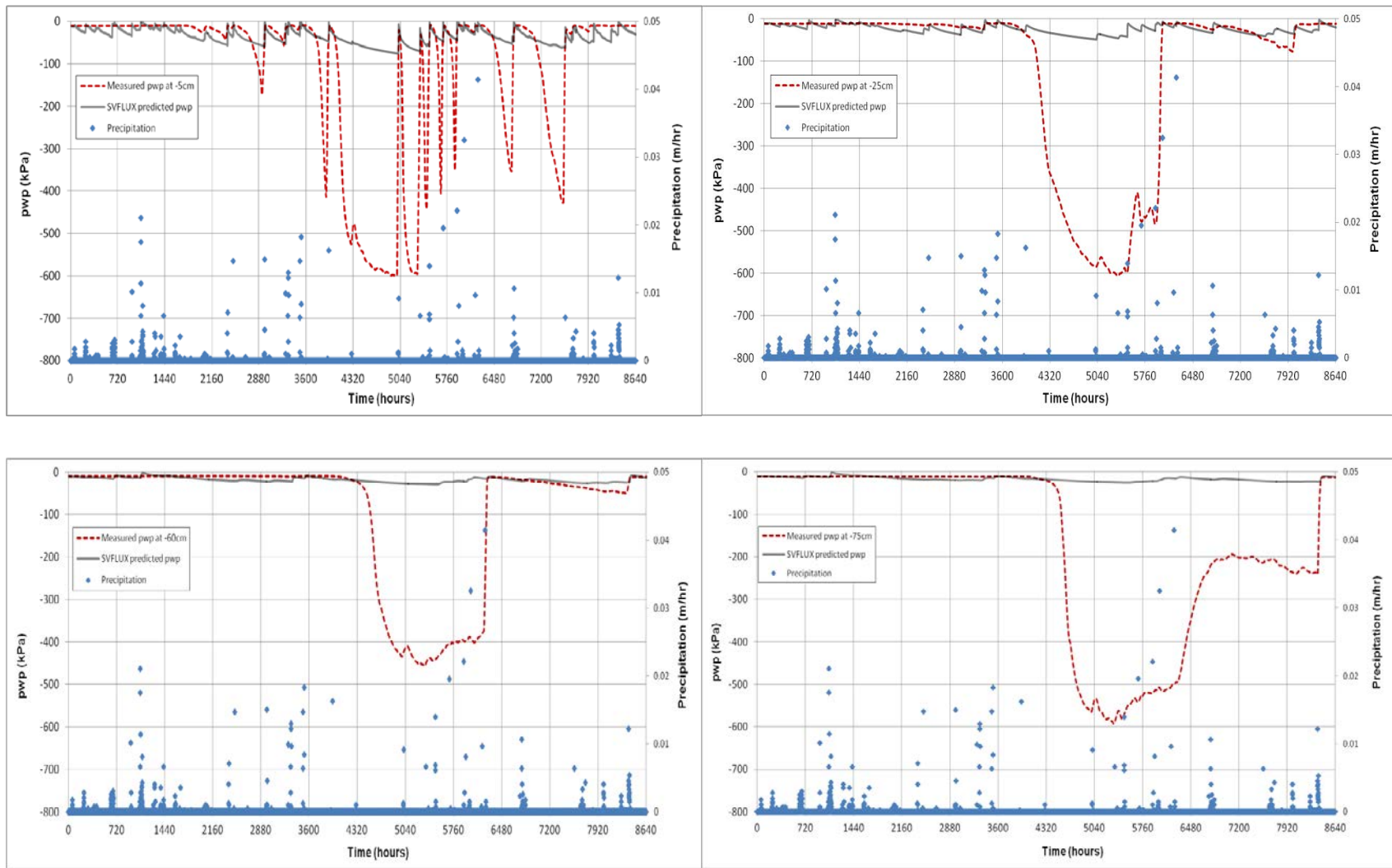


Figure 6.10. Measured and Predicted Pore Water Pressures at the WAUR Station.

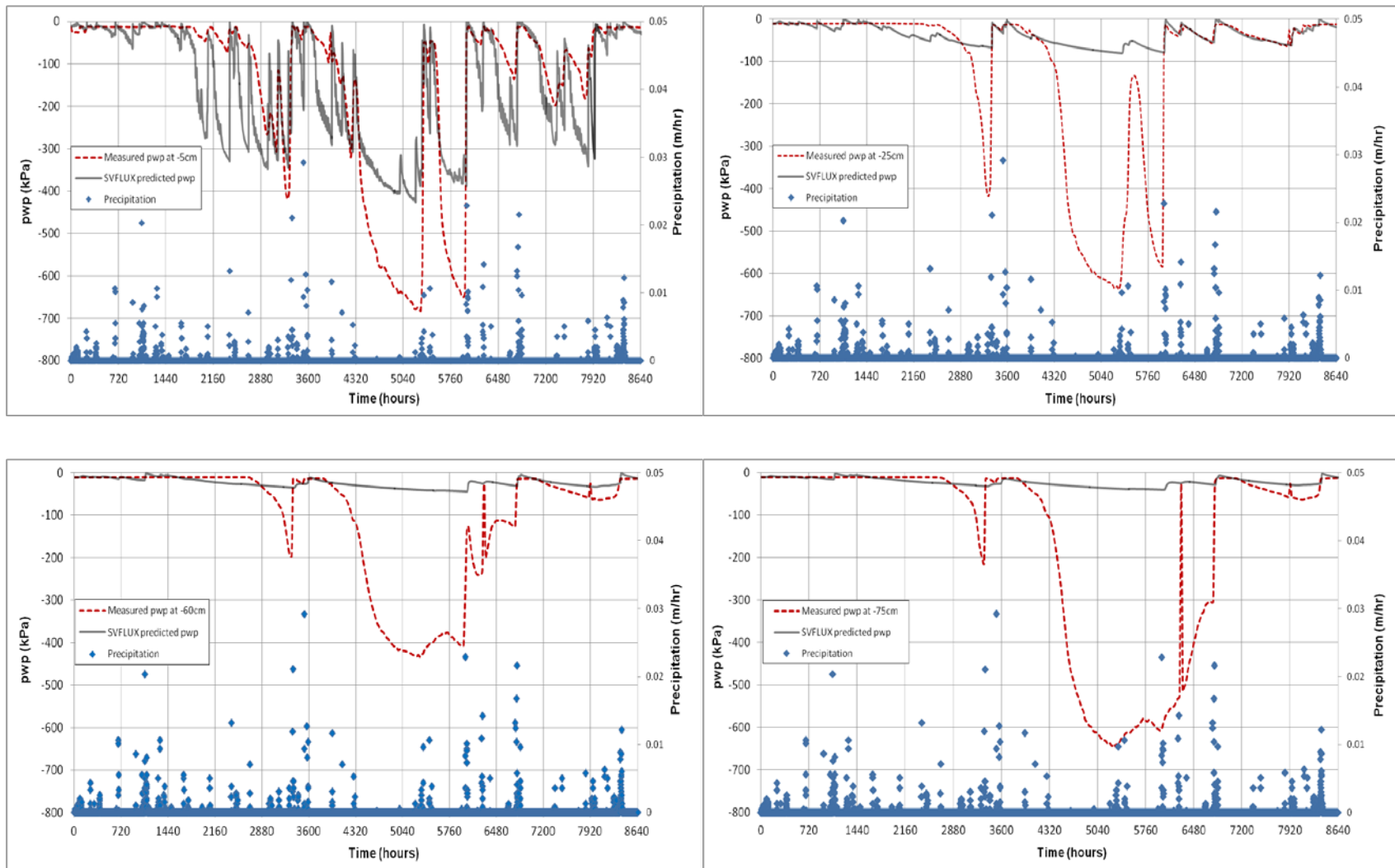


Figure 6.11. Measured and Predicted and Pore Water Pressures at the WIST Station.

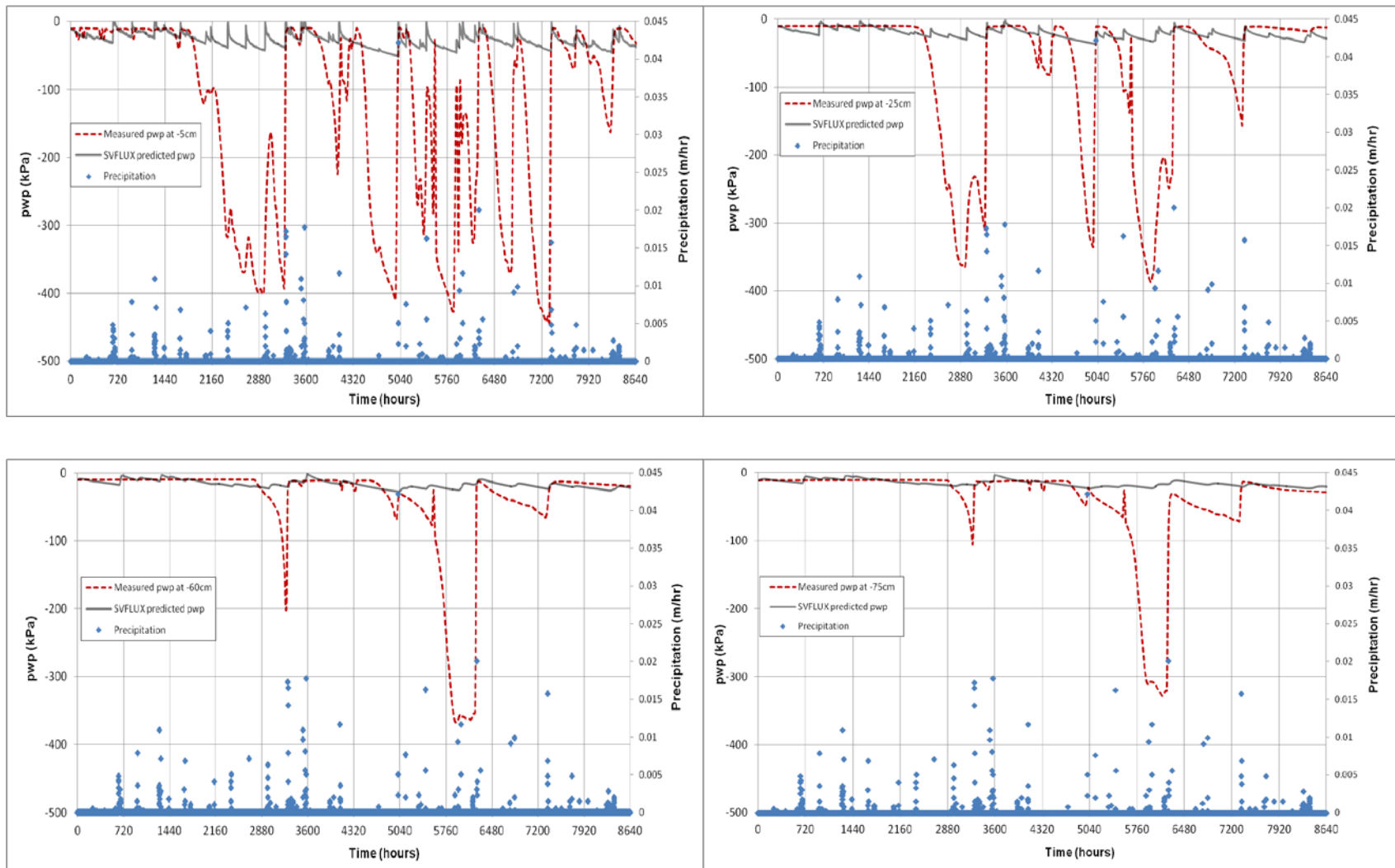


Figure 6.12. Measured and Predicted Pore Water Pressures at the STIL Station.

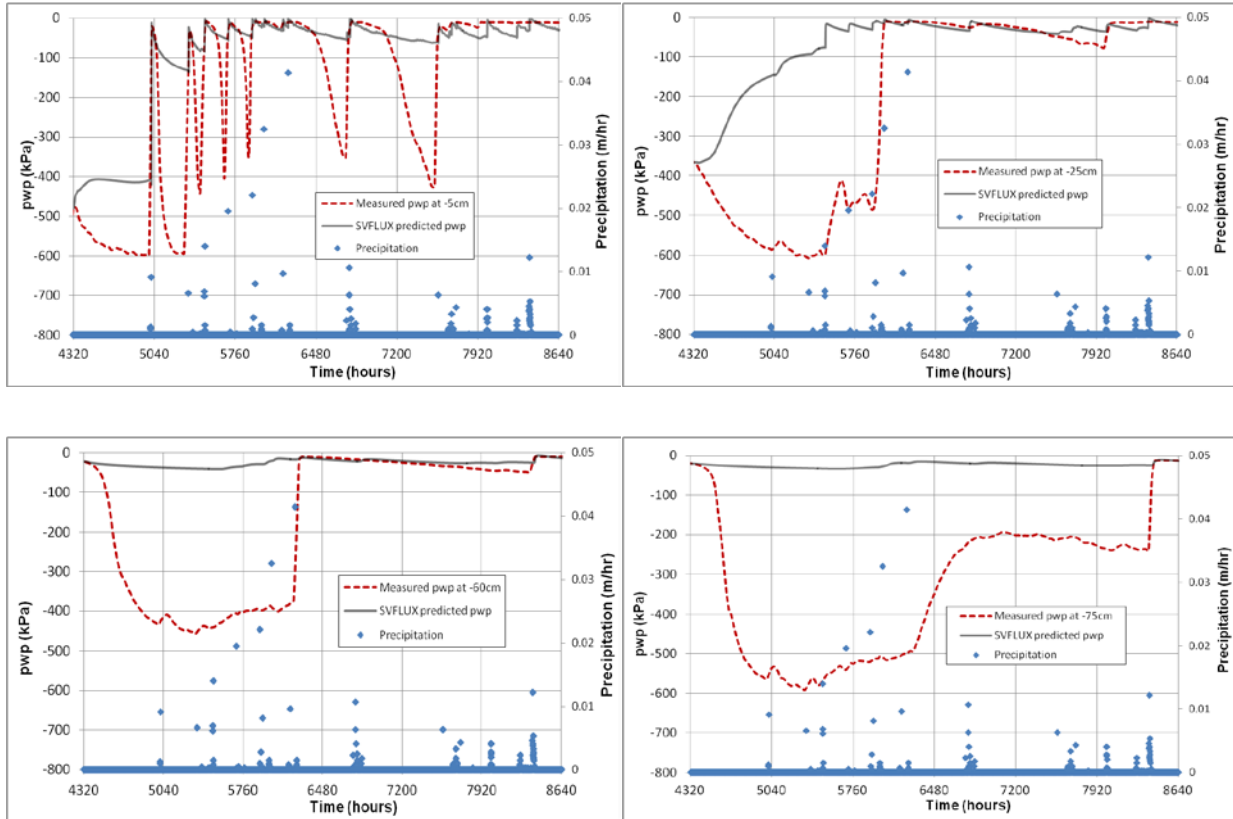


Figure 6.13. Measured and Predicted Pore Water Pressures at the WAUR Station with Initial Conditions at 4320 Hours.

7 CONCLUSIONS

The climate plays a significant role in controlling the material properties of pavements. Among the climatic variables, temperature, precipitation, relative humidity, percent sunshine, and wind speed make up the climatic input files for the EICM model in the mechanistic-empirical design guide. Furthermore, the depth to ground water table and Thornthwaite Moisture Index (TMI) control the boundary conditions in the pavement profile. In this study, large cluster of raw climate and soil moisture data were obtained from Oklahoma Mesonet for evaluation and used in creating the necessary input parameters for the climatic model in the MEPDG. The research team also gathered a large number of soil data from the USDA Web Soil Survey and the Oklahoma Mesonet. This study created 77 EICM input files representing the climate of each of the Oklahoma counties. These files were verified and are ready to be used in the EICM model in MEPDG. Furthermore, the research project also produced maps of ground water table using raw data obtained from the Oklahoma Water Resources Board (OWRB). These color and line contour maps can be used to determine the required lower bound moisture boundary conditions in the pavement analysis in the MEPDG. In addition, Thornthwaite Moisture Index (TMI) contour maps were created for Oklahoma using three different models.

Based on the historical climatic and soil data, the research team identified unique climatic and soil regions using the cluster analysis. The climatic regions indicate some climatic patterns throughout Oklahoma and since these regions were developed using the same climatic parameters employed in the creation of the climatic input files, the equilibrium suction ranges and depths to equilibrium (constant) suction values are expected to have similar values within each region. However, the soil regions do not show any clear clustering patterns, which is believed to be the limited number and range of soil data that was employed in the formation of the regions, and the variability (not showing a unique trend from one point to another) in the soil types across Oklahoma.

This study also established soil matric suction versus time history plots for 71 counties across Oklahoma using field measurements conducted by Mesonet over a long period of time. Some of these plots were employed in the validation of the moisture migration model in the EICM model as compared to the well-established model in the commercially available software SVFLUX. In the analysis, the predictions were compared to the measured values for the BOWL, STIL, WAUR, and WIST weather stations. In general, measured and predicted pore water pressures show more variation near the surface. Overall trends in pore water pressures and therefore moisture contents are predicted reasonably well by SVFLUX.

The results of this study can lead to some recommendations that could be considered in improving the climatic data and moisture (suction) boundary conditions for the mechanistic empirical design guide. Using the current and historical climatic data pertaining to Oklahoma future trends of the climatic parameters could be predicted using improved models. It is also believed that a careful analysis and interpretation of the climatic and soil data could be used in establishing realistic depths to constant suction and equilibrium suction profiles that are essential in establishing the envelope values of the moisture regime.

REFERENCES

Allen, R. G., I. A. Walter, R. Elliott, T. Howell, D. Itenfisu, and M. Jensen (2005). The ASCE Standardized Reference Evapotranspiration Equation. Environmental and Water Resources Institute of the American Society of Civil Engineers Final Report.

Arya, L. M. and Paris, J. F. (1981). A physicoempirical model to predict the soil moisture characteristic from practical-size distribution and bulk density data. *Soil Sci. Soc. Amer. J.*, 45, pp. 1023-1030.

ASCE Standardization of Reference Evapotranspiration Task Committee. (2005). "The ASCE Standardized Reference Evaporation Equation," Final Report.

Fredlund, D. G., and Rahardjo, H. (1993). "Soil Mechanics for Unsaturated Soils," John Wiley & Sons, New York.

Gupta, S., A. Ranaivoson, T. Edil, C. Benson, and A. Sawangsuriya (2007). Pavement Design Using Unsaturated Soil Technology. Report No. MN/RC-2007-11, Final Report.

Guttman, N.B. and Quayle, R. G. 1985. A Historical Perspective of U.S. Climate Divisions. *Bulletin of the American Meteorological Society*.

Heitzman, M., D. Timm, G. Tackle, D. Herzmann, and D. D. Truax (2011). Developing MEPDG Climatic Data Input Files for Mississippi. FHWA/MS-DOT RD-11-233 Final Report.

Illston, B. G., J. B. Basara, and K. C. Crawford (2004). Seasonal to Interannual Variations of Soil Moisture Measured in Oklahoma. *International Journal of Climate*, Vol. 24, pp. 1883-1896.

Illston, B. G., J. B. Basara, D. K. Fisher, R. Elliott, C. A. Fiebrich, K. C. Crawford, K. Humes, and E. Hunt. (2008). Mesoscale Monitoring of Soil Moisture across a Statewide Network. *Journal of Atmospheric and Oceanic Technology*, Vol. 25, pp. 167-182.

Mallery, D. and George, P. (2012). IBM SPSS Statistics 19 Step by Step A Simple Guide and Reference. Pearson, Boston.

Mather, J. R. (1974). Climatology: fundamentals and applications. McGraw-Hill, Inc.

McKeen, R. G. and L. D. Johnson (1990). Climate Controlled Soil Design Parameters for Mat Foundations. ASCE Journal of Geotechnical Engineering, Vol. 116, No. 7, pp. 1073-1094.

McPherson, R. A. (2007). Statewide Monitoring of the Mesoscale Environment: A Technical Update on the Oklahoma Mesonet. Journal of Atmospheric and Oceanic Technology, Vol. 24, pp. 301-321.

Nazarian, S., I. Abdallah, L. N. Mohammad, M. Abu-Farsakh, A. Puppala, and R. Bulut (2011). Modulus-Based Construction Specification for Compaction of Earthwork and Unbound Aggregate. Interim Report, National Cooperative Research Program NCHRP Project 10-84.

NCHRP, Calibration and Validation of the Enhanced Integrated Climatic Model for Pavement Design, National Cooperative Highway Research Program (NCHRP), Report No. 602, Transportation Research Board of the National Academies, Washington D.C., 2008.

Oh, J., D. Ryu, E. G. Fernando, and R. L. Lytton (2006). Estimation of Expected Moisture Contents for Pavements by Environmental and Soil Characteristics. Transportation Research Record: Journal of the Transportation Research Board, No. 1967, pp. 135-147.

Personal Communication (e-mail) with Chris Wagner, Team Leader, Federal Highway Administration Resource Center, Pavement and Materials Technical Services Team, Phone (404) 562-3693, E-mail: christopher.wagner@dot.gov

Personal Communication (e-mail and telephone) with Gregg Larson, Applied Research Associates, Inc., <http://www.ara.com/index.html>, E-mail: glarson@ara.com

Puppala, A. J., T. Manosuthikji, L. Hoyos, and S. Nazarian (2009). Moisture and Suction in Clay Subgrades Prior to Initiation of Pavement Cracking. TRB 88th Annual Meeting Compendium of Papers DVD, Transportation Research Board Annual Meeting 2009 Paper #09-1522, 13p.

Scott, B. L., Ochsner, T. E., Illston, B. G., Fiebrich, C. A., Basara, J. B., and Sutherland, A. J. (2013). New soil property improves Oklahoma Mesonet soil moisture estimates. American Meteorological Society, Vol. 00, pp. 1-11.

Swenson, S., J. Famiglietti, J. Basara, and J. Wahr (2008). Estimating Profile Soil Moisture and Groundwater Variations using GRACE and Oklahoma Mesonet Soil Moisture Data. Water Resources Research Journal, Vol. 44, pp. 1-12.

Thode, R., Gitirana, G., and Fredlund, M. (2011). "SVFLUX Saturated/Unsaturated Finite Element 2D/3D Seepage Modeling-Theory Manual," SoilVision Systems Ltd, Saskatoon, Saskatchewan, Canada.

Thornthwaite, C. W. (1948). An Approach Toward a Rational Classification of Climate. Geographical Review, Vol. 38, No. 1, pp. 54-94.

Thornthwaite, C. W. and J. R. Mather (1955). The Water Balance. Publication of Climatology, Vol. 8, No. 1, 104p.

van Genuchten, M. T., Leij, F. J., and Yates, S. R (1991). The RETC code for quantifying the hydraulic functions of unsaturated soils. U.S. Environmental Protection Agency Rep. EPA/600-91/065, pp. 93.

Witczak, M. W., C. E. Zapata, and W. N. Houston (2006). Models Incorporated into the Current Enhanced Integrated Climatic Model for Version 1.0 of the ME-PDG. NCHRP 9-23 Project Report.

Zapata, C. E., D. Andrei, M. W. Witczak, and W. N. Houston (2007). Incorporation of Environmental Effects in Pavement Design. Transportation Research Record: Journal of the Transportation Research Board, pp. 667-693.

APPENDICES

Appendix A

Table A1. Climatic Input Files

Weather Station ID	City	County	Latitude (°)	Longitude (°)	Elevation (m)	Data Available Period	MEPDG Input File Name
ADAX	Ada	Pontotoc	34.79851	-96.66909	295	01/01/1994-06/30/2012	ADAX.hcd
ALTU	Altus	Jackson	34.58722	-99.33808	416	01/01/1994-06/30/2012	ALTU.hcd
ARD2	Ardmore	Carter	34.19258	-97.08568	266	02/22/2004-06/30/2012	ARD2.hcd
ARDM*	Ardmore	Carter	34.19220	-97.08500	266	01/01/1994-02/18/2004	ARD2.hcd
ARNE	Arnett	Ellis	36.07204	-99.90308	719	01/01/1994-06/30/2012	ARNE.hcd
BEAV	Beaver	Beaver	36.80253	-100.53012	758	01/01/1994-06/30/2012	BEAV.hcd
BESS	Bessie	Washita	35.40185	-99.05847	511	01/01/1994-06/30/2012	BESS.hcd
BIXB	Bixby	Tulsa	35.96305	-95.86621	184	01/01/1994-06/30/2012	BIXB.hcd
BOIS	Boise City	Cimarron	36.69256	-102.49713	1267	01/01/1994-06/30/2012	BOIS.hcd
BOWL	Bowlegs	Seminole	35.17156	-96.63121	281	01/01/1994-06/30/2012	BOWL.hcd
BREC	Breckinridge	Garfield	36.41201	-97.69394	352	01/01/1994-06/30/2012	BREC.hcd
BUFF	Buffalo	Harper	36.83129	-99.64101	559	01/01/1994-06/30/2012	BUFF.hcd
BURN	Burneyville	Love	33.89376	-97.26918	228	01/01/1994-06/30/2012	BURN.hcd
BUTL	Butler	Custer	35.59150	-99.27059	520	01/01/1994-06/30/2012	BUTL.hcd
CENT	Centrahoma	Coal	34.60896	-96.33309	208	01/01/1994-06/30/2012	CENT.hcd
CHAN	Chandler	Lincoln	35.65282	-96.80407	291	01/01/1994-06/30/2012	CHAN.hcd

Weather Station ID	City	County	Latitude (°)	Longitude (°)	Elevation (m)	Data Available Period	MEPDG Input File Name
CHER	Cherokee	Alfalfa	36.74813	-98.36274	362	01/01/1994-06/30/2012	CHER.hcd
CHEY	Cheyenne	Roger Mills	35.54615	-99.72790	694	01/01/1994-06/30/2012	CHEY.hcd
CHIC	Chickasha	Grady	35.03236	-97.91446	328	01/01/1994-06/30/2012	CHIC.hcd
CLOU	Cloudy	Pushmataha	34.22321	-95.24870	221	01/01/1994-06/30/2012	CLOU.hcd
CLRM	Claremore	Rogers	36.32112	-95.64617	207	07/10/2002-06/30/2012	CLRM.hcd
CLAR*	Claremore	Rogers	36.31720	-95.64170	213	01/01/1994-07/07/2002	CLRM.hcd
COPA	Copan	Washington	36.90980	-95.88553	250	01/01/1994-06/30/2012	COPA.hcd
DURA	Durant	Bryan	33.92075	-96.32027	197	01/01/1994-06/30/2012	DURA.hcd
ELRE	El Reno	Canadian	35.54848	-98.03654	419	01/01/1994-06/30/2012	ELRE.hcd
ERIC	Erick	Beckham	35.20494	-99.80344	603	01/01/1994-06/30/2012	ERIC.hcd
EUFA	Eufaula	McIntosh	35.30324	-95.65707	200	01/01/1994-06/30/2012	EUFA.hcd
FAIR	Fairview	Major	36.26353	-98.49766	405	01/01/1994-06/30/2012	FAIR.hcd
FTCB	Fort Cobb	Caddo	35.14887	-98.46607	422	01/01/1994-06/30/2012	FTCB.hcd
GOOD	Goodwell	Texas	36.60183	-101.60130	997	01/01/1994-06/30/2012	GOOD.hcd
GRA2	Grandfield	Tillman	34.23944	-98.74358	341	04/01/1999-06/30/2012	GRA2.hcd
GRAN*	Grandfield	Tillman	34.23920	-98.73970	342	01/01/1994-03/16/1999	GRA2.hcd
GUTH	Guthrie	Logan	35.84891	-97.47978	330	01/01/1994-06/30/2012	GUTH.hcd
HOBA	Hobart	Kiowa	34.98971	-99.05283	478	01/01/1994-06/30/2012	HOBA.hcd
HOLD	Holdenville	Hughes	35.07073	-96.35595	280	05/28/2009-06/30/2012	HOLD.hcd

Weather Station ID	City	County	Latitude (°)	Longitude (°)	Elevation (m)	Data Available Period	MEPDG Input File Name
CALV*	Calvin	Hughes	34.99240	-96.33422	234	01/01/1994-03/18/2009	HOLD.hcd
HOLL	Gould	Harmon	34.68550	-99.83331	497	01/01/1994-06/30/2012	HOLL.hcd
HUGO	Hugo	Choctaw	34.03084	-95.54011	175	01/01/1994-06/30/2012	HUGO.hcd
IDAB	Idabel	McCurtain	33.83013	-94.88030	110	01/01/1994-06/30/2012	IDAB.hcd
JAYX	Jay	Delaware	36.48210	-94.78287	304	01/01/1994-06/30/2012	JAYX.hcd
KETC	Ketchum Ranch	Stephens	34.52887	-97.76484	341	01/01/1994-06/30/2012	KETC.hcd
KIN2	Kingfisher	Kingfisher	35.85431	-97.95442	323	03/05/2009-06/30/2012	KIN2.hcd
KING*	Kingfisher	Kingfisher	35.88050	-97.91121	319	01/01/1994-03/05/2009	KIN2.hcd
LANE	Lane	Atoka	34.30876	-95.99716	181	01/01/1994-06/30/2012	LANE.hcd
MADI	Medicine Park	Marshall	34.03579	-96.94394	232	01/01/1994-06/30/2012	MADI.hcd
MANG	Mangum	Greer	34.83592	-99.42398	460	01/01/1994-06/30/2012	MANG.hcd
MAYR	May Ranch	Woods	36.98707	-99.01109	555	01/01/1994-06/30/2012	MAYR.hcd
MCAL	McAlester	Pittsburg	34.88231	-95.78096	230	01/01/1994-06/30/2012	MCAL.hcd
MEDF	Medford	Grant	36.79242	-97.74577	332	01/01/1994-06/30/2012	MEDF.hcd
MEDI	Medicine Park	Comanche	34.72921	-98.56936	487	01/01/1994-06/30/2012	MEDI.hcd
MIAM	Miami	Ottawa	36.88832	-94.84437	247	01/01/1994-06/30/2012	MIAM.hcd
NEWK	Newkirk	Kay	36.89810	-96.91035	366	01/01/1994-06/30/2012	NEWK.hcd
NOWA	Delaware	Nowata	36.74374	-95.60795	206	01/01/1994-06/30/2012	NOWA.hcd
NRMN	Norman	Cleveland	35.23611	-97.46488	357	07/31/2002-06/30/2012	NRMN.hcd

Weather Station ID	City	County	Latitude (°)	Longitude (°)	Elevation (m)	Data Available Period	MEPDG Input File Name
NORM*	Norman	Cleveland	35.25560	-97.48360	360	01/01/1994-06/30/2002	NRMN.hcd
OILT	Oilton	Creek	36.03126	-96.49749	255	01/01/1994-06/30/2012	OILT.hcd
OKEM	Okemah	Okfuskee	35.43172	-96.26265	263	01/01/1994-06/30/2012	OKEM.hcd
OKMU	Morris	Okmulgee	35.58211	-95.91473	205	01/01/1994-06/30/2012	OKMU.hcd
PAUL	Pauls Valley	Garvin	34.71550	-97.22924	291	01/01/1994-06/30/2012	PAUL.hcd
PAWN	Pawnee	Pawnee	36.36114	-96.76986	283	01/01/1994-06/30/2012	PAWN.hcd
PORT	Clarksville	Wagoner	35.82570	-95.55976	193	11/05/1999-06/30/2012	PORT.hcd
TULL*	Tulahassee	Wagoner	35.83970	-95.41330	189	01/01/1994-11/04/1999	PORT.hcd
PRYO	Adair	Mayes	36.36914	-95.27138	201	01/01/1994-06/30/2012	PRYO.hcd
PUTN	Putnam	Dewey	35.89904	-98.96038	589	01/01/1994-06/30/2012	PUTN.hcd
REDR	Red Rock	Noble	36.35590	-97.15306	293	01/01/1994-06/30/2012	REDR.hcd
SALL	Sallisaw	Sequoyah	35.43815	-94.79805	157	01/01/1994-06/30/2012	SALL.hcd
SHAW	Shawnee	Pottawatomie	35.36492	-96.94822	328	01/01/1994-06/30/2012	SHAW.hcd
SPEN	Spencer	Oklahoma	35.54208	-97.34146	373	01/01/1994-06/30/2012	SPEN.hcd
STIG	Stigler	Haskell	35.26527	-95.18116	173	01/01/1994-06/30/2012	STIG.hcd
STIL	Stillwater	Payne	36.12093	-97.09527	272	01/01/1994-06/30/2012	STIL.hcd
SULP	Sulphur	Murray	34.56610	-96.95048	320	01/01/1994-06/30/2012	SULP.hcd
TAHL	Tahlequah	Cherokee	35.97235	-94.98671	290	01/01/1994-06/30/2012	TAHL.hcd
TISH	Tishomingo	Johnston	34.33262	-96.67895	268	01/01/1994-06/30/2012	TISH.hcd

Weather Station ID	City	County	Latitude (°)	Longitude (°)	Elevation (m)	Data Available Period	MEPDG Input File Name
VINI	Vinita	Craig	36.77536	-95.22094	236	01/01/1994-06/30/2012	VINI.hcd
WAL2	Walters	Cotton	34.39957	-98.34569	323	03/12/2012-06/30/2012	WAL2.hcd
WALT*	Walters	Cotton	34.36470	-98.32025	308	01/01/1994-03/12/2012	WAL2.hcd
WASH	Washington	McClain	34.98224	-97.52109	345	01/01/1994-06/30/2012	WASH.hcd
WATO	Watonga	Blaine	35.84185	-98.52615	517	01/01/1994-06/30/2012	WATO.hcd
WAUR	Waurika	Jefferson	34.16775	-97.98815	283	01/01/1994-06/30/2012	WAUR.hcd
WEBR	Webbers Falls	Muskogee	35.48900	-95.12330	145	04/16/2008-06/30/2012	WEBR.hcd
WEBB*	Webbers Falls	Muskogee	35.47298	-95.13209	145	01/01/1994-04/16/2008	WEBR.hcd
WEST	Westville	Adair	36.01100	-94.64496	348	01/01/1994-06/30/2012	WEST.hcd
WILB	Wilburton	Latimer	34.90092	-95.34805	199	01/01/1994-06/30/2012	WILB.hcd
WIST	Wister	LeFlore	34.98426	-94.68778	143	01/01/1994-06/30/2012	WIST.hcd
WOOD	Woodward	Woodward	36.42329	-99.41682	625	01/01/1994-06/30/2012	WOOD.hcd
WYNO	Wynona	Osage	36.51806	-96.34222	269	01/01/1994-06/30/2012	WYNO.hcd

Retired Stations. The retired station information is given in Table A2.

Table A2. Retired Station Information

Station ID	Information
ARDM	The site was moved 180 feet northwest and renamed ARD2.
CALV	The site was moved 5 1/2 miles north-northwest and renamed HOLD.
CLAR	The site was moved 4/10 of a mile northwest and renamed CLRM.
GRAN	The site was moved 1/4 of a mile west and renamed GRA2.
KING	The site was moved 3 miles southwest and renamed KIN2.
NORM	The site was moved 1 mile south-southeast and renamed NRMN.
TULL	The site was moved 8 1/4 miles west and renamed PORT.
WALT	The site was moved 2 3/4 miles northwest and renamed WAL2.
WEBB	The site was moved 1 1/4 miles north-northeast and renamed WEBR.

Appendix B Matric Suction versus Time Plots at Various Depths at STIL Mesonet Weather Station.

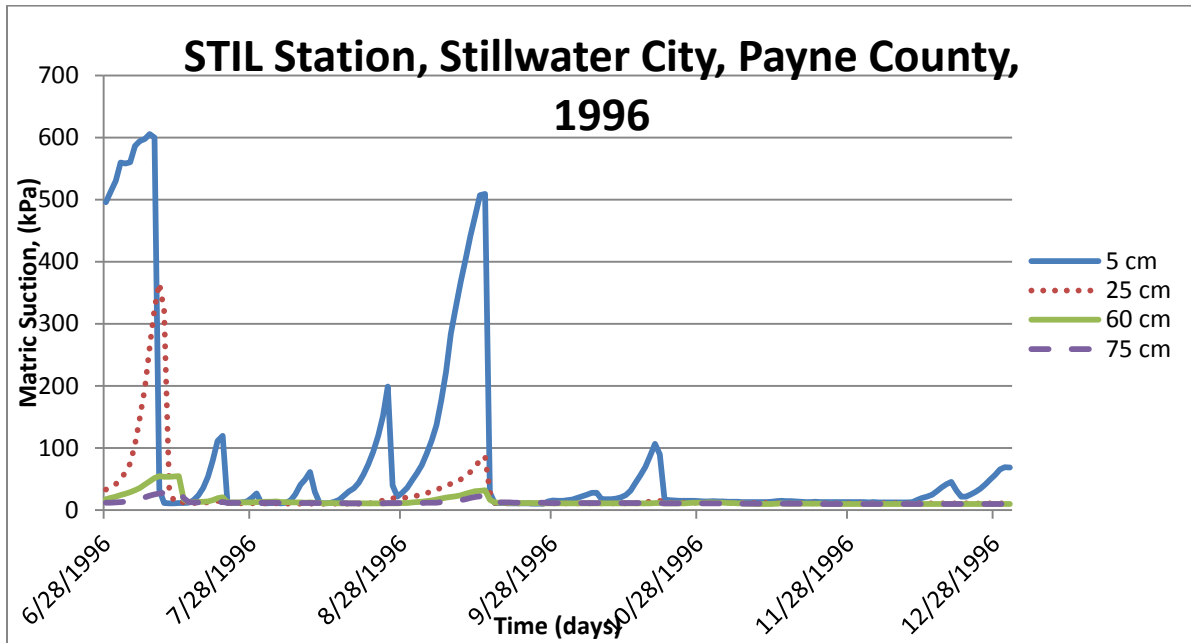


Figure B1. Matric Suction versus Time Plots For 1996.

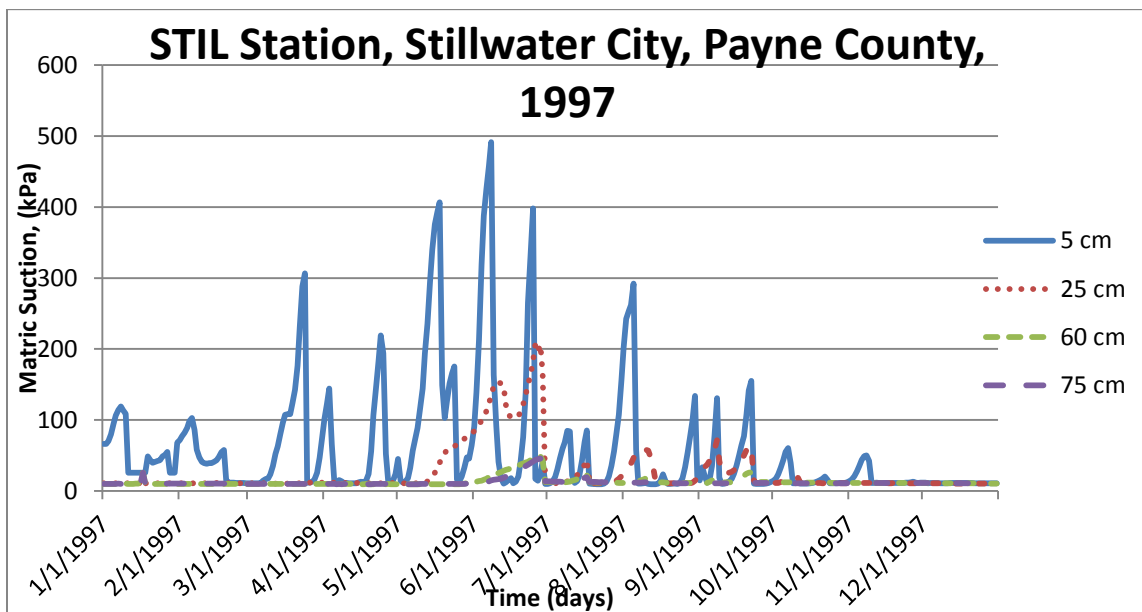


Figure B2. Matric Suction versus Time Plots For 1997.

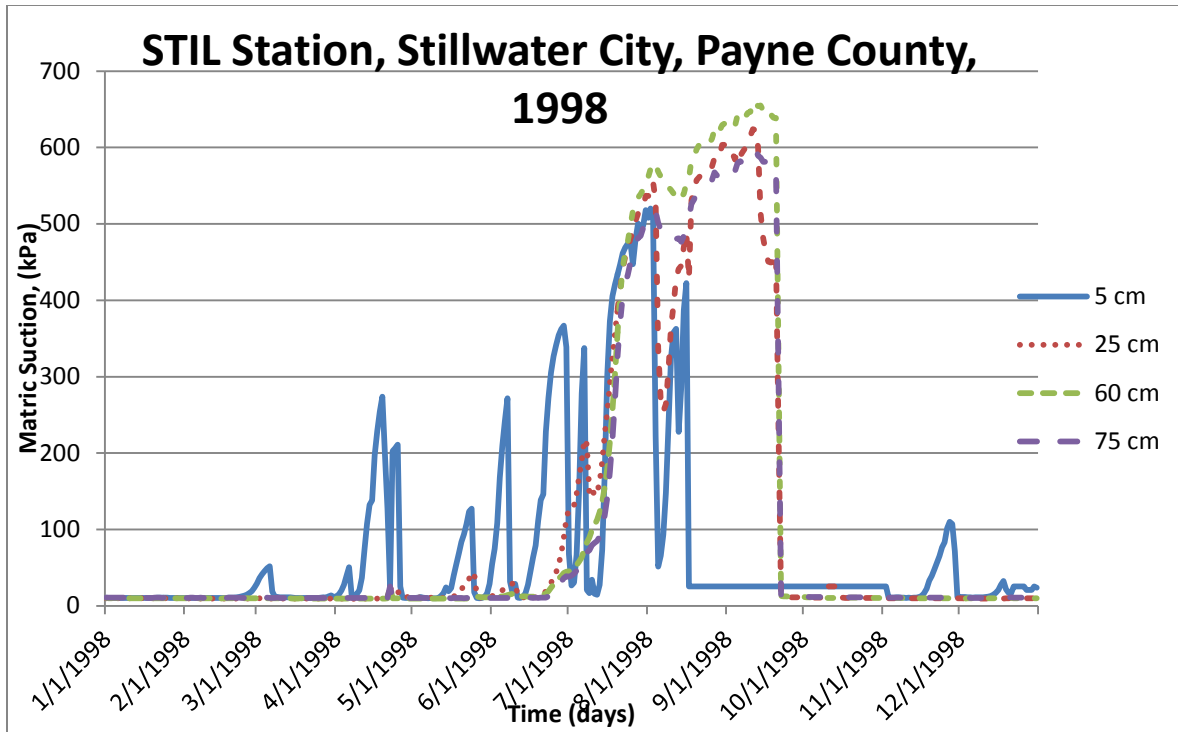


Figure B3. Matric Suction versus Time Plots For 1998.

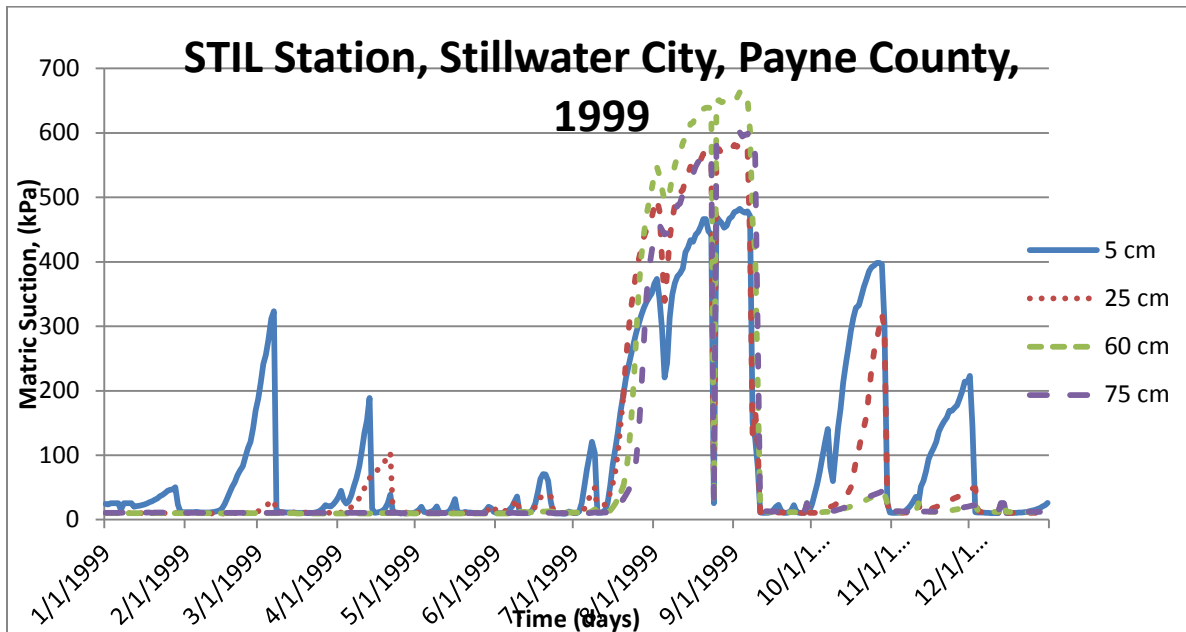


Figure B4. Matric Suction versus Time Plots For 1999.

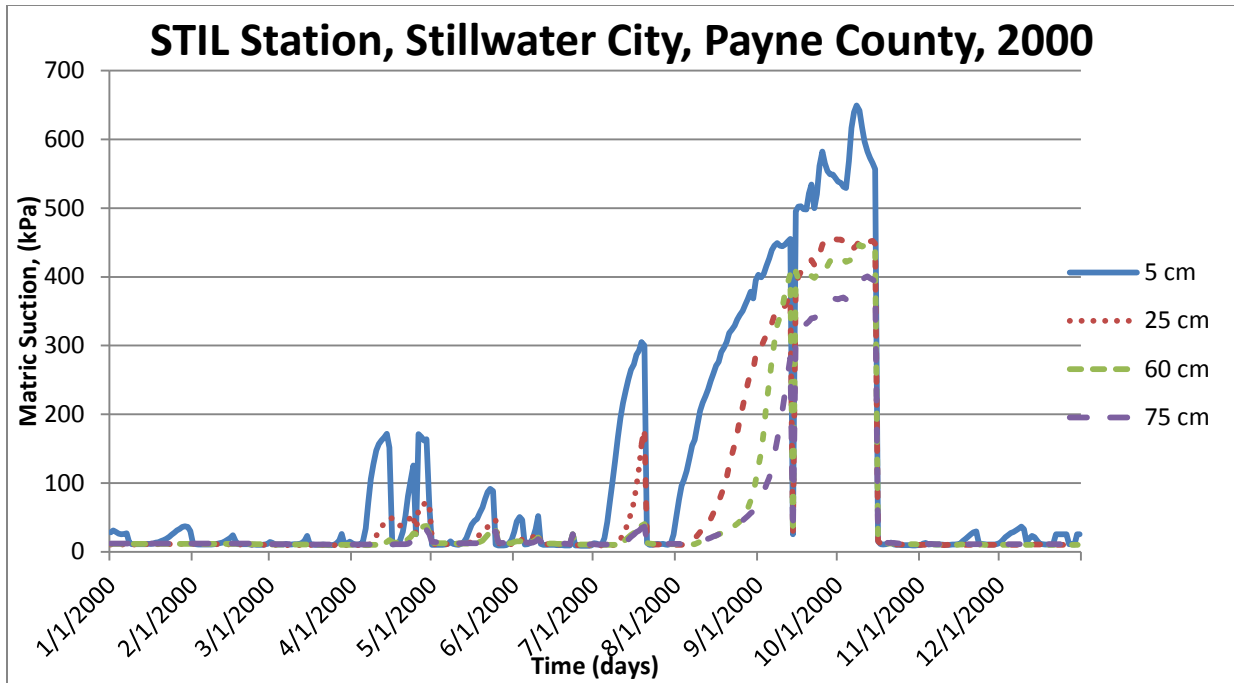


Figure B5. Matric Suction versus Time Plots For 2000.

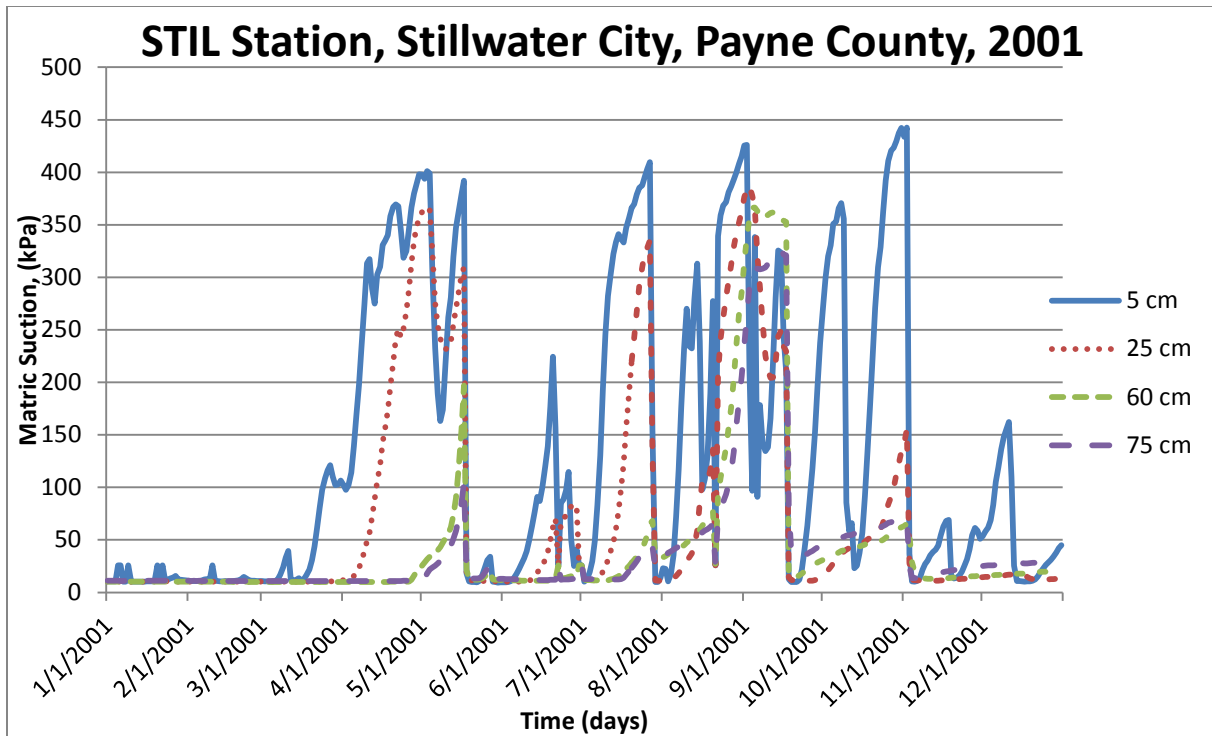


Figure B6. Matric Suction versus Time Plots For 2001.

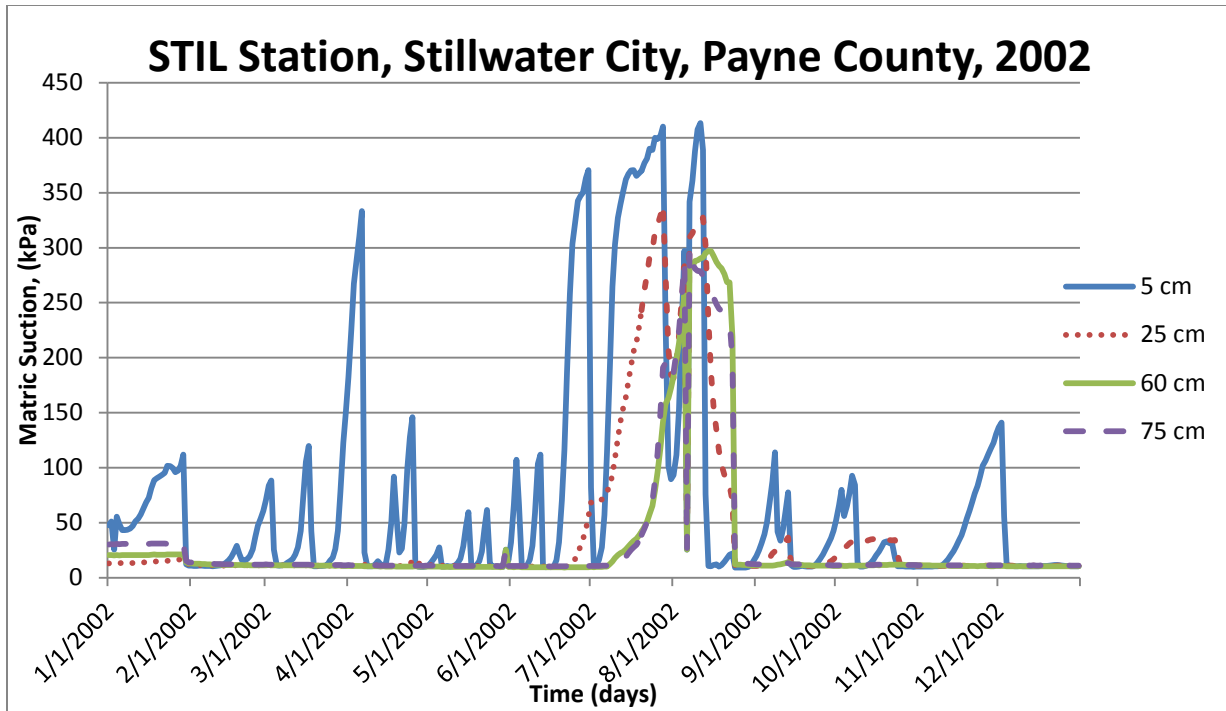


Figure B7. Matric Suction versus Time Plots For 2002.

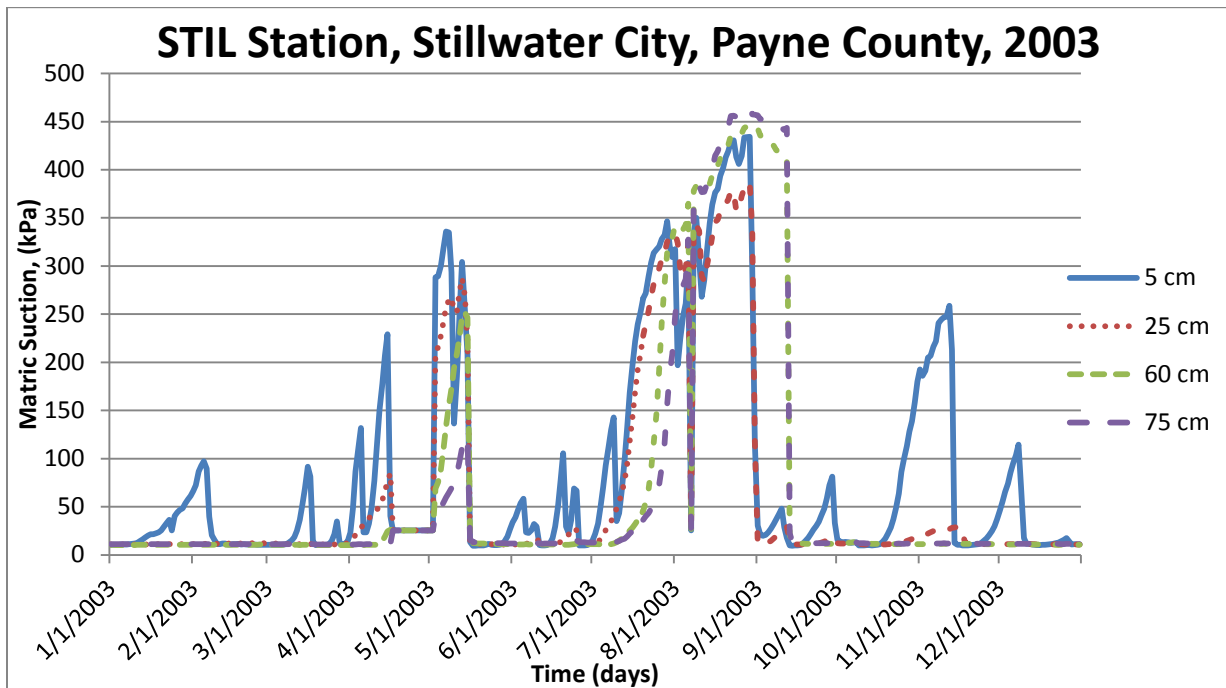


Figure B8. Matric Suction versus Time Plots For 2003.

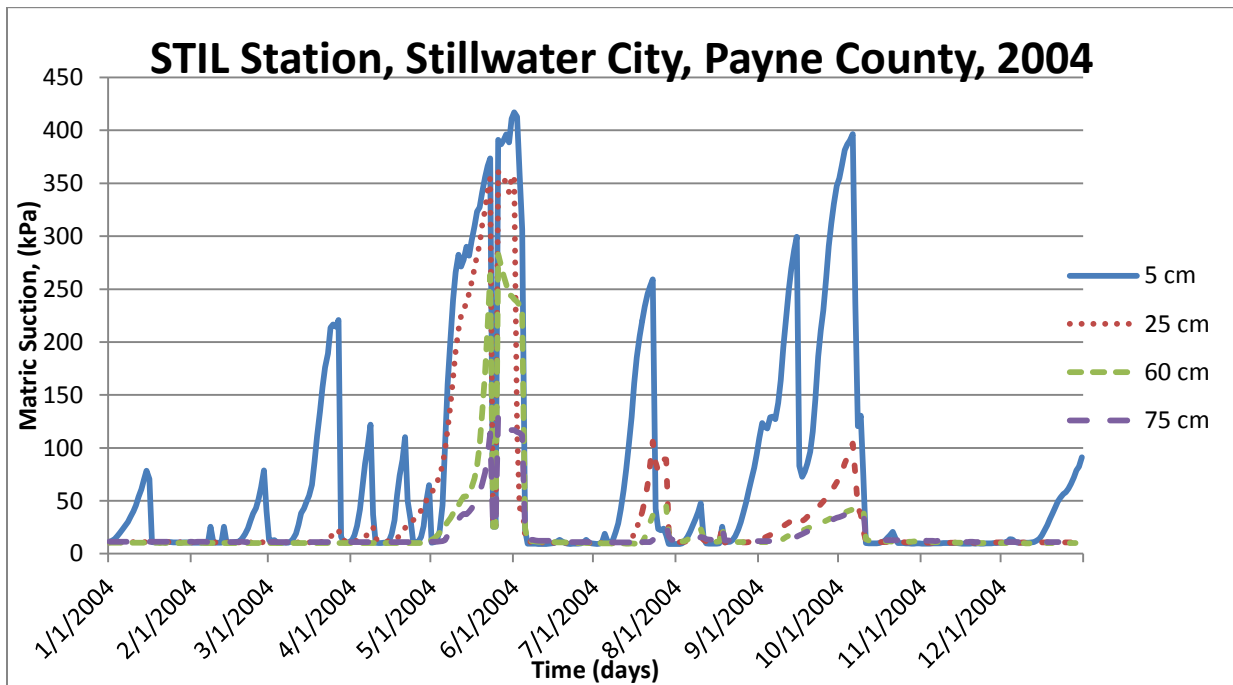


Figure B9. Matrix Suction versus Time Plots For 2004.

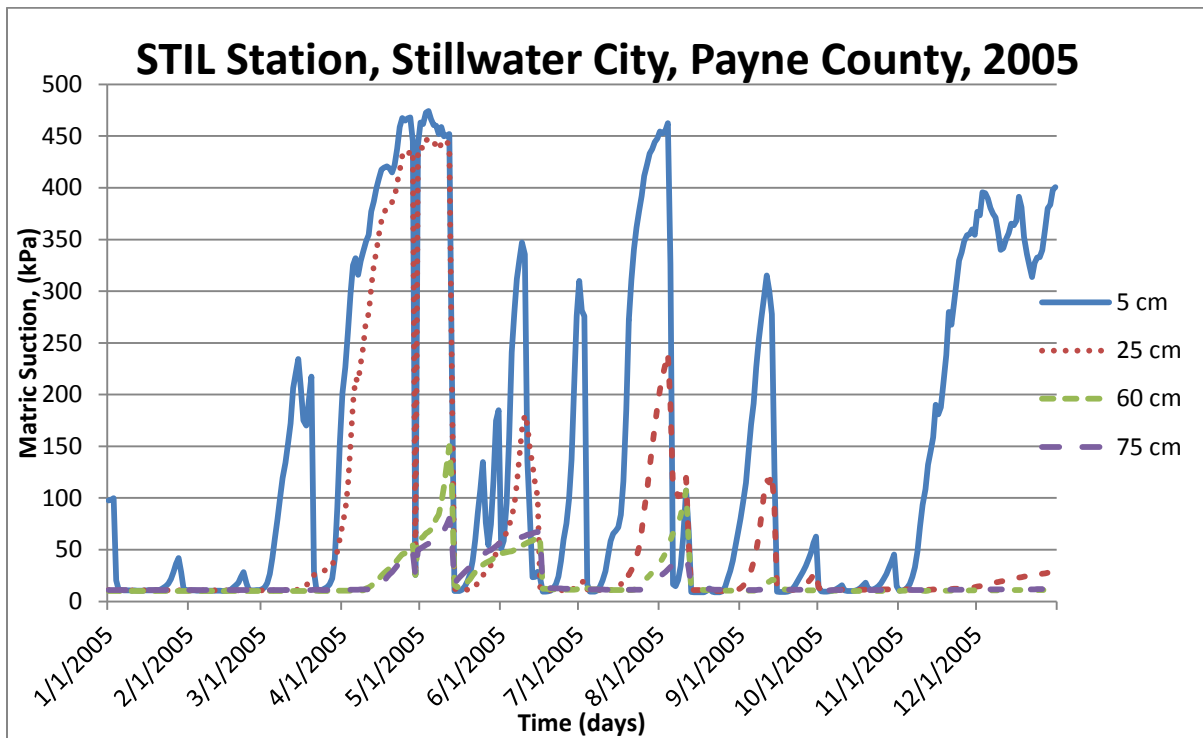


Figure B10. Matrix Suction versus Time Plots For 2005.

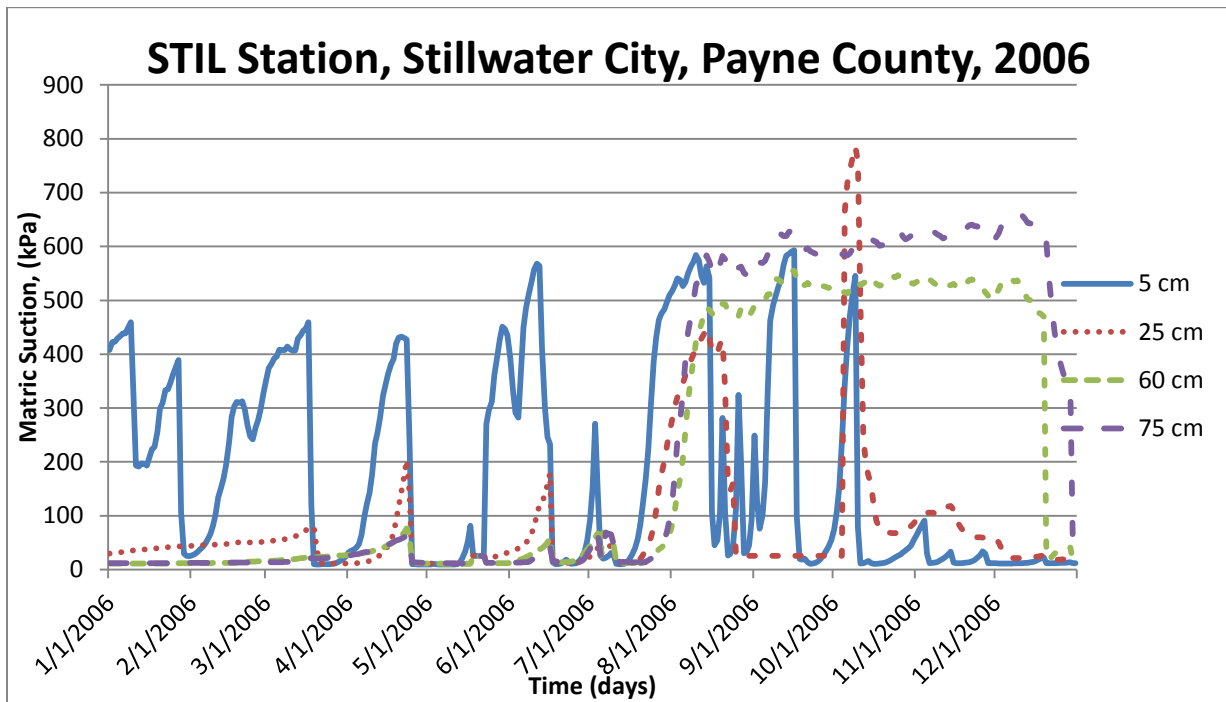


Figure B11. Matric Suction versus Time Plots For 2006.

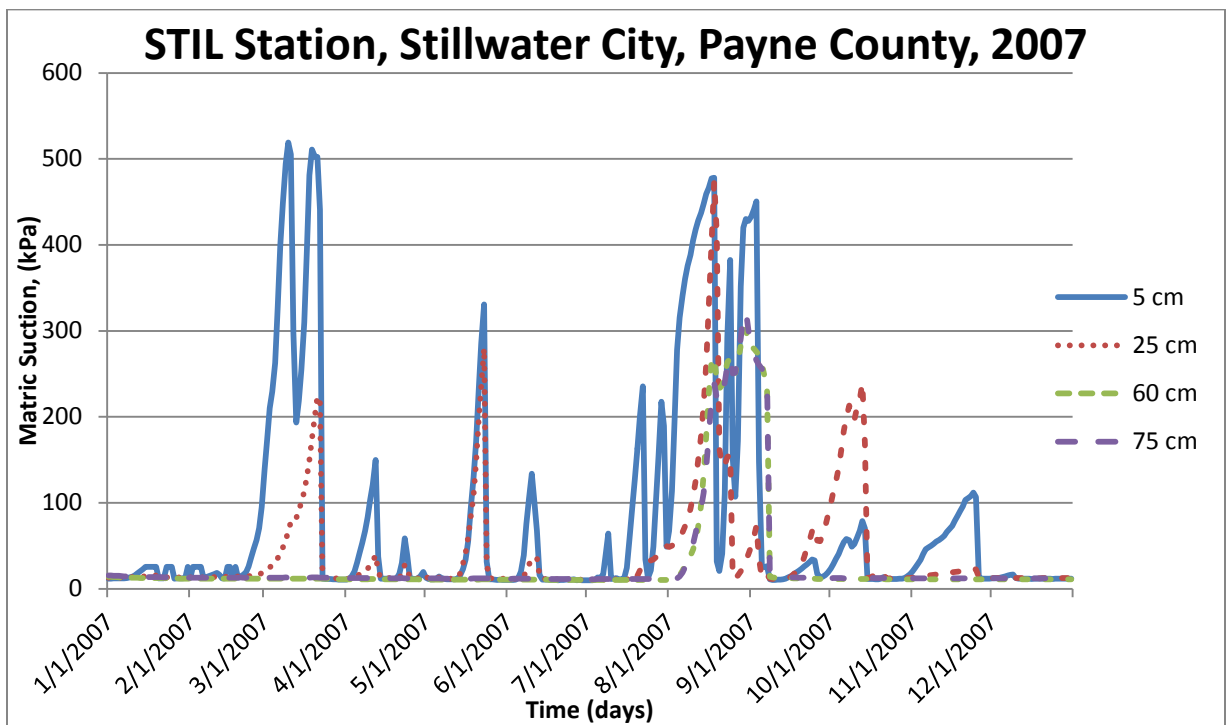


Figure B12. Matric Suction versus Time Plots For 2007.

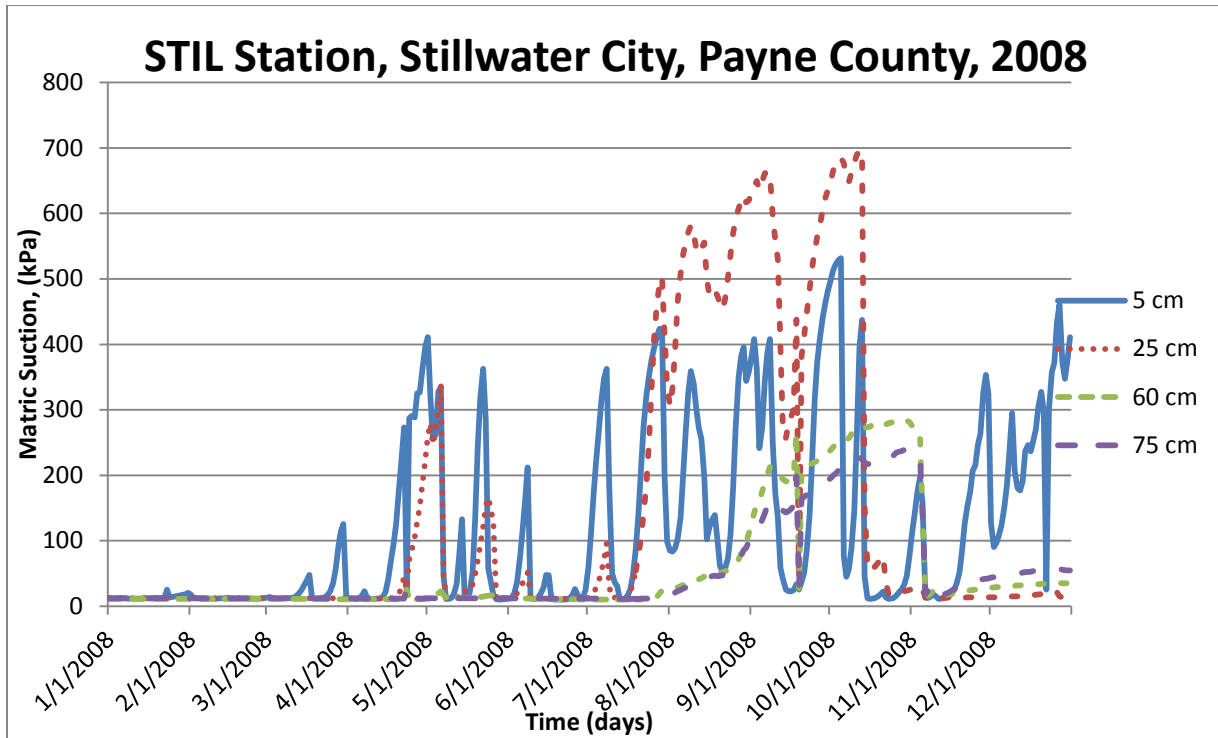


Figure B13. Matric Suction versus Time Plots For 2008.

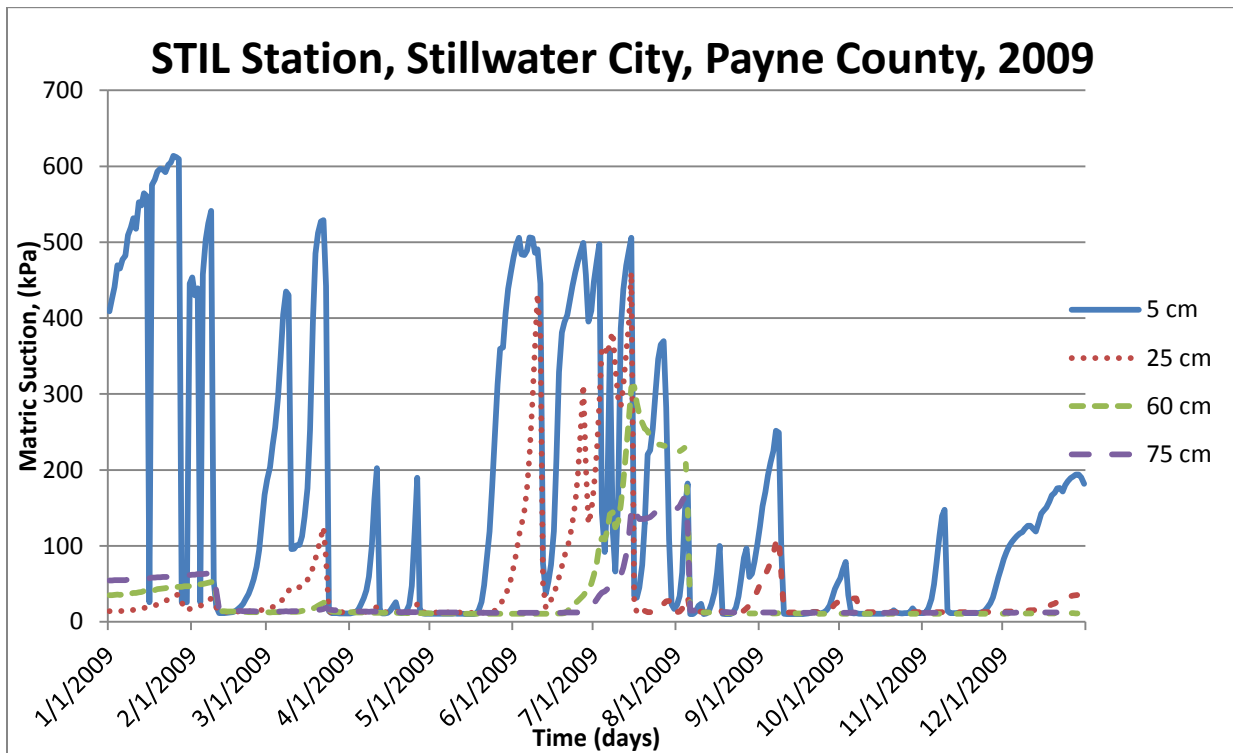


Figure B14. Matric Suction versus Time Plots For 2009.

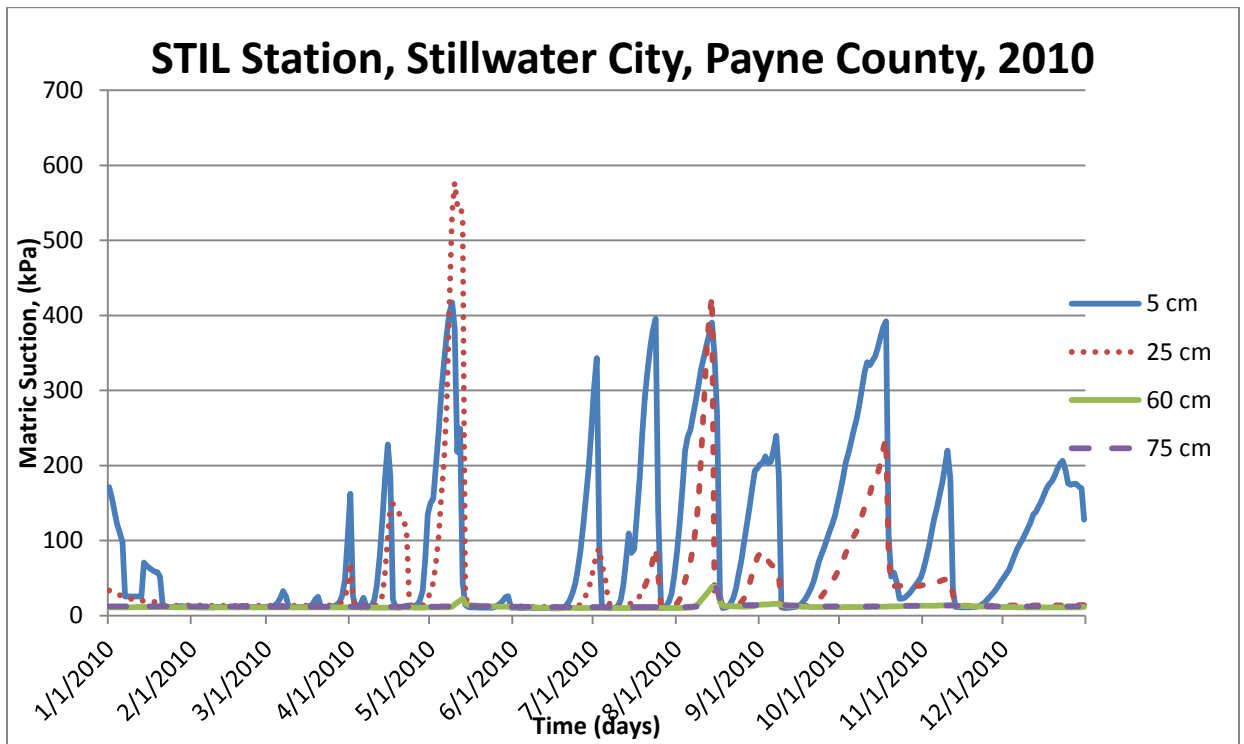


Figure B15. Matric Suction versus Time Plots For 2010.

Table B1. Time Period over which Matric Suction Measurements were Collected.

Weather Station ID	City	County	Latitude (°)	Longitude (°)	Elevation (m)	Data Available Period
ADAX	Ada	Pontotoc	34.79851	-96.66909	295	01/01/00-12/31/12
ALTU	Altus	Jackson	34.58722	-99.33808	416	05/06/97-12/31/12
ARDM	Ardmore	Carter	34.19220	-97.08500	266	10/11/96-02/16/04
ARNE	Arnett	Ellis	36.07204	-99.90308	719	01/01/97-12/31/12
BEAV	Beaver	Beaver	36.80253	-100.53012	758	01/01/97-12/31/10
BESS	Bessie	Washita	35.40185	-99.05847	511	05/10/99-12/31/12
BIXB	Bixby	Tulsa	35.96305	-95.86621	184	01/01/97-12/31/12
BOIS	Boise City	Cimarron	36.69256	-102.49713	1267	10/23/96-12/31/12
BOWL	Bowlegs	Seminole	35.17156	-96.63121	281	06/24/96-12/31/10
BREC	Breckinridge	Garfield	36.41201	-97.69394	352	10/05/99-12/31/12
BUFF	Buffalo	Harper	36.83129	-99.64101	559	11/18/99-12/31/12
BURN	Burneyville	Love	33.89376	-97.26918	228	03/06/97-12/31/12
BUTL	Butler	Custer	35.59150	-99.27059	520	01/22/97-12/31/10
CENT	Centrahoma	Coal	34.60896	-96.33309	208	01/01/97-12/31/12
CHAN	Chandler	Lincoln	35.65282	-96.80407	291	06/24/96-12/31/12
CHER	Cherokee	Alfalfa	36.74813	-98.36274	362	01/01/00-12/31/10
CHEY	Cheyenne	Roger Mills	35.54615	-99.72790	694	12/12/96-12/31/12
CLOU	Cloudy	Pushmataha	34.22321	-95.24870	221	01/05/00-12/31/12
COPA	Copan	Washington	36.90980	-95.88553	250	08/12/99-12/31/12
DURA	Durant	Bryan	33.92075	-96.32027	197	12/05/96-12/31/12
ELRE	El Reno	Canadian	35.54848	-98.03654	419	06/25/96-12/31/12
ERIC	Erick	Beckham	35.20494	-99.80344	603	06/24/00-12/31/12
EUFA	Eufaula	McIntosh	35.30324	-95.65707	200	05/20/97-06/01/06
FAIR	Fairview	Major	36.26353	-98.49766	405	02/18/97-04/29/12
FTCB	Fort Cobb	Caddo	35.14887	-98.46607	422	03/01/97-12/31/12
GOOD	Goodwell	Texas	36.60183	-101.60130	997	08/06/97-12/31/12
GRA2	Grandfield	Tillman	34.23944	-98.74358	341	05/12/99-12/31/12
GUTH	Guthrie	Logan	35.84891	-97.47978	330	10/14/99-12/31/12
HOBA	Hobart	Kiowa	34.98971	-99.05283	478	02/19/97-07/01/05
HOLD	Holdenville	Hughes	35.07073	-96.35595	280	09/22/09-12/31/12
HOLL	Gould	Harmon	34.68550	-99.83331	497	03/17/97-12/31/12
HUGO	Hugo	Choctaw	34.03084	-95.54011	175	01/06/00-12/31/12
IDAB	Idabel	McCurtain	33.83013	-94.88030	110	06/10/99-12/31/12
JAYX	Jay	Delaware	36.48210	-94.78287	304	09/22/99-12/31/12
KETC	Ketchum Ranch	Stephens	34.52887	-97.76484	341	03/08/97-12/31/12
KING	Kingfisher	Kingfisher	35.88050	-97.91121	319	06/25/96-03/02/09

Weather Station ID	City	County	Latitude (°)	Longitude (°)	Elevation (m)	Data Available Period
LANE	Lane	Atoka	34.30876	-95.99716	181	02/01/97-12/31/12
MANG	Mangum	Greer	34.83592	-99.42398	460	03/06/97-06/01/12
MAYR	May Ranch	Woods	36.98707	-99.01109	555	10/16/96-12/31/12
MCAL	McAlester	Pittsburg	34.88231	-95.78096	230	02/15/00-12/31/12
MEDI	Medicine Park	Comanche	34.72921	-98.56936	487	12/28/99-12/31/12
MIAM	Miami	Ottawa	36.88832	-94.84437	247	11/23/96-12/31/12
NEWK	Newkirk	Kay	36.89810	-96.91035	366	08/11/99-12/31/12
NOWA	Delaware	Nowata	36.74374	-95.60795	206	08/29/97-12/31/12
NRMN	Norman	Cleveland	35.23611	-97.46488	357	09/24/02-12/31/12
OILT	Oilton	Creek	36.03126	-96.49749	255	10/13/99-12/31/12
OKEM	Okemah	Okfuskee	35.43172	-96.26265	263	02/15/00-12/31/12
OKMU	Morris	Okmulgee	35.58211	-95.91473	205	02/09/00-12/31/12
PAUL	Pauls Valley	Garvin	34.71550	-97.22924	291	10/28/99-12/31/12
PAWN	Pawnee	Pawnee	36.36114	-96.76986	283	11/13/96-12/31/12
PORT	Clarksville	Wagoner	35.82570	-95.55976	193	11/26/99-12/31/12
PRYO	Adair	Mayes	36.36914	-95.27138	201	09/23/99-12/31/12
PUTN	Putnam	Dewey	35.89904	-98.96038	589	12/17/96-12/31/12
REDR	Red Rock	Noble	36.35590	-97.15306	293	08/25/99-12/31/12
SALL	Sallisaw	Sequoyah	35.43815	-94.79805	157	10/12/04-12/31/12
SHAW	Shawnee	Pottawatomie	35.36492	-96.94822	328	08/03/99-12/31/12
SPEN	Spencer	Oklahoma	35.54208	-97.34146	373	12/07/99-12/31/12
STIG	Stigler	Haskell	35.26527	-95.18116	173	09/09/99-05/27/12
STIL	Stillwater	Payne	36.12093	-97.09527	272	06/28/96-12/31/10
TAHL	Tahlequah	Cherokee	35.97235	-94.98671	290	09/21/99-12/31/12
TISH	Tishomingo	Johnston	34.33262	-96.67895	268	02/01/00-12/31/12
VINI	Vinita	Craig	36.77536	-95.22094	236	11/03/99-12/31/12
WALT	Walters	Cotton	34.36470	-98.32025	308	03/06/97-03/11/12
WASH	Washington	McClain	34.98224	-97.52109	345	06/17/99-12/31/12
WATO	Watonga	Blaine	35.84185	-98.52615	517	10/19/99-12/31/12
WAUR	Waurika	Jefferson	34.16775	-97.98815	283	03/06/97-02/16/10
WEST	Westville	Adair	36.01100	-94.64496	348	11/14/96-12/31/12
WILB	Wilburton	Latimer	34.90092	-95.34805	199	11/11/99-12/31/12
WIST	Wister	LeFlore	34.98426	-94.68778	143	10/03/96-12/31/10
WOOD	Woodward	Woodward	36.42329	-99.41682	625	12/10/96-12/31/12
WYNO	Wynona	Osage	36.51806	-96.34222	269	08/26/99-12/31/12

Appendix C Maps Of Climatic Regions

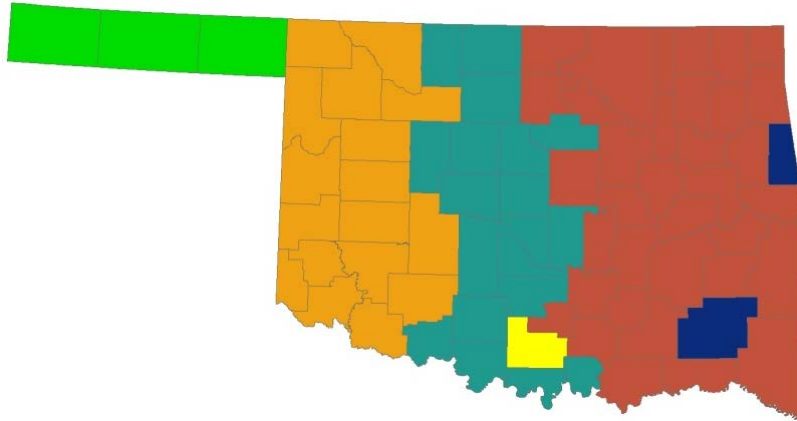


Figure C1. Six Climatic Regions (Hierarchical Clustering)

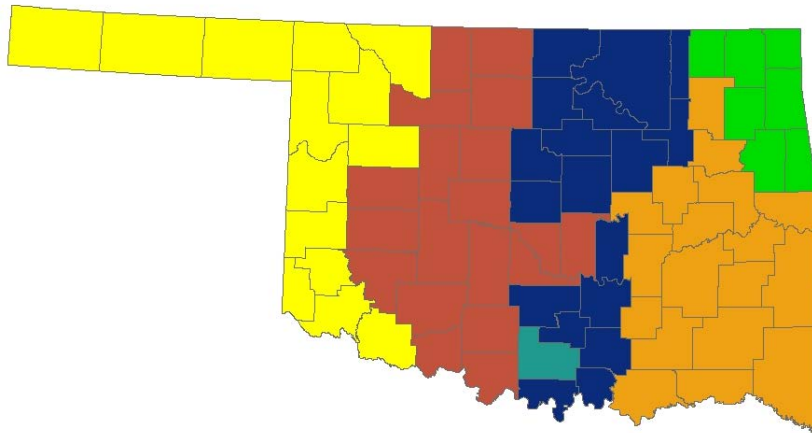


Figure C2. Six Climatic Regions (K-Means Clustering)

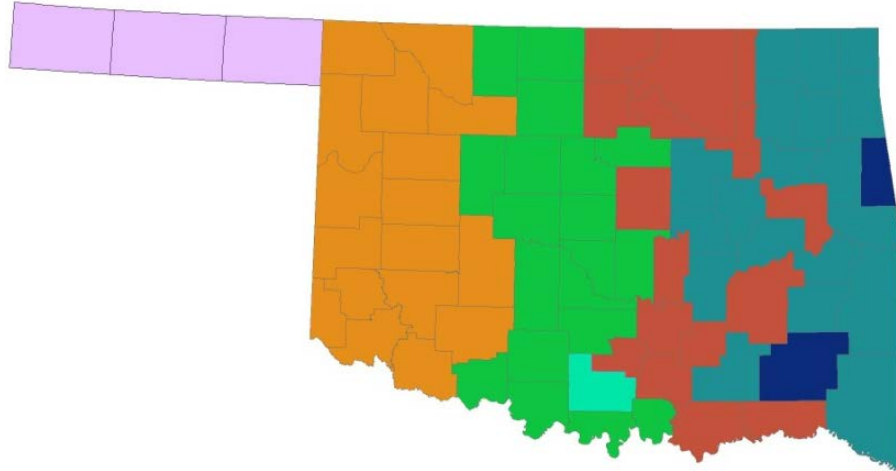


Figure C3. Seven Climatic Regions (Hierarchical Clustering).

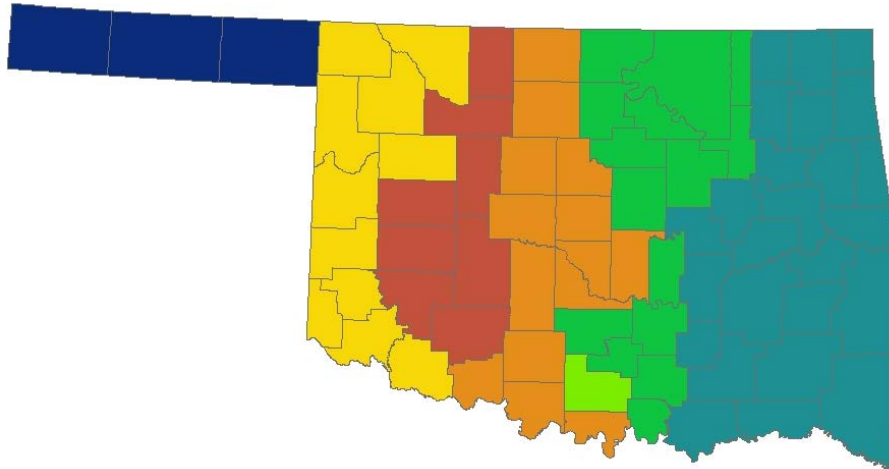


Figure C4. Seven Climatic Regions (K-Means Clustering).

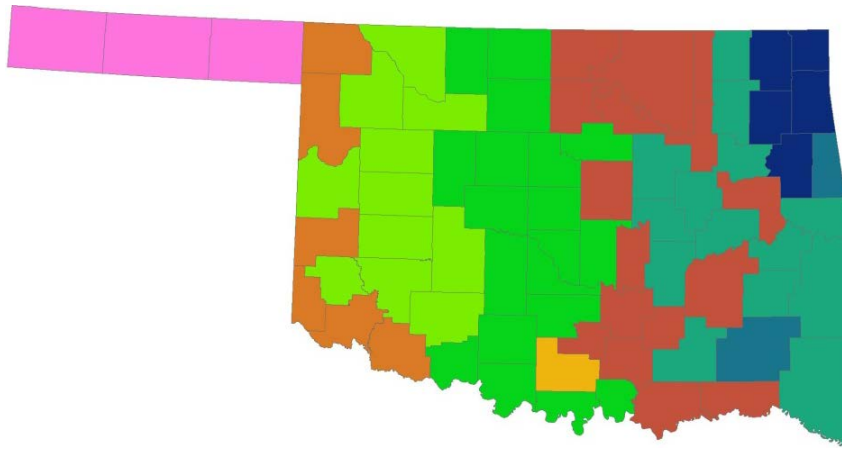


Figure C5. Nine Climatic Regions (Hierarchical Clustering).

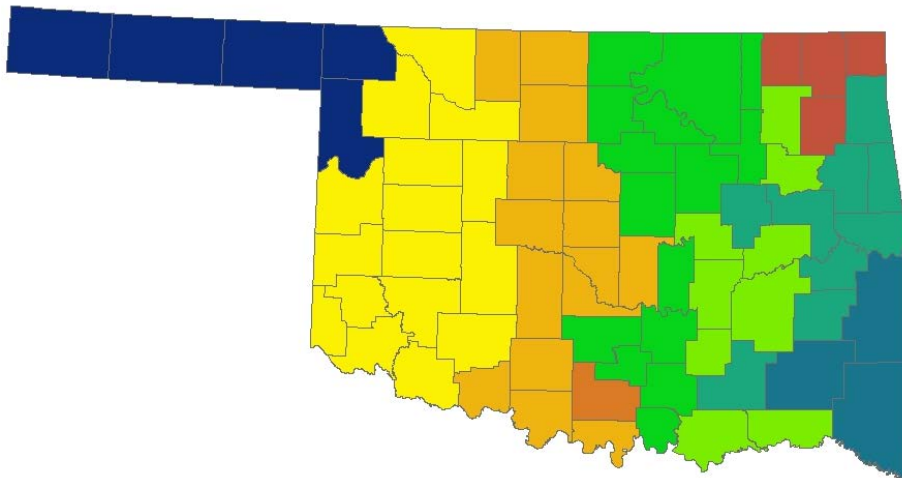


Figure C6. Nine Climatic Regions (K-Means Clustering).

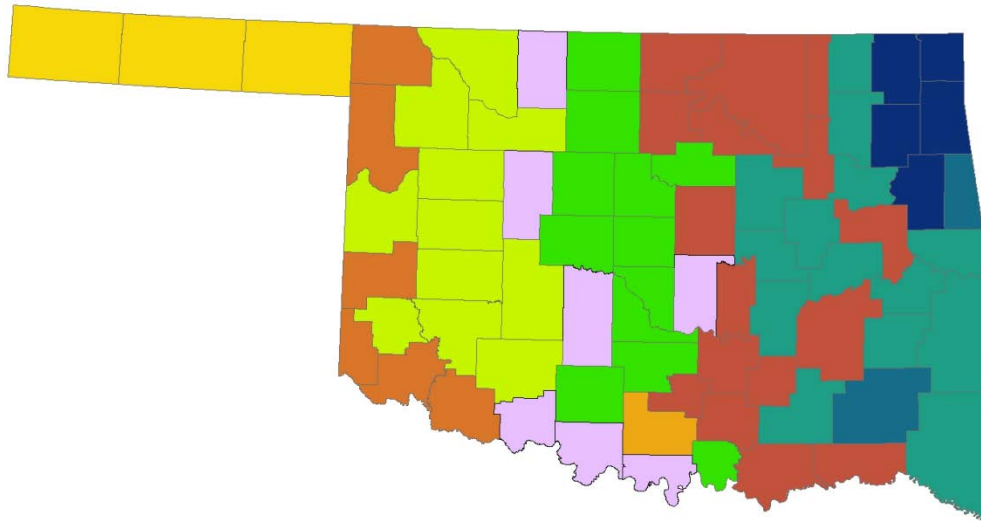


Figure C7. Ten Climatic Regions (Hierarchical Clustering).

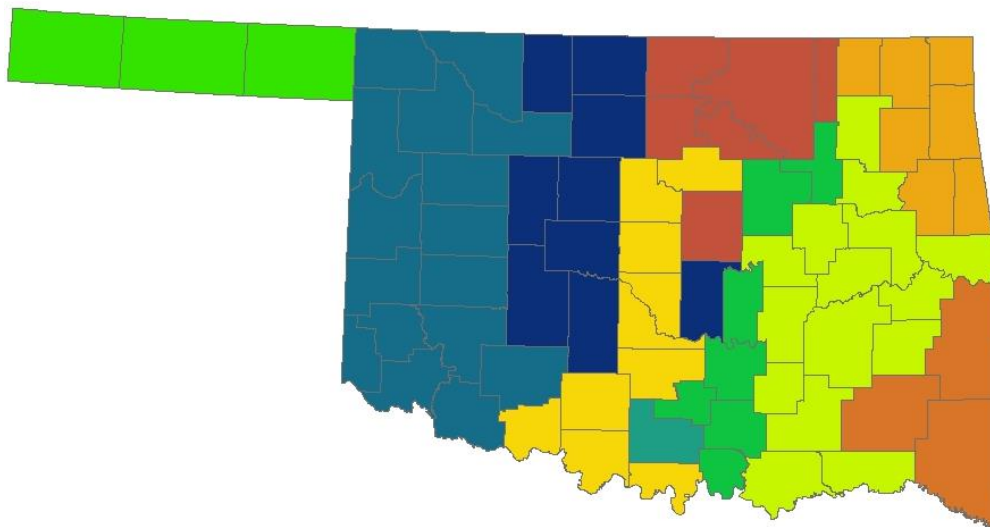


Figure C8. Ten Climatic Regions (K-Means Clustering).

Appendix D Maps Of Soil Regions Using Soil Parameters From USDA Web Soil Survey and The Oklahoma Mesonet

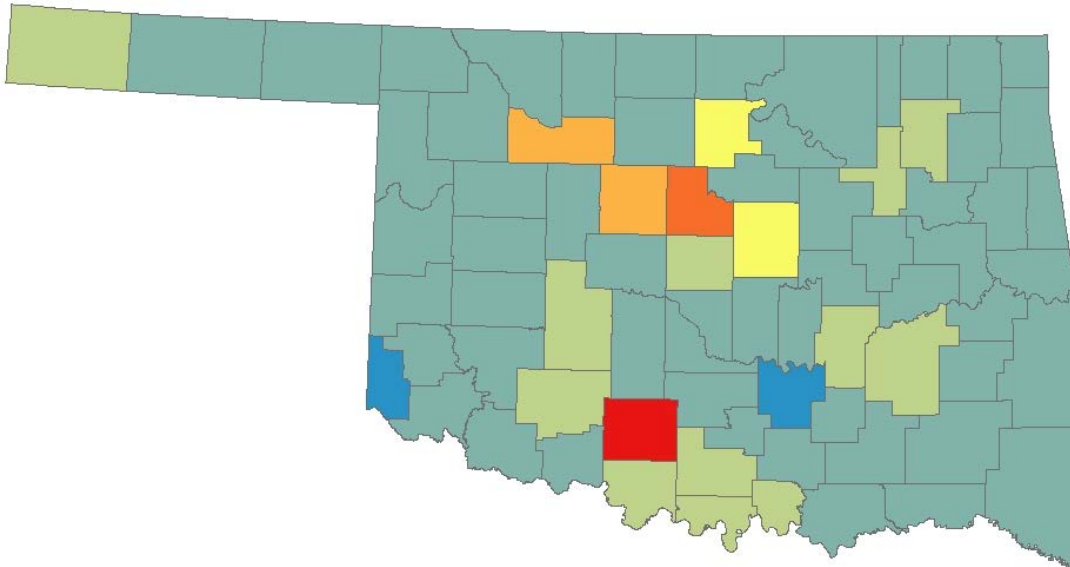


Figure D1. Seven Soil Regions at 5 cm.

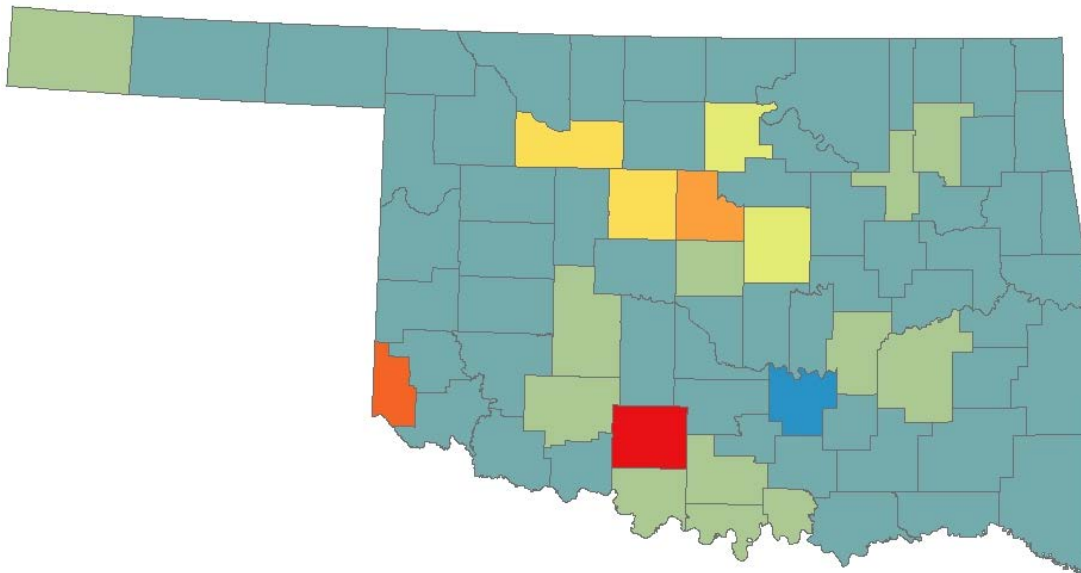


Figure D2. Eight Soil Regions at 5 cm.

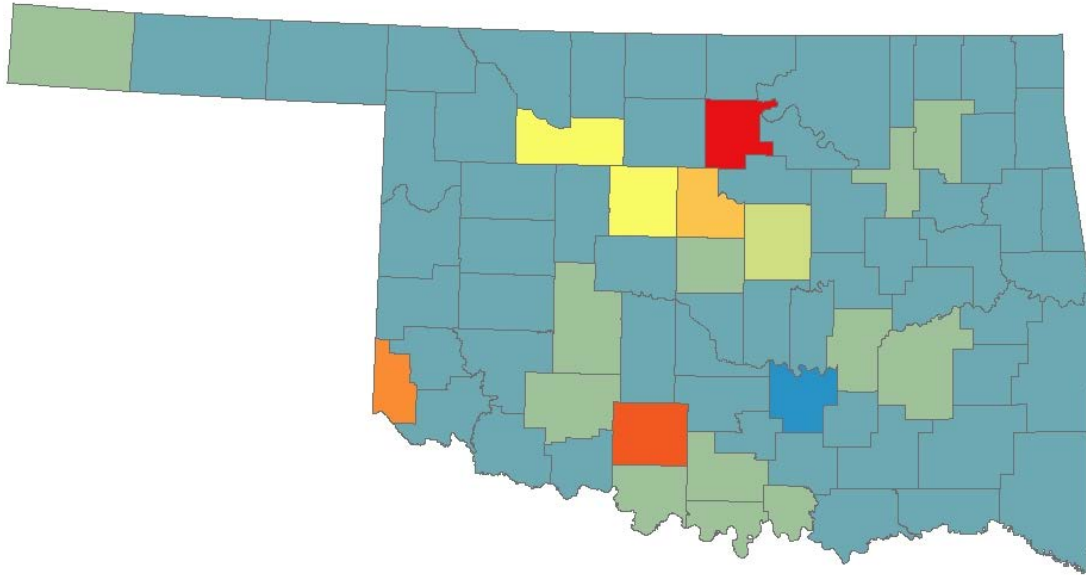


Figure D3. Nine Soil Regions at 5 cm.

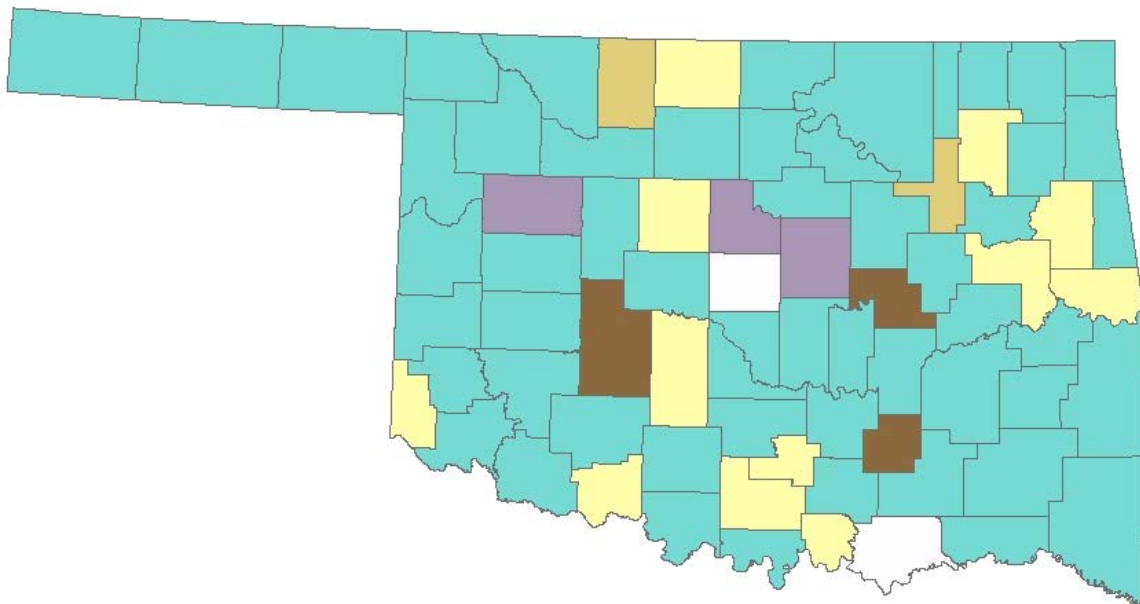


Figure D4. Six Soil Regions at 25 cm.

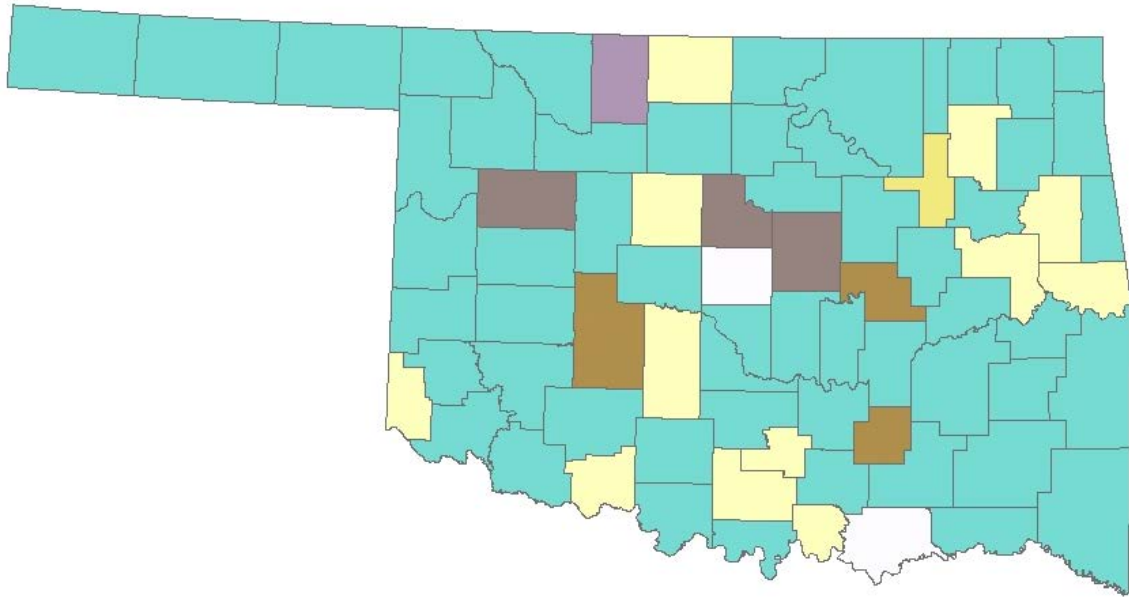


Figure D5. Seven Soil Regions at 25 cm.

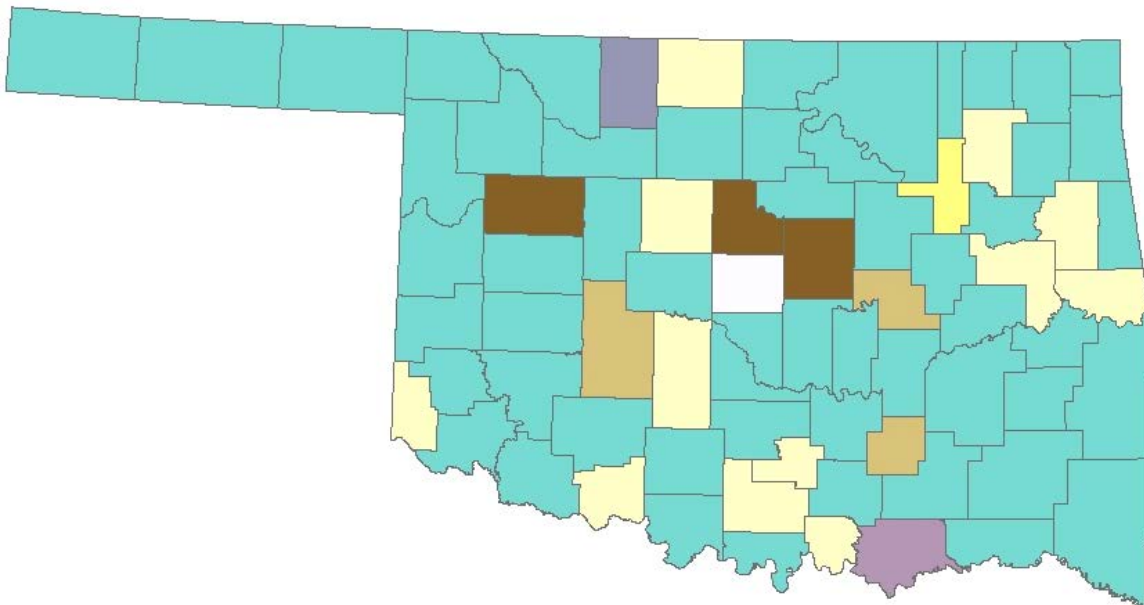


Figure D6. Eight Soil Regions at 25 cm.

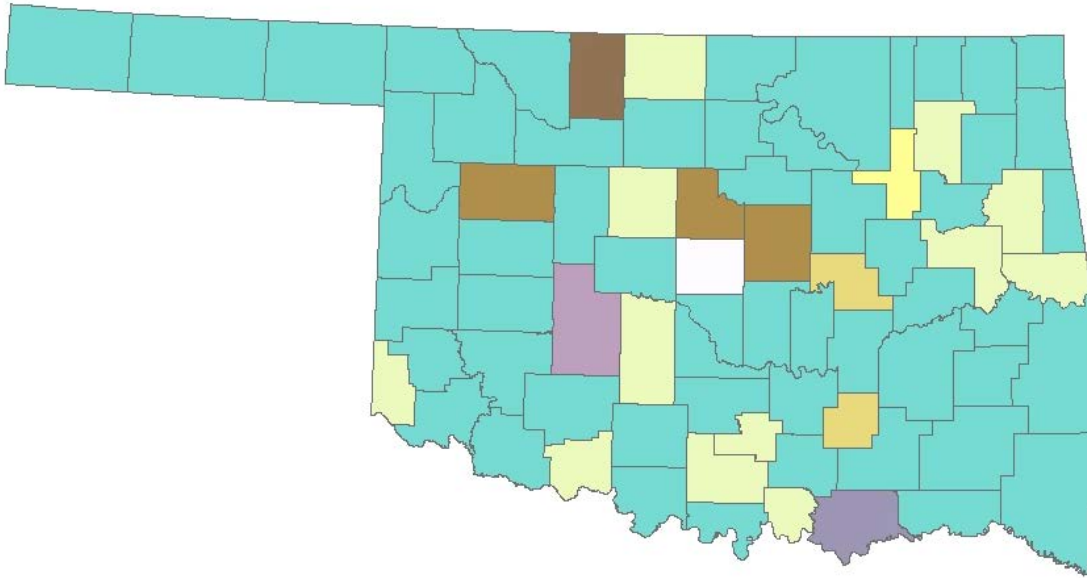


Figure D7. Nine Soil Regions at 25 cm.

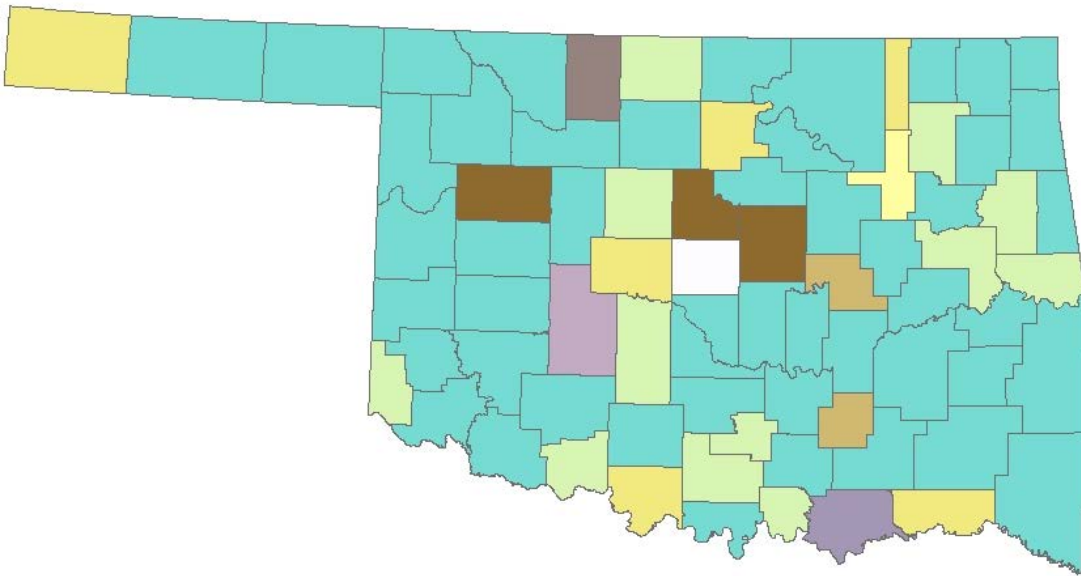


Figure D8. Ten Soil Regions at 25 cm.

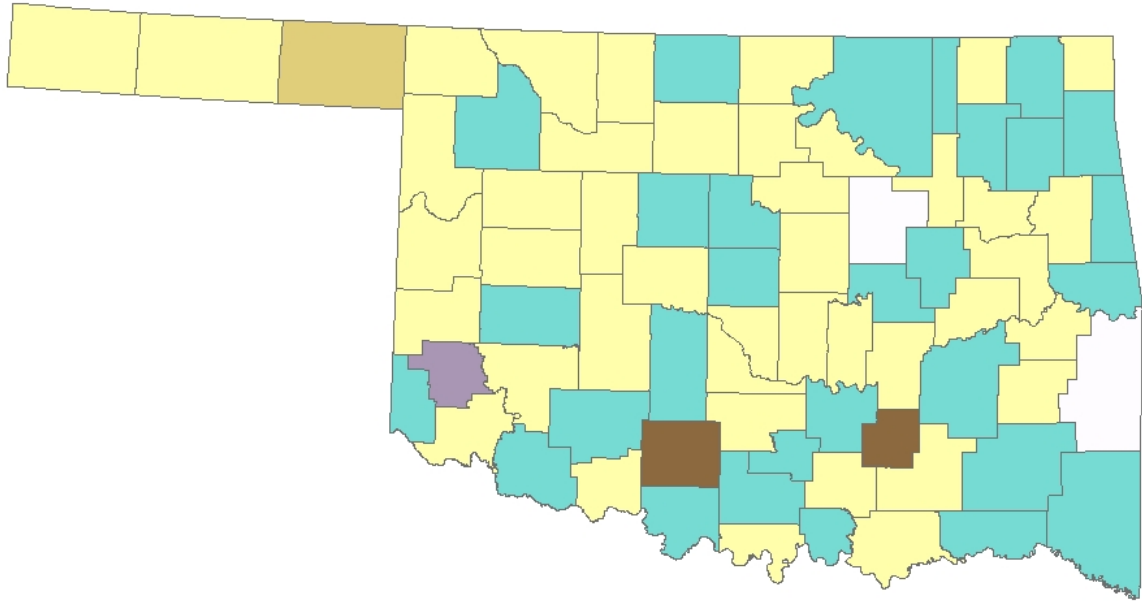


Figure D9. Six Soil Regions at 60 cm.

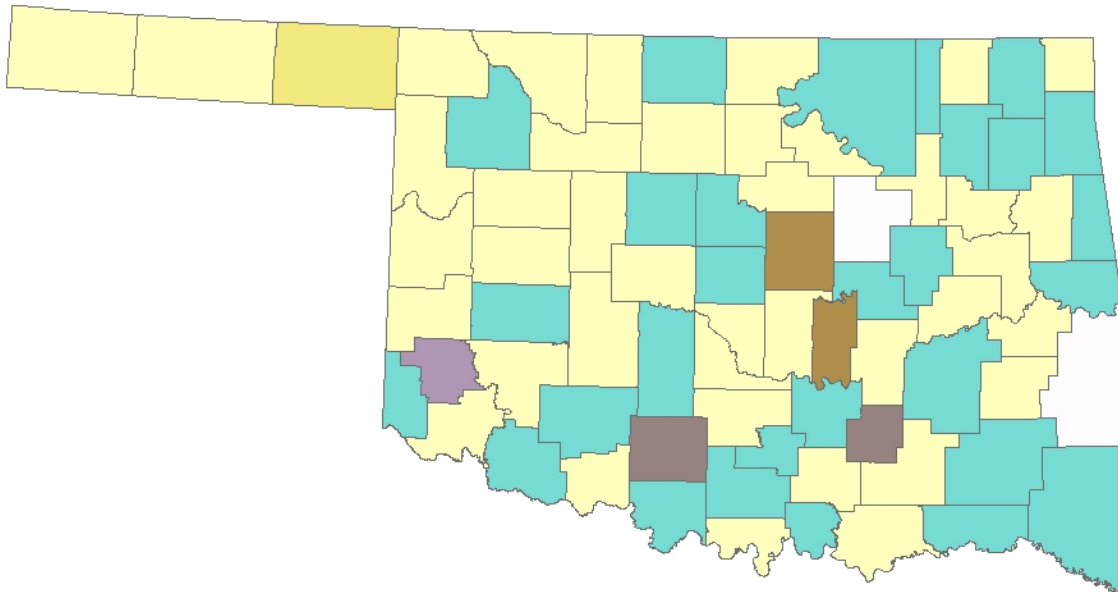


Figure D10. Seven Soil Regions at 60 cm.

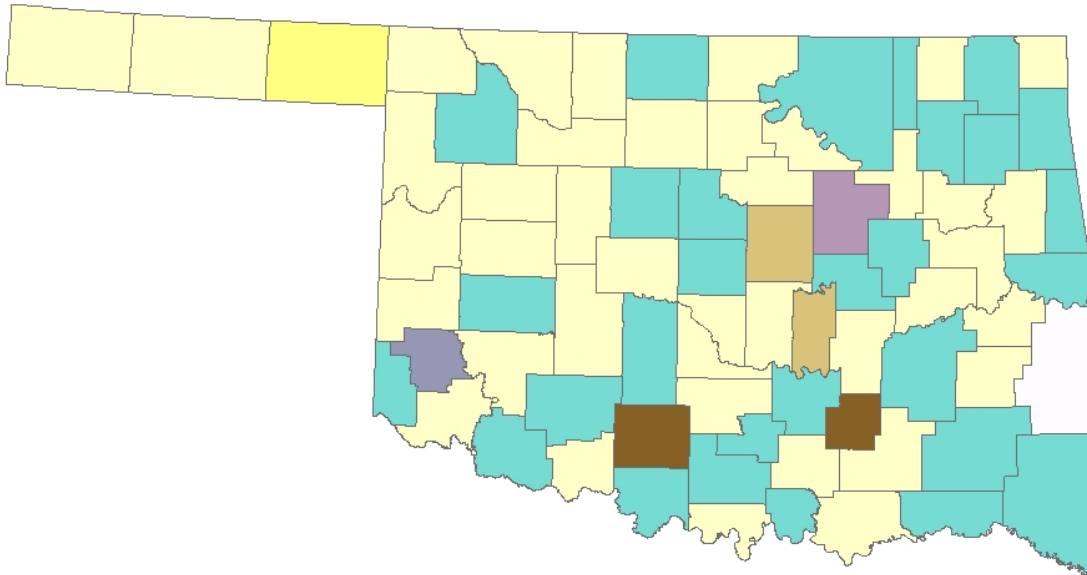


Figure D11. Eight Soil Regions at 60 cm.

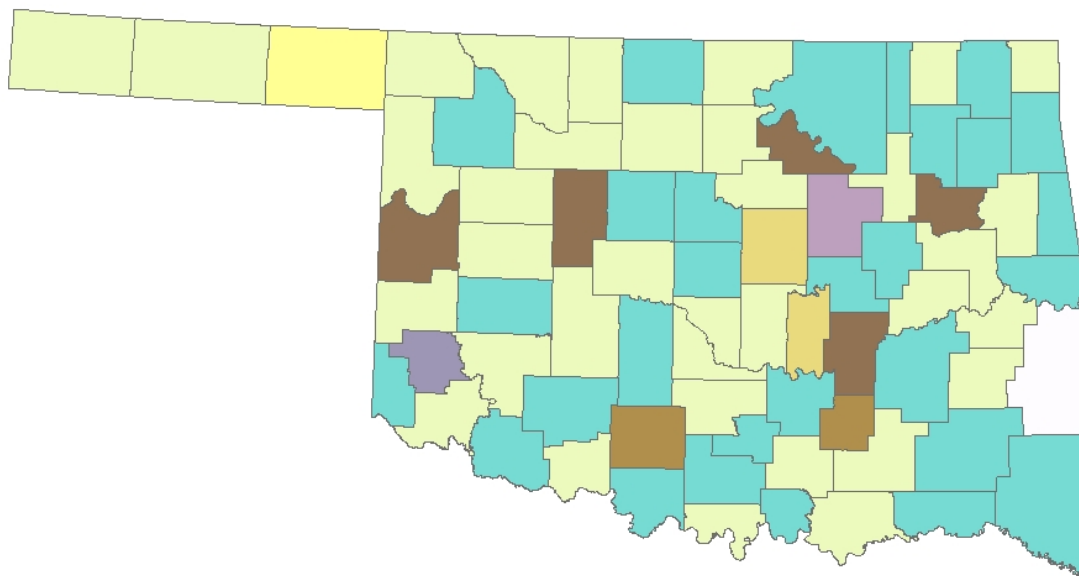


Figure D12. Nine Soil Regions at 60 cm.

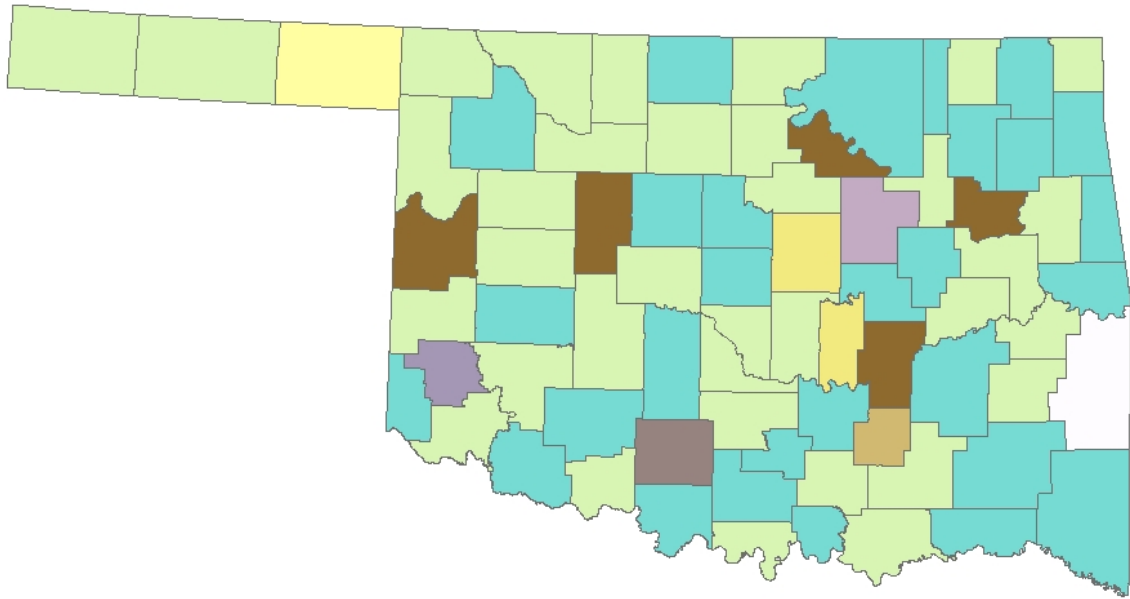


Figure D13. Ten Soil Regions at 60 cm.

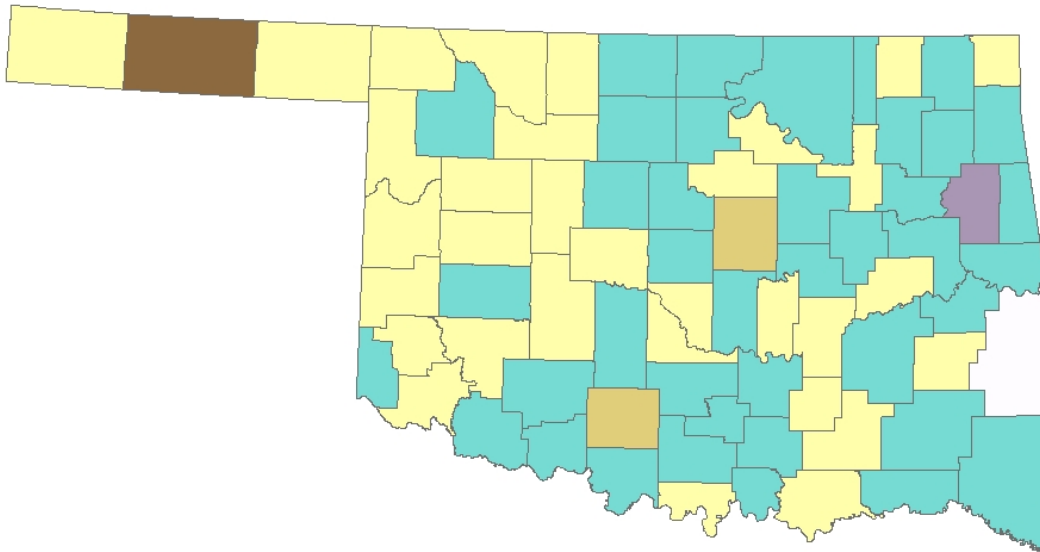


Figure D14. Six Soil Regions at 75 cm.

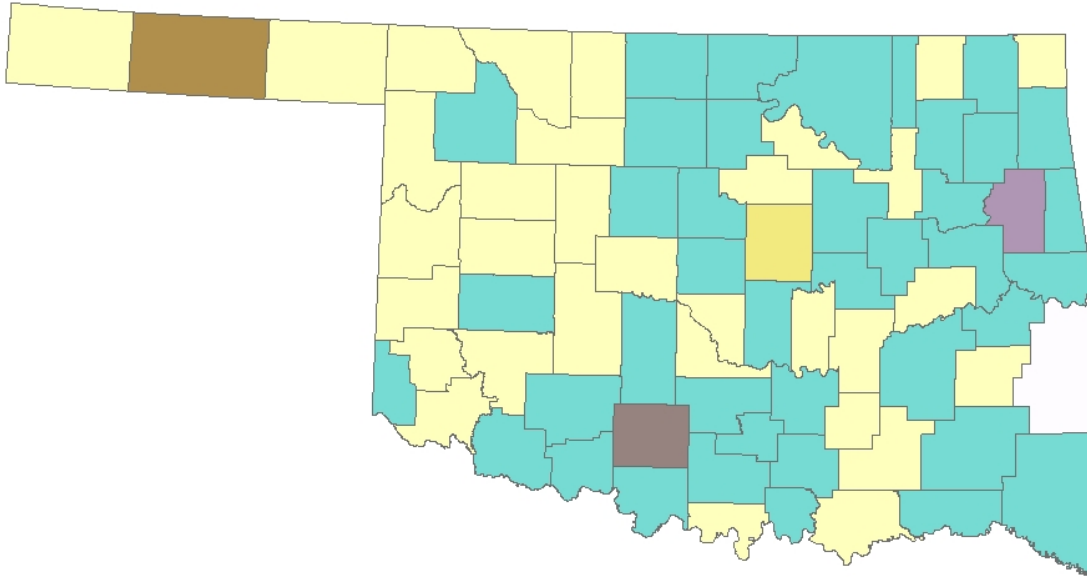


Figure D15. Seven Soil Regions at 75 cm.

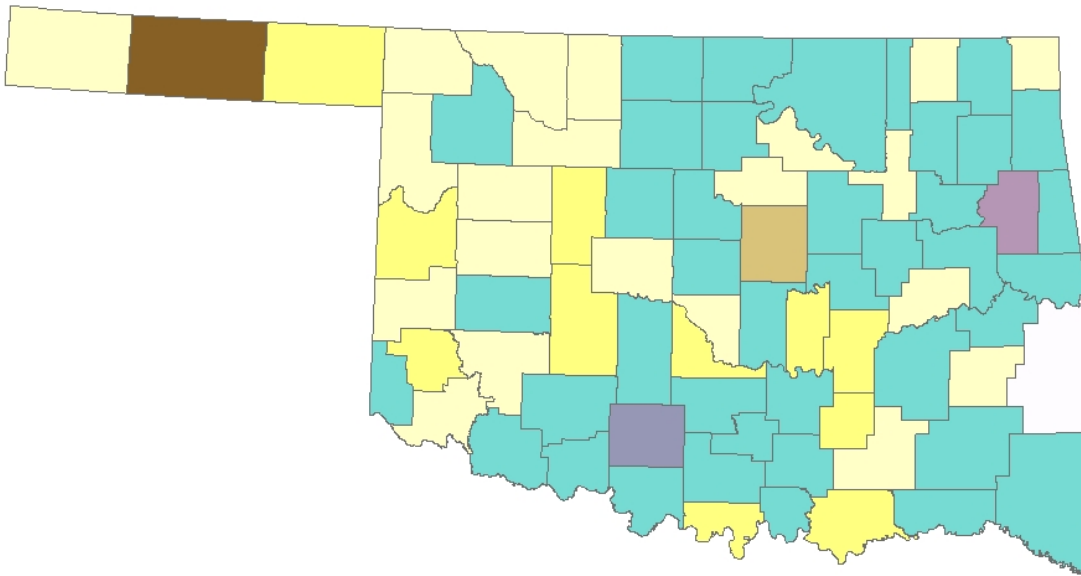


Figure D16. Eight Soil Regions at 75 cm.

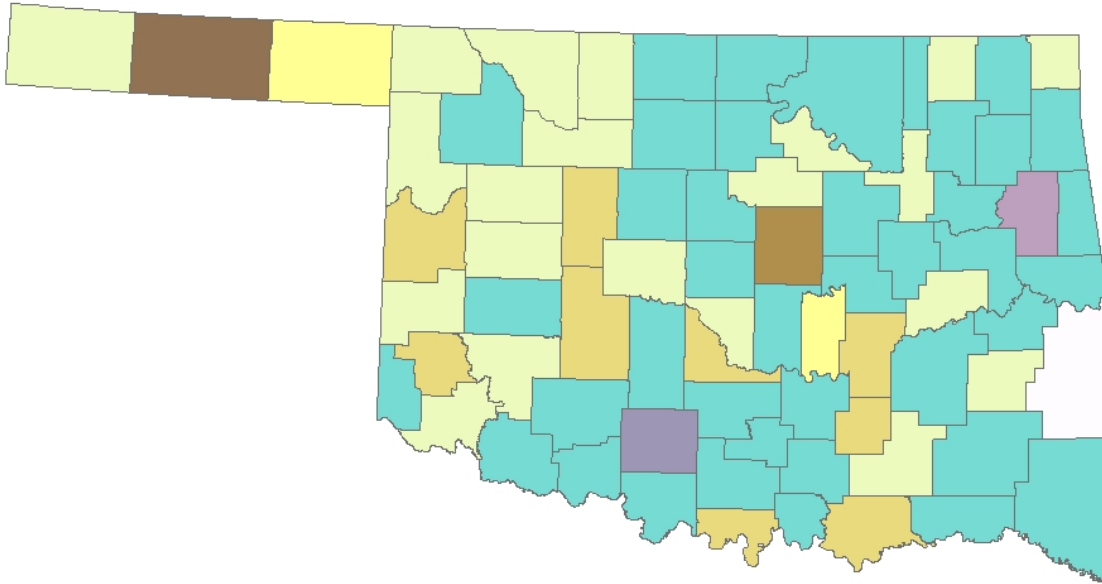


Figure D17. Nine Soil Regions at 75 cm.

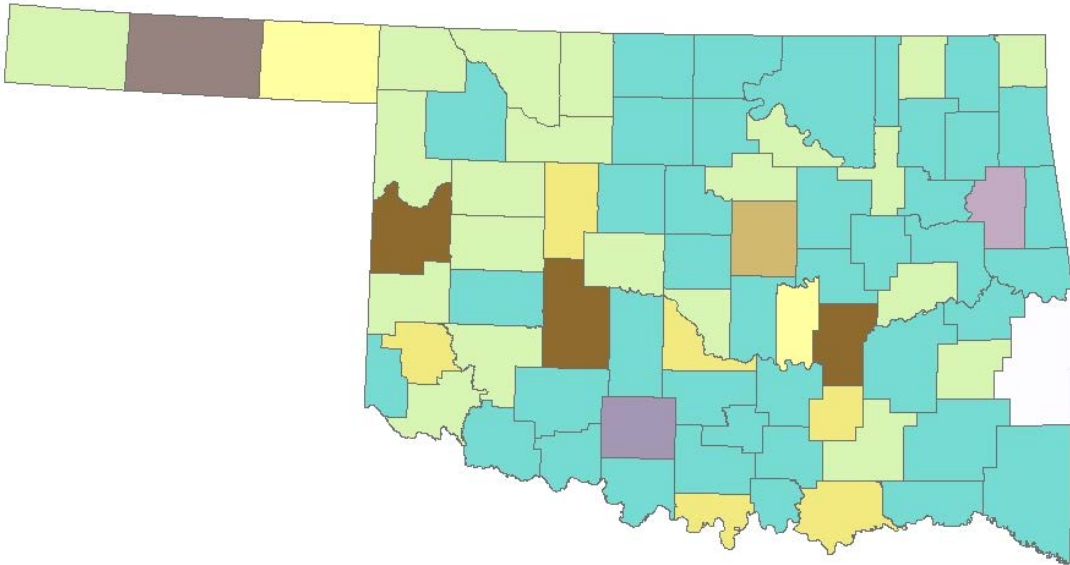


Figure D18. Ten Soil Regions at 75 cm.

Appendix E Maps of Soil Regions Using New Soil Property Database

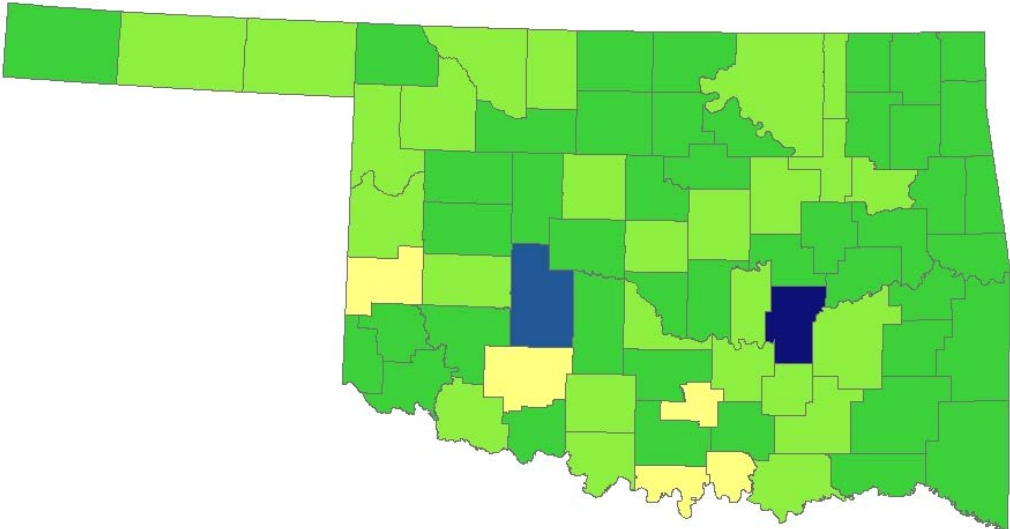


Figure E1. Six Soil Regions at 20 cm.

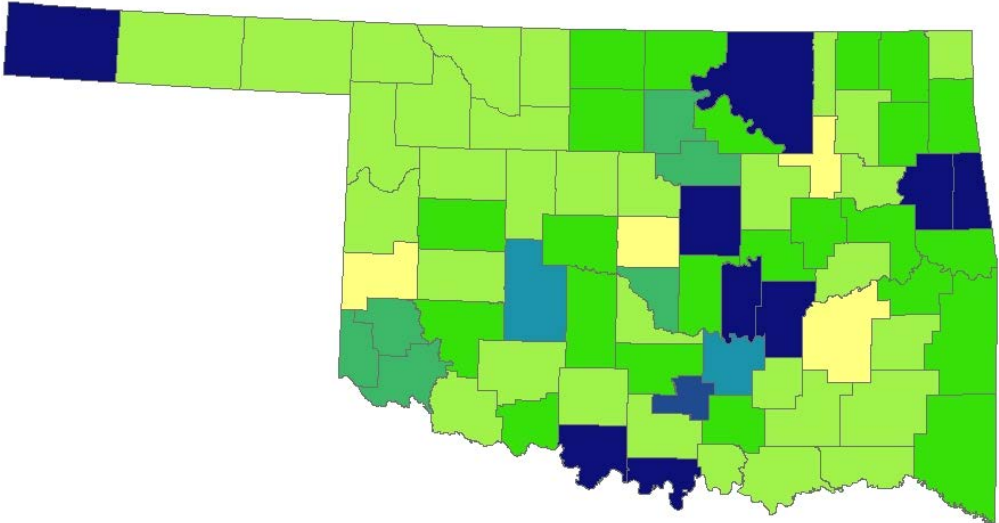


Figure E2. Seven Soil Regions at 3 cm.

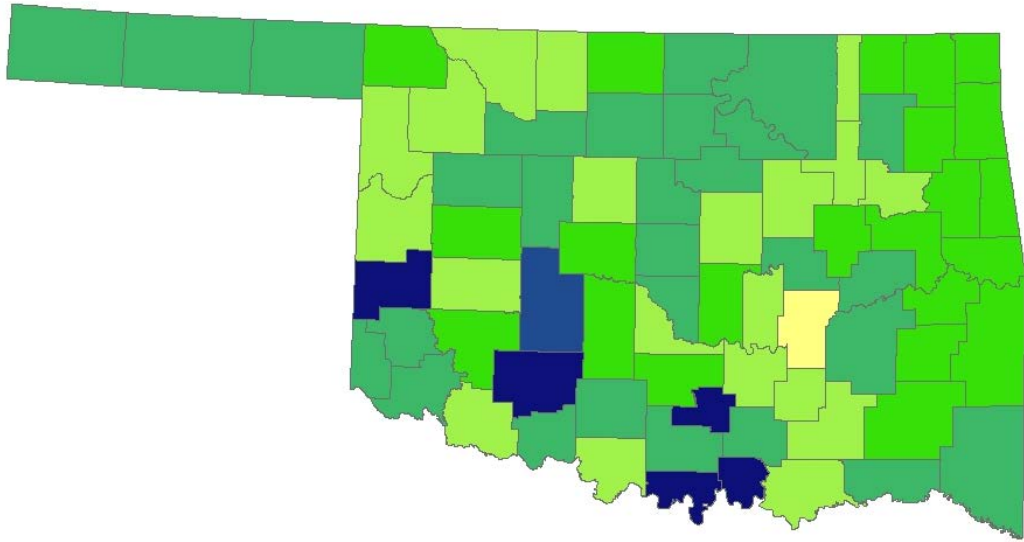


Figure E3. Seven Soil Regions at 20 cm.

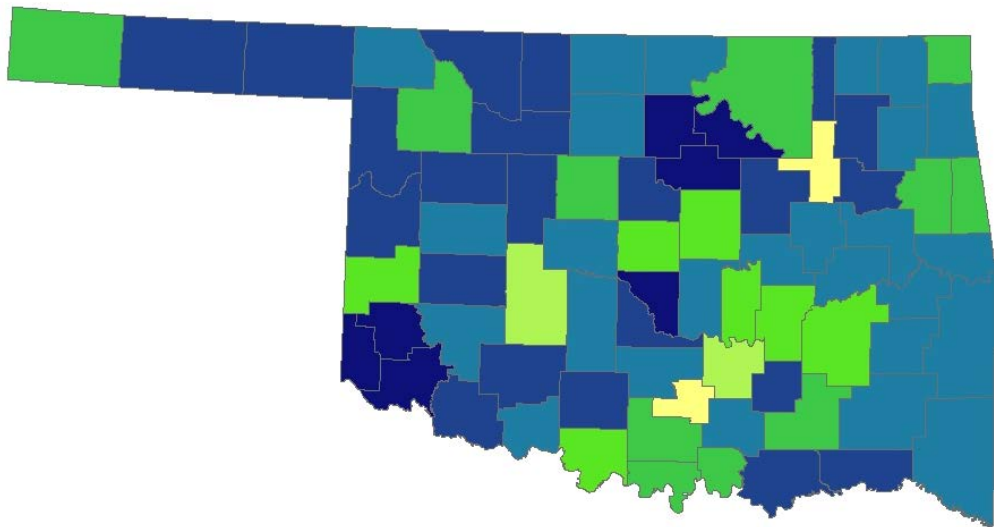


Figure E4. Eight Soil Regions at 3 cm.

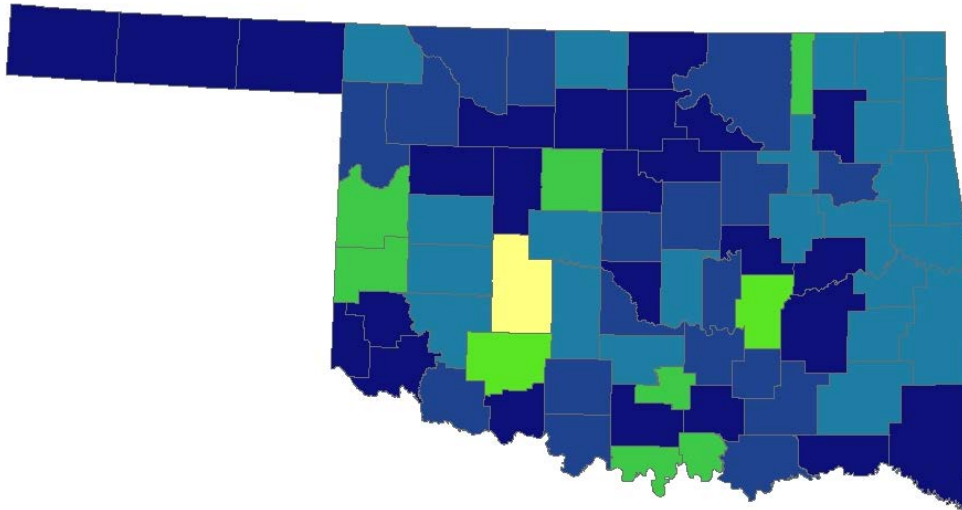


Figure E5. Eight Soil Regions at 20 cm.

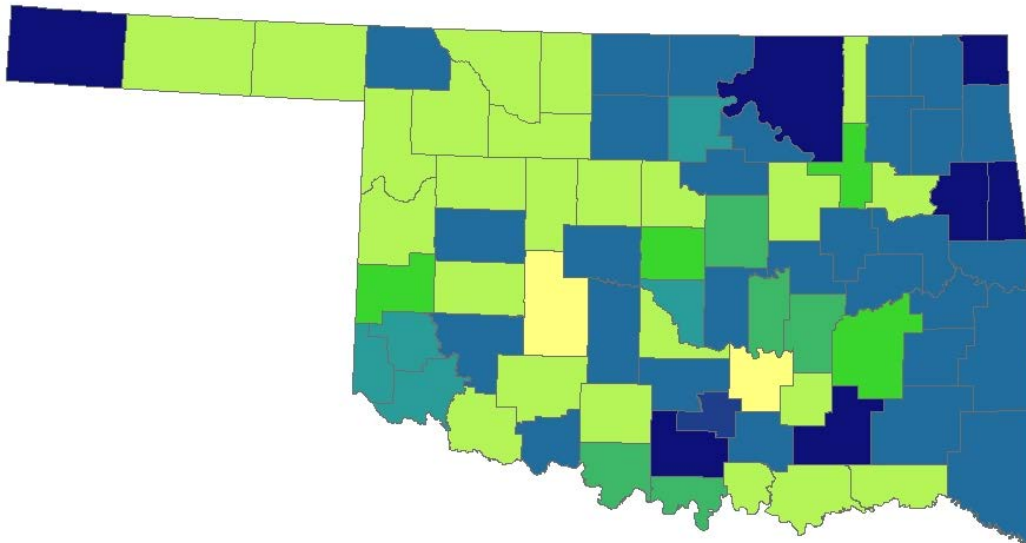


Figure E6. Nine Soil Regions at 3 cm.

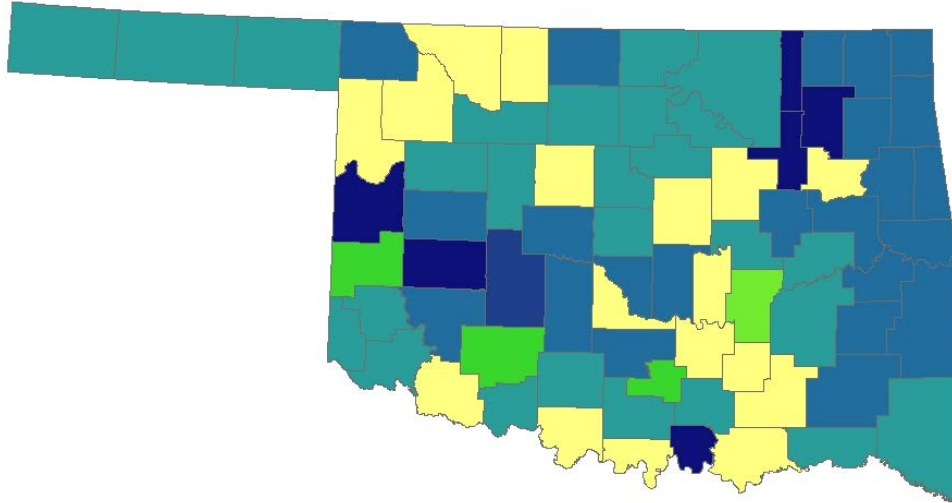


Figure E7. Nine Soil Regions at 20 cm.

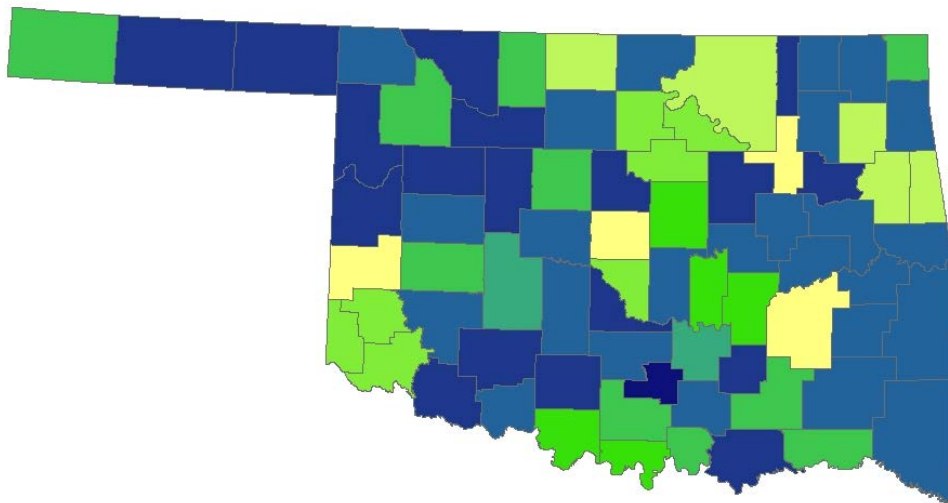


Figure E8. Ten Soil Regions at 3 cm.

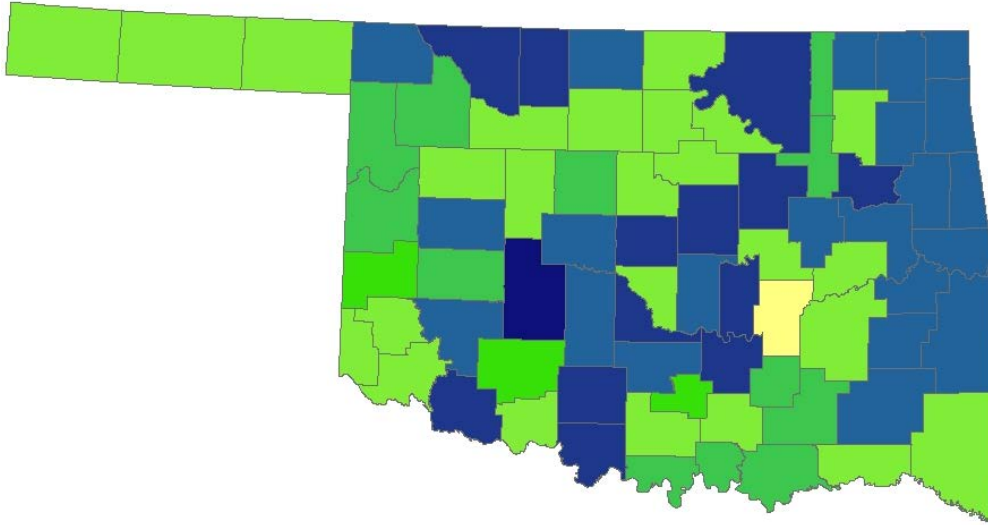


Figure E9. Ten Soil Regions at 20 cm.

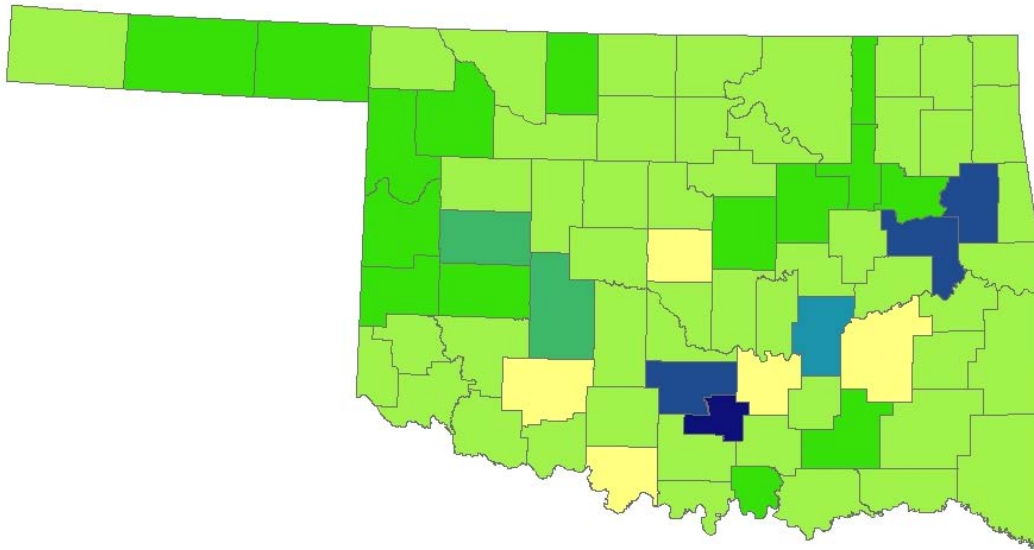


Figure E10. Seven Soil Regions (Weighted Average).

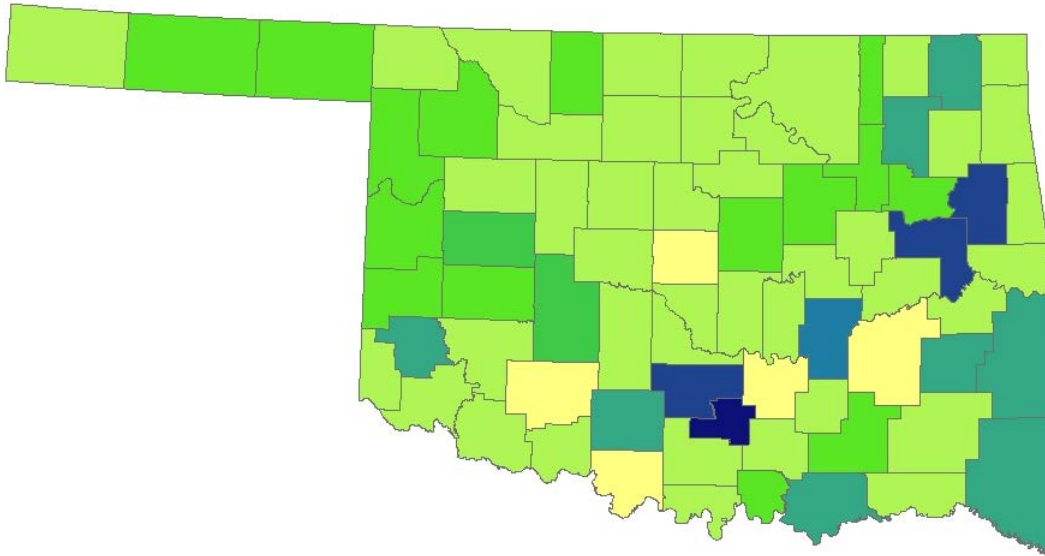


Figure E11. Eight Soil Regions (Weighted Average).

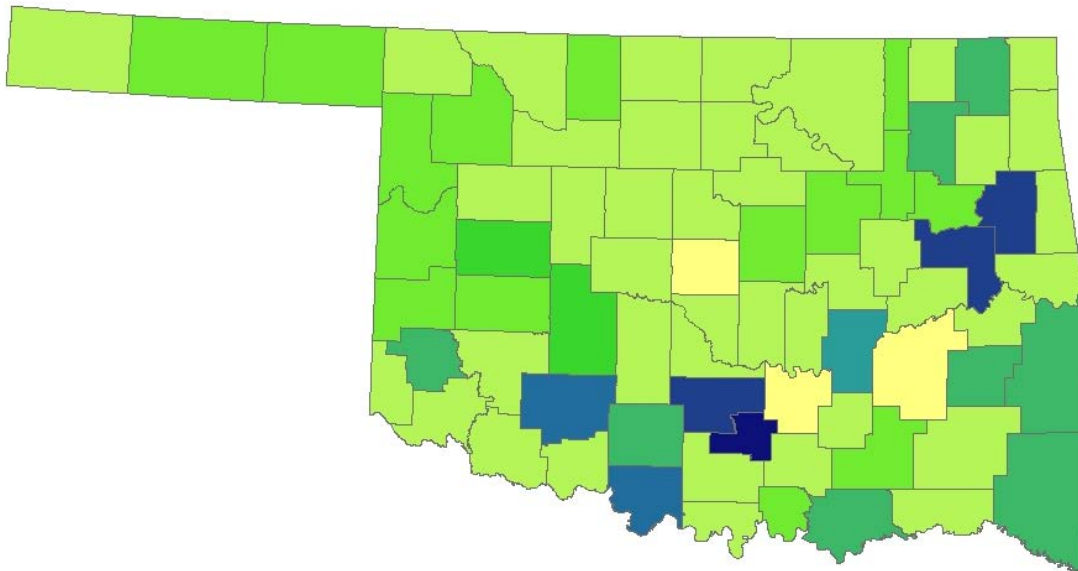


Figure E12. Nine Soil Regions (Weighted Average).

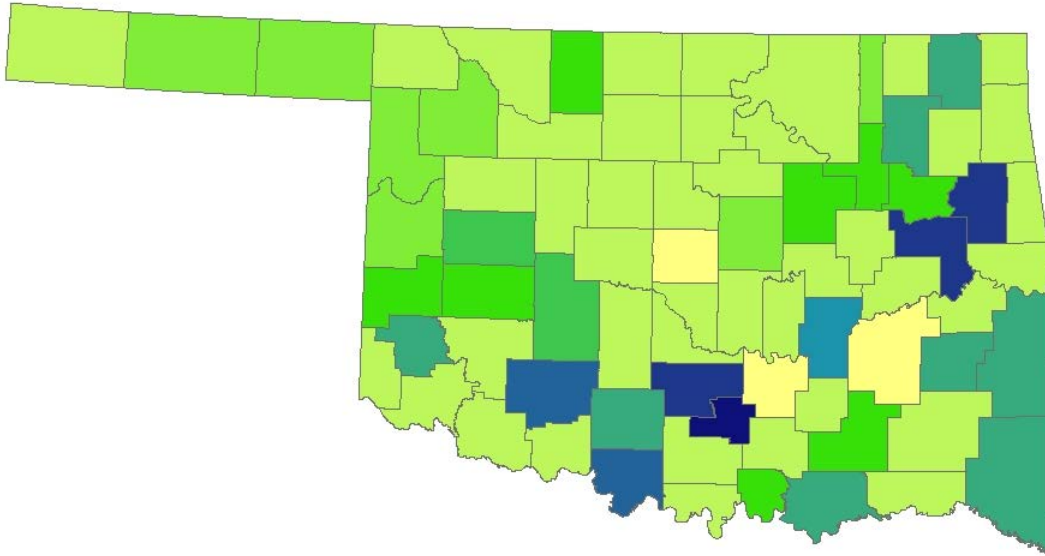


Figure E13. Ten Soil Regions (Weighted Average).